CENTRO INTERNACIONAL DE MÉTODOS NUMÉRICOS EN INGENIERÍA

Decision Support System for Cardiovascular Problems

E. Soudah
R. López
M. Bordone
E. Oñate

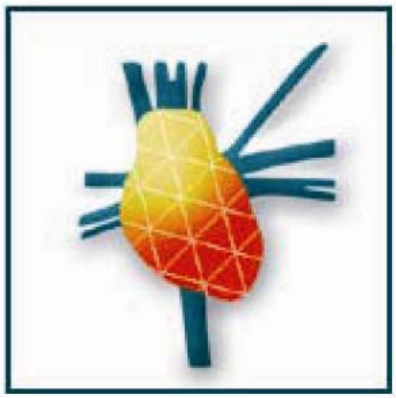

Monograph CIMNE Nº-108, February 2008

Decision Support System for Cardiovascular Problems

E. Soudah
R. López
M. Bordone
E. Oñate

Monograph CIMNE Nº-108, February 2008

Research project sponsored by the European Commission (EC) through the 6th Framework PROGRAMME HORIZONTAL RESEARCH ACTIVITIES INVOLVING SME'S CO-OPERATIVE RESEARCH.
DISHEART Project nºFP6-2002-SME-1

INTERNATIONAL CENTER FOR NUMERICAL METHODS IN ENGINEERING
Gran Capitán s/n, 08034 Barcelona, Spain

INTERNATIONAL CENTER FOR NUMERICAL METHODS IN ENGINEERING
Edificio C1, Campus Norte UPC
Gran Capitán s/n
08034 Barcelona, España
www.cimne.upc.es

First edition: February 2008

DECISION SUPPORT SYSTEM FOR CARDIOVASCULAR PROBLEMS
Monograph CIMNE M108

ISBN: 978-84-96736-43-6

INDEX.

ILLUSTRATION

1 SUMMARY

The DISHEART project aims at developing a new computer based decision support system (DSS) integrating medical image data, modelling, simulation, computational Grid technologies and artificial intelligence methods for assisting clinical diagnosis and intervention in cardiovascular problems. The RTD goal is to improve and link existing state of the art technologies in order to build a computerised cardiovascular model for the analysis of the heart and blood vessels.

The resulting DISHEART DSS interfaces computational biomechanical analysis tools with the information coming from multimodal medical images. The computational model is coupled to an artificial neural network (ANN) based decision model that can be educated for each particular patient with data coming from his/her images and/or analyses. The DISHEART DSS system is validated in trials of clinical diagnosis, surgical intervention and subject-specific design of medical devices in the cardiovascular domain. The DISHEART DSS also contributes to a better understanding of cardiovascular morphology and function as inferred from routine imaging examinations.

Four reputable medical centers in Europe took an active role in the validation and dissemination of the DISHEART DSS as well as the elaboration of computational material and medical images. The integrated DISHEART DSS supports health professionals in taking promptly the best possible decision for prevention, diagnosis and treatment. Emphasis was put in the development of user-friendly, fast and reliable tools and interfaces providing access to heterogeneous health information sources, as well as on new methods for decision support and risk analysis.

The use of Grid computing technology is essential in order to optimise and distribute the heavy computational work required for physical modelling and numerical simulations and especially for the parametric analysis required for educating the DSS for every particular application.

The four end user SME's participating in the project benefits from the new DISHEART DSS. The companies COMPASS, QUANTECH and Heartcore will market the DSS among public and private organizations related to the cardiovascular field. EndoArt will exploit the DISHEART DSS as a support for enhanced design and production of clinical devices.

The partnership was sought in order to gather the maximum complementary of skills for the successful development of the project Disheart DSS, requiring experts in Mechanical sciences, Medical sciences, Informatic, and FEM technique to grow up the testes. All the partners are called below:, divided into:

RTD Performers

- International Center for Numerical Methods in Engineering (CIMNE) (Barcelona Spain)
- The Aragon Institute of Engineering University of Zaragoza (I3A) (Zaragoza-Spain)
- Technical University of Graz (Graz Austria)
- Laboratoire Techinque de l'Imagerie de la Modélisation et de la Cognition (Grenouble France
- Vascular Fluid Dynamics (USA)
- Sant Pau Hospital (Barcelona Spain)

SME'S

- COMPASS Ingenieria y Sistemas S.A. (Barcelona Spain)
- HeartCore B.V. (Nederland)
- EndoArt S.A. (Switzerland)
- Quantech ATZ S.A. (Barcelona Spain)

2 PROJECT BACKGROUND AND OBJECTIVES

The DISHEART project aims at developing a new computer based decision support system (DSS) integrating image analysis, modelling, simulation, computational Grid technologies and artificial intelligence methods for assisting clinical diagnosis and intervention in cardiovascular problems. The aim is to build a computerised cardiovascular model for the analysis of the heart and arteries interfacing biomechanical and computational fluid dynamics information with the information coming from medical images obtained through different techniques. The computational model will be coupled to an artificial neural network (ANN) based decision model that will be educated for each particular patient with data coming from his/her images and/or analyses.

The two main lines of medical research in this project are vascular anatomy (large vessels around the heart, coronaries and peripheral arteries) and heart chambers. Geometric models will be constructed to aid clinical diagnosis or multiphysical modelling and simulation. Two levels of complexity will be considered. For heart modelling, the first level will concentrate on models of the left and right ventricular cavities for robust and efficient extraction of simple clinical indexes of geometry, volume, mass, and wall kinetics. The second level will aim at more complex, four-chambered models, which will be important in developing comprehensive solid and fluid models to assist the design of medical devices.

Following the successful development of the DISHEART DSS, a crucial activity of the project will be the in-depth calibration, validation and assessment of the performance, scalability and effectiveness of the DSS in its application to a number of cardiovascular problems including the study of implants and devices, the simulation of surgical intervention and the application to heart valve interventions. This task will be developed in close collaboration between the RTD performers, the SME's and the supporting medical centres. In assumptions:

1. The DISHEART system will be applicable to computer analysis of the heart and blood vessels.

2. The resulting DISHEART DSS will interface computational biomechanical analysis tools with the information coming from medical images.

3. The DISHEART system will be developed following:
    - Definition of the levels of users.
    - User friendly interface
    - Easy access to the new decision support system
    - Access to heterogeneous health information sources
    - With the most actual communication tools by Internet

3 NEED AND RELEVANCE OF THE PROPOSED RESEARCH

According to WHO estimates, 17 million people around the globe die of cardiovascular disease (CVD) each year. In 1998 there were 7.3 million deaths from heart attack and 5.1 million from stroke. About 600 million people with high blood pressure are at risk of heart attack, stroke and cardiac failure. In 1999 CVD contributed to one-third of global deaths. Low- and middle-income countries contributed to 78 percent of CVD deaths. By 2010 CVD is estimated to be the leading cause of death in developing countries. Heart disease has no geographic, gender or socio-economic boundaries [WHO, AHA03, AHA02, Rayner 2000, Petersen 2003].

CVD is not only the main cause of death in Europe and the EU but is also the main cause of years lost due to an early death. The Global Burden of Disease Study has shown that on average 31% of years of life lost are due to CVD in 'Established Market economies' (mostly Northern, Southern and Western countries in Europe and all the member states of the EU).

As CVD keeps on being the world leading cause of death the need to find ways are procedures to mitigate this problem increases. Hence any effort to improve early diagnosis and therapy by advanced computer-aided technology will have a highly beneficial impact on society. *The DISHEART project is concerned with integrating efforts from the medical image, physical modelling, numerical simulation and Grid computing communities to provide new tools and procedures to facilitate the diagnosis, treatment and therapies of CVDs.*

The outcomes of the DISHEART project will be strategic to enhance the competitiveness of the four participating SME's in the area of computer-aided clinical diagnosis and intervention in the cardiovascular sector. The SME's will actively exploit both externally and internally the new tools and procedures resulting from the RTD activities as described below.

3.1 Specific research and innovation activities of the project

Medical treatment of cardiovascular problems is a decision-making process bordering between the art and science of making choices for desirable change in order to make accurate clinical diagnosis and choose the optimal path for surgical interventions. There will be six innovative roles for the DISHEART DSS:

1. *Guiding role* through the decision-making process during diagnosis, interventions and recovery stages;
2. *Assisting role* in establishing the optimal intervention path;
3. *Supporting role* in describing the cardiovascular problem to be solved in terms of predefined objectives, and constraints for generation of alternative actions;
4. *Active role* in collection and integration of information that will support a clinical diagnosis or an intervention, evaluation of consequences of actions, and learning;
5. *Aiding role* in evaluation of alternatives using multiple and often conflicting interventions paths;
6. *Educational role* in learning from the decision process itself and from outcomes of the implemented clinical decisions.

In order to achieve these six innovative roles during the DISHEART project will be developed the following modules:

1. *Simulation module:* this module will be integrated by a blood and vessel interaction simulation

tool and a heart chambers simulation tool;

2. *Decision module:* a specific support system will be developed to assist in the decision of clinicians in two specific cardiovascular problems of interest;

3. *Design or validation module:* four different specific problems of computer-aided design will be tackled during this project.

The integration of these three modules in a unique system will conform the DISHEART system.

4 OVERVIEW OF PROJECT TASKS.

The project work was split in the following work packages:

WP1. Specification of DISHEART

WP2. Database of material properties and medical images.

WP3. Generation of data for computer simulation from medical images.

WP4. Development of blood flow simulation module.

WP5. Development of computational module for analysis of blood vessels and heart mechanics.

WP6. Integration of DISHEART DSS.

WP7. Validation and enhancement of the DISHEART system.

WP8. Dissemination and exploitation plan.

WP9. Project management.

The following sections describe the work carried out in the project with emphasis in the main achievements toward development and the user interface of DISHEART.DSS- The descriptions of the project work following the activities planned in the different workpackage.

5 SIMULATION MODULE

Cardiovascular diseases, in their multiple forms, can either be local (i.e., atherosclerosis), where local geometry and tissue properties and local haemodynamics play a role, or global, where systemic factors and the global interaction of heart with arterial system play an important role (i.e., isolated systolic hypertension, heart failure, etc). Depending on the type of arterial disease, effective diagnosis and treatment of arterial disease may necessitate precise local measurements of the tissue geometry, the material properties and the associated haemodynamics but may also require the ability to characterize global cardiac and arterial functions on a per patient specific basis. Subject-specific cardiovascular modelling, i.e., the ability to derive from a set of limited non-invasive measurements of vascular or cardiac parameters, a patient-specific assessment of arterial and cardiac functions is a significant step towards the better diagnosis and treatment of cardiovascular disease. This accentuates the need of subject-specific cardiovascular modelling based on local or global non-invasive cardiovascular measurements.

Detailed knowledge of the biomechanical properties of vascular tissues is crucial for the understanding of the changes in the cardiovascular system due to age, atherosclerosis and hypertension [see, for example, Berry 1976, Cox 1982, Rachev 1998, Stefanadis 1997, Salunke 1997, Topo1eski 1997, Wuyts 1995]. Within the physiological domain, constitutive equations attempt to reflect the (visco) elastic response of the vascular tissues. For an overview see [Abé 1996, Humphrey 2002, Holzapfel 2003], with a particular focus on arterial wall mechanics provided in, e.g., [Hayashi 1993, Holzapfel, Gasser & Oogden 2000, Holzapfel 2001]. For interventional treatments such as (coronary) balloon angioplasty loading is frequently much higher than within the physiological domain, and modelling issues have to be extended to more advances theories such as damage, (visco) plasticity and so forth [Holzapfel, Schulze-Bauer & Stadler 2000, 2001, Gasser 2002, among others]. Physical models aim to incorporate the structure of the associated tissue [Guccione 1995, McCuloch 1995, Holzapfel, Gasser & Oogden 2000, Xie 2000] with the goal to find physically meaningful parameters. For example, to incorporate the (collagen) fibres in arterial walls in the constitutive model advances our knowledge of the interaction of the associated structure and function.

Much effort has been invested in recent years in the development of robust and efficient computational techniques for large-scale computations typical of biomechanical problems. Note that various types of biological soft tissues show a very high resistance to volumetric changes compared with that to isochoric changes [Humphrey 2002]. Hence, due to the nearly incompressible or incompressible deformation behaviour of soft tissues a very careful numerical treatment is required. Efficient and stable mixed finite elements, which can be used in computational cardiovascular mechanics, have been developed by some of the project teams [Holzapfel 2000, Cervera 2003, Chiumenti 2002, 2003, Oñate et al. 2004]. These elements circumvent numerical difficulties that arise from the over stiffening of the numerical solution associated with the analysis of isochoric constitutive responses of vascular tissues. Finite element models in cardiovascular and cardiac mechanics can be seen, for example, in [Simon 1993, McColloch 1995, Gasser, Schulze-Bauer & Holzapfel 2002, Holzapfel 2003].

Soft tissues as living material are able of adapt themselves to their mechanical environment. This phenomenon, usually known as tissue remodelling, is responsible of the stiffening of blood vessels, reduction or increase of the thickness of the vessel walls and the change of the mechanical properties of this wall and with this of the long-term redistribution of the stress distribution in the tissue. This effect is significant in the case of different pathologies can be simulated using remodelling theories, both in hard and soft tissues.

Computer-based numerical flow and mass transport simulation tools, such as Computational Fluid Dynamics (CFD), can provide detailed, three-dimensional predictions of fluid flow and mass

transport in complex geometries. Commercially, general purpose CFD software has been applied to predict flow and mass transfer in various medical devices. CFD is recognized as a very useful tool to assist the diagnosis process of cardiovascular diseases and the development process of artificial organs [Bludszuweit 1995a,b, 1997, Kelly 2002, Ku 2002, Lawford 2002, Preim 2000, Luo 2003a, Soto 2003, Löhner 2003a, Hernandez 1998].

The physical aspects of transport phenomena in the macro scale are governed by fundamental principles of mass, momentum and energy conservation expressed in terms of algebraic equations, ordinary/partial differential equations or integral representations. A number of numerical techniques exist (including finite volume, finite difference and finite element methods) for solving these equations and obtaining a numerical description of the fluid flow in time and/or space domain. Applications of simulation method to complex cardiovascular problem are intimately related to the advances in computer technology fulfilling the increasing demand for speed and storage required by the numerical simulation of the flow and mass transport in the cardiovascular domain.
When combined with medical imaging techniques, CFD is capable of performing subject-specific flow simulations based on in-vivo anatomical and flow data. Several groups among the project partners have made progress towards developing an "image-based" CFD modelling tool for subject- and patient-specific arterial flow simulations [Cebral 2003, Löhner 2003a,b, Gonzalez 1998]. In addition to physiological studies aimed at giving more insight into the complex flow phenomena in the cardiovascular system, image-based CFD modelling is also being developed as an aid to the design of interventional diagnostic, measuring and treatment devices.

Modelling the mechanics of vessel and heart requires the effective coupling of computational blood flow models with structural analysis methods. The interaction between blood flow and the structural mechanical response of vessel and heart are intimately coupled. The use of advanced fluid-structure interaction (FSI) techniques is essential for the fully modelling and understanding of the coupled problems. Recent advances in FSI analysis performed by CIMNE will be taken as starting point of this work [Oñate 2001, Idelsohn 2003].

In this project we aim at providing patient-specific 3D biomechanical computer analysis models through the use of available advanced image analysis tools and non-invasive imaging and measurement techniques for anatomy reconstruction and characterization of the different soft biological tissues and boundary conditions necessary for each specific numerical simulation.

The development of computer simulation models of specific regions of the cardiovascular system will require the development and integration of methods and software for coupled fluid-structure interactions and state-of the-art constitutive models for soft tissue and for modelling the heart mechanics.

6 DECISION MODULE

The intelligent decision support concept chosen in this project will link four basic elements of decision-making: (a) medical expertise; (b) a systems approach; (c) medical image data; and (d) a decision module based on neural network tools. As such, this concept becomes very similar to the integrated model-base decision support approach [Goicoechea et al., 1982; Mittra, 1986; Loucks and daCosta, 1991; Simonovic, 1996]. Applications of the concept in predictive medicine are found in Taylor 1999. The concept envisions, technical specialists and a group of medical experts as the potential users of the DSS. In this environment, the DSS is seen as a link between the field expert and the decision-maker. Therefore, the DISHEART DSS will not only be a tool for assisting medical staff, but an instrument for communication, training, forecasting and management of clinical cardiovascular problems in a cooperative manner. The innovative aspect of this concept is that the DSS is application and problem-oriented rather than methodology oriented. In this project, advanced AI technology through neural nets will provide real time response necessary for taking decision in practical clinical situations. The neural net technology will be combined with advanced techniques of biomaterial modelling, medical image data processing and computer simulation.

Three levels of functional support will be provided within the new DISHEART DSS to different users:

- *Information support* is the first level of support provided by the DISHEART DSS. It includes plots, animations, video and reports to all potential users classified as information users.
- *Technical support* is the second level of support. It will include access to databases (archival, spatial, real-time, etc.) and modelling tools to all medical users responsible for treating cardiovascular diseases.
- *Application support* is the third level provided by the DISHEART DSS mostly to final decision-makers (typically medical staff) at different levels. Application users will be able with the assistance of the DISHEART DSS to focus on a practical problem for initial implementation, test and fine-tune various aspects of clinical diagnosis and surgical intervention in the solution of cardiovascular problems. Also the impacts of different measures, decisions and procedures can be tested and analyzed in prototype clinical problems before moving on to full medical implementation.

There are several innovative aspects underlying the use of the new DISHEART DSS resulting from this project. Among these we will focous our efforts in the following problems:

- Study the mechanical factors that may be important in triggering the rupture of aneurysms;
- Determine mechanical risk factors for plaque rupture and stability.

Two specific decision support modules will be created in order to assist the clinicians in this two practice problems.

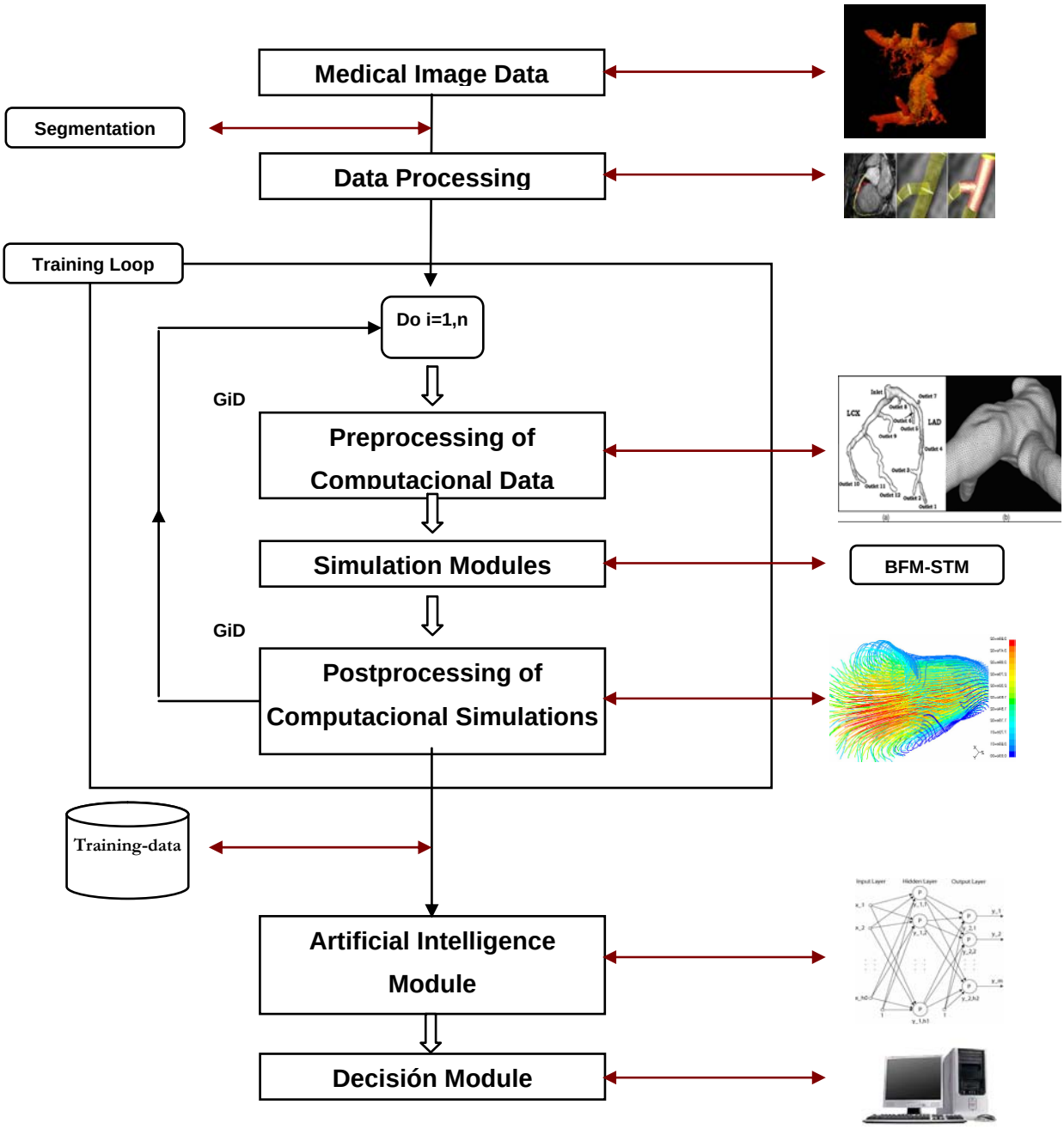

Figure 1: Acquisition data process. Different slices stored in DICOM format.

7 DESIGN OR VALIDATION MODULE

Cardiovascular devices interact with the cardiac or vascular tissue and, in consequence, optimal device design requires deep understanding and appropriate testing of this interaction. To illustrate the complexity of the problem, one may consider the design of an optimal vascular access graft for haemodialysis. These grafts, usually fail due to neo-intimal growth at the anastomosis, where a significant compliance mismatch and strongly perturbed flows exists. The complex anastomosis geometry, nonlinear material properties and blood flow phenomena are important considerations for optimal graft design. Similar conclusions can be drawn for all other cardiovascular implants, where precise biomechanical modelling is needed in the design process.

Currently, there are many experimental approaches to developing test methods for devices and materials involving performance requirements such as strength, durability, abrasion resistance, puncture resistance, etc. EndoArt uses some of these methods in everyday practice. However, it would be desirable to have computational models of devices and organs to simulate the interaction between them under specific conditions (geometries, material properties, flow, etc.). These models will facilitate non-invasive analysis of the performance of a given device and therefore, to help in optimizing the design. Again, this would mean a substantial saving in R&D efforts by yielding CAD techniques for subject-specific devices.

A major benefit of the DISHEART system will be the ability to evaluate designs at early stage quickly, before committing the expense of prototype manufacture and testing. When applied with sound engineering judgement, the new DSS will therefore reduce the costs, timescales and risks associated to the development of a new design.

The availability of the DISHEART system will help to predict biological responses and complications of a device, such as undesirable haemolysis rates and thrombosis. The need for an extensive in-vitro testing using blood circuits or animal testing will thus be drastically reduced.

DISHEART system will also help to quickly investigate the effects of device design changes on blood flow, to reduce the risk of unexpected knock-on effects which otherwise would only become apparent at a later stage. When a final device design has been reached, computational analysis will be used to confirm that the design goals have been achieved. The detailed picture of the flow field will be used to support and explain experimental results, and to predict the device performance, strengthening regulatory submissions and providing a scientific base for clinical use.

The DISHEART system will be applicable and valuable in the development of any blood medical device with demanding performance and reliability requirements, including bioprosthetic and flexible synthetic heart valves, blood pumps, stents, grafts, blood access and purification devices and others. Used at appropriate stages of the design cycle, the DISHEART system will offer a detailed understanding of vessel and heart mechanics, thus complementing the clinical, technical and experimental experience of the design team.

Innovative industrial applications of the DISHEART system for the enhanced design or validation of the medical devices will include:

- Analysis of the stent deployment procedure in-vivo. There is data available from the BloodSim project, to look at the effect of stent deployment upon a patient and compare the results of simulations with the experimental data;
- Optimize the design of arterial prostheses such as stents;
- Validation of the Flowatch Endoart's implant.

There are several innovative aspects underlying the use of the new DISHEART system resulting from this project. Among these we will focous our efforts in the following problems:

- Determine optimal interventional protocols with respect to certain target quantities for grafting interventions (improved outcome, increased safety);
- Determine optimal interventional protocols with respect to certain target quantities for ballon interventions (improved outcome, increased safety);

8 MEDICAL IMAGE DATA ACQUISITION AND PROCESSING

Within the duration of the DISHEART project will be developed an image tool, which will permit the clinician to accede to different kind of diagnostic images and to analyse and process this images, aiding him/her in his/her decision.

The image-based diagnosis is acquiring more importance in the everyday clinical activity, since its beginnings three decades ago, due to the commercialisation of new equipments (computerized tomography, magnetic resonance). The great volumes of information that these news equipments generate have produced the need to create a tool to efficiently administrate images and its associated data. This tool will facilitate the clinicians' work in favour of the patient.

A more detailed explanation of the medical image data acquisition and processing will be done in the deliverable D2.2.

8.1 Data acquisition

The medical images will be obtained by Computed Tomography (CT), sometimes called CAT scan, uses special x-ray equipment to obtain image data from different angles around the body, and then uses computer processing of the information to show a cross-section of body tissues and organs. A CT scanner is more detailed than a x-ray regular equipment, and it also reduces the risk of radiation exposure.

The Clinic Creu Blanca has various centres in Barcelona and Zaragoza for image-based diagnosis and possesses various multi-detector CT scanner with 32 and 64 detectors Toshiba Aquilion System. Clinicians from the Sant Pau Hospital will support the project in the interpretation of medical images obtained from these CT scanners. The medical images acquired by this way will be stored in the DICOM standard (Digital Imaging Communication in Medicine).

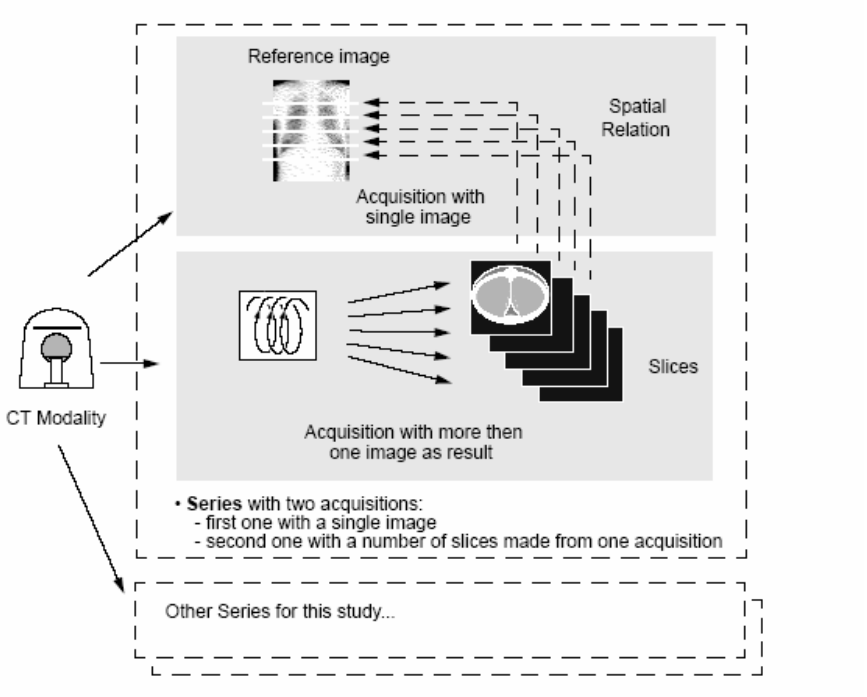

Figure 2: Example of mapping CT Series:.

CT imaging is particularly useful because it can show different types of tissue—lung, bone, soft tissue and blood vessels—with great clarity. A CT examination often requires the use of different contrast materials to enhance the visibility of certain tissues or blood vessels. The contrast material may be injected through an IV directly into the blood stream, swallowed or administered by enema, depending on the type of study to be performed.

8.2 Image segmentation

The segmentation is the process of dividing an image in regions with similar properties. There are many segmentation techniques due to its complexity. The acquisition of the image is a non-linear, noisy and discrete process, which acts on heterogeneous tissues.

The first segmentation process that will be implemented during the project is based on the grey level intensity. The image voxels that have Hounsfield units in the selected rang of interest will be selected.

TABLE I
HOUNSFIELD'Scale

Substance o material	TC Number
Cortical Bone	1000
	800
	600
	400
	200
Congealed Blood	56-76
Grey matter	36-46
White matter	22-32
Blood	12
Water	0
Fat	-100
	-200

	-400
	-600
	-800
Air	-1000

Figure 3: Hounsfield's scale

Other segmentation methods exist (as contours detection, seed expansion, snakes, etc), that will be implemented if is needed in any point during the development of the project.

8.3 Draw Regions of Interest (ROI).

The region of interest (ROI) is the zone where the pathology studied is localized. The well delimitation of this ROI will facilitate the posterior work of clinicians and engineers in order to carry out a specific simulation.

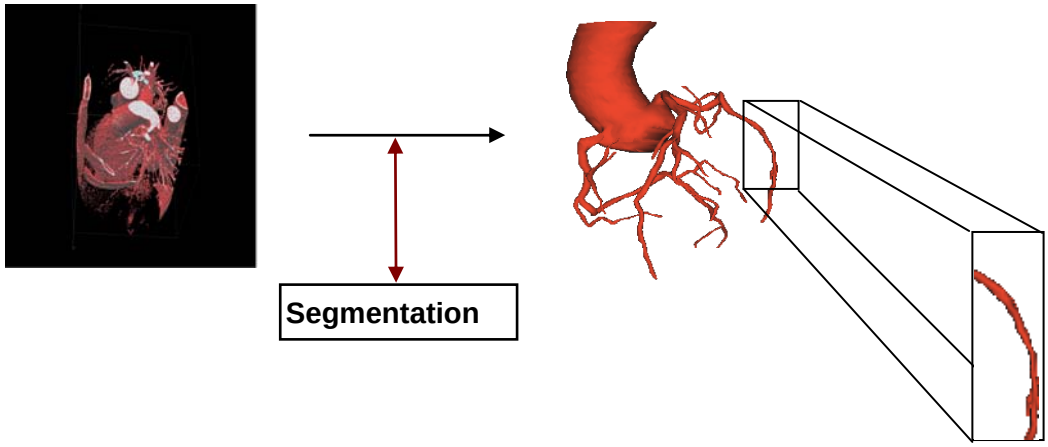

Figure 4: ROI

9 SIMULATION MODULES

In this section we will address the problem of developing models for the numerical simulation of the human circulatory system. In particular, we will focus our attention on the problem of haemodynamics in large human arteries.

Indeed, the mathematical investigation of blood flow in the human circulatory system and it interaction with the vessel is certainly one of the major challenges of the next years. The social and economical relevance of these studies is highlighted by the unfortunate fact that cardiovascular diseases represent the major cause of death in developed countries.

Altered flow conditions, such as: separation, flow reversal, low and oscillatory shear stress areas, are now recognised by the medical research community as important factors in the development of arterial diseases. An understanding of the local haemodynamics can then have useful applications for the medical research and, in a longer-term perspective, to surgical planning and therapy.

Since blood flow interacts mechanically with the vessel walls, it gives rise to a rather complex fluid-structure interaction problem, which requires algorithms able to correctly describe the energy transfer between the fluid (typically modelled by the Navier-Stokes equations) and the structure (the vessel).

The principal quantities, which describe blood flow, are the velocity and pressure. Knowing these fields allows the computation of the stresses to which an arterial wall is subjected due to the blood movement. Since we will treat fluid-structure interaction problems, the displacement of the vessel wall due to the action of the flow field is another quantity of relevance. Pressure, velocity and vessel wall displacement will be functions of time and the spatial position.

9.1 Blood flow simulation module

Computational modelling of blood flow requires solving, in the general case, three dimensional, transient flow equations in deforming blood vessels. The appropriate framework for problems of this type is the arbitrary Lagrangian-Eulerian (ALE) description of continuous media in which the fluid and solid domains are allowed to move to follow the distensible vessel and deforming fluid domain

Blood flow is obviously pulsatile. This means that one cannot neglect the time by considering a steady state solution, function only of the spatial position, as it is often done in many other situations. With some approximation one may think the blood to be a periodic in time. Yet, this is usually true only for relatively short periods, since the various human activities require changing the amount of blood sent to the various organs.

9.1.1 Mathematical modelling of blood flow

The complexity of the cardiovascular system features a tremendous variety of districts like large arteries, vases of medium calibre as well as capillaries. Their size ranges from few centimetres in

diameter down to few micrometers. Except for the very tiny capillaries, the blood flow can be assumed to behave as a continuum (see e.g. [Cokelet, 1987], [Sedeghipour et al., 1995]), as well as incompressible, apart from severe pathological situations. As such, its velocity and pressure fields, related by the momentum and mass conservation laws, which we are going to illustrate, can describe its macroscopic behaviour.

We adopt the following notation: Ω is a three-dimensional region denoting the portion of the district on which we focus our attention, and $\mathbf{x}=(x_1, x_2, x_3)$ is an arbitrary point of Ω; $\mathbf{v}=\mathbf{v}(\mathbf{x}, t)$ denotes the blood velocity. For $\mathbf{x}\in\Omega$ and $t>0$, the conservation of momentum and mass is described by the following equations:

$$\begin{cases} \rho\dfrac{D\mathbf{v}}{Dt} - \nabla\cdot\mathbf{T} = \rho\mathbf{f} & \mathbf{x}\in\Omega,\ t>0 \\ \nabla\cdot\mathbf{v} = 0 & \mathbf{x}\in\Omega\ ,\ t> 0 \end{cases}; \qquad (1.3.1.1)$$

where ρ is the density of the fluid and $\mathbf{f}=\mathbf{f}(\mathbf{x},t)$ is a possible volume force term which is prescribed for all $\mathbf{x}\in\Omega$ and $t>0$. Actually, the blood density ρ depends on the red-cell concentration c. However, in physiological conditions, the value of ρ is almost constant (for the sake of simplicity, ρ will be considered constant).

In this section, we investigate the specific features and the limits of system (1.3.1.1) as a mathematical model of blood. First of all, we consider the features of the blood as a fluid. Particularly, we consider the functional dependence of $\mathbf{T}$ and $\mathbf{v}$ and the blood pressure $P=P(\mathbf{x},t)$, which is the field of blood rheology.
Then, we analyse some relevant properties of blood flow in specific districts such as arteries. A peculiar feature is the flow unsteadiness, or, more precisely, the pulsatility induced by the periodic contractive and relaxing motion of the heart. Another feature is the absence of turbulence in almost every vascular district. These issues will be discussed in Sect. 1.3.1.1.2.

In view of the numerical solution of equations (1.3.1.1) in a specific vascular district, a suitable set of conditions has to be prescribed at the initial time t_0 and at the domain boundary Γ.
This issue is far from being trivial, especially as far as the boundary conditions are concerned, since the assigned data have to be mathematically correct, and, on the other hand, they have to correspond to quantities actually measurable. We will face this problem in Sect. 1.3.1.1.3.

9.1.1.1 Blood rheology

In order to provide a brief acquaintance with the complex field of blood rheology, let us recall some basic notions from fluid mechanics. We denote by the $\mathbf{T}$ the stress tensor of the fluid and by d the strain rate tensor, defined as follows:

$$\mathbf{d} = \frac{1}{2}(\nabla\mathbf{v} + \nabla\mathbf{v}^T),$$

which is obviously symmetric. Assessing the dependence law of $\mathbf{T}$ from $\mathbf{d}$ is the field of rheology. This relation is called the constitutive law and, in many cases, it can be expressed by an equation in the following form:

$$\mathbf{T} = -P\mathbf{I} + \mathbf{S}, \qquad (1.3.1.2)$$

where **I** is the Kronecker tensor (identified by an identity matrix). In this case, tensor P**I** is called the isotropic tensor (P is the pressure of the fluid), while **S** is the so-called extra-stress tensor.

If S is a linear function of the rate-of-strain tensor, i.e.:

$$\mathbf{S} = 2\mu\mathbf{d} = \mu(\nabla\mathbf{v} + \nabla\mathbf{v}^T), \tag{1.3.1.3}$$

the fluid is called Newtonian. The constant μ represents the (dynamic) viscosity of the fluid. The Newtonian law (1.3.1.3) is the simplest one that can be encountered in the study of viscous flows. Other relations between the stress tensor and the rate-of-strain tensor are actually observed in the experiments, identified under the general definition of non-Newtonian fluids. Strictly speaking, blood is not Newtonian, due to its complex nature.

The rheological properties of blood, however, may depend dramatically on the vessel size. For instance, when the vessel diameter reduces to a size comparable with one of the red cells (bellow 12μm), blood could no longer be considered a continuum. However, as the vascular bed size decreases below 500μm, a further reduction of apparent viscosity is observed (Fahraeus-Lindqvist effect) due to the physiological decreasing of red-cell concentration in capillaries.
In the framework of large and medium vessels, it is generally agreed that, under physiological conditions, the Newtonian model for blood rheology can be considered acceptable at a first level of approximation (see [Nichols et al., 1990], [Perktold et al., 1991], [Xu et al., 1992]). For this reason, in the sequel, we will consider blood as a Newtonian fluid, even if we are aware that a more precise accounting of the rheological properties of blood could bring a meaningful improvement to the investigation of specific clinical cases.

9.1.1.2 Features of blood flow in arteries

The motion of blood in arteries is induced by the periodic contraction of the heart muscles that pump the fluid down to the arterial system from the aorta to the capillaries. More precisely, a heartbeat consists of two phases. During the first one, called systole, the left ventricular pressure becomes higher than the aortic one, due to an isovolumetric contraction of the muscular fibres. The aortic valve opens and the blood is pumped into the aorta. In physiological cases, this phase occupies about one third of the whole beat. During the second phase, called diastole, the aortic pressure balances the ventricular pressure, the valve closes, the ventricular pressure falls quickly, while the aortic pressure decreases slowly and the blood flows to the peripheral sites.

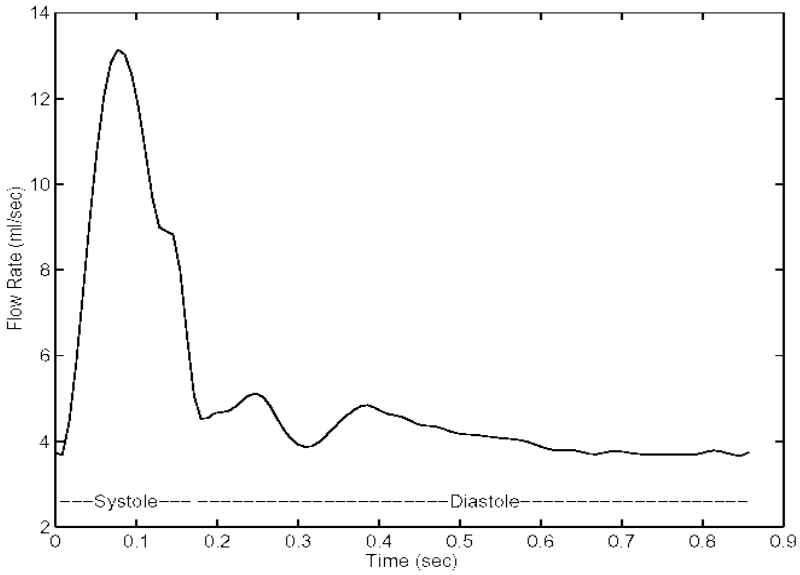

Figure 5: Waveforms of the flow rate at the entrance of the carotid (see [Perktold, 1991])

Therefore, one of the most evident features of blood flow in arteries is the periodic unsteadiness or, more precisely, the pulsatility [Nichols, 1990]. This term refers properly to the feature of a first rapid increase and decrease of the flow rate, followed by a longer phase, when the flow rate becomes small and almost constant. Figure 7 for instance illustrate the flow rate during a heartbeat at the entrance of the carotid bifurcation.

The periodic pulsatility influences in a decisive way the actual velocity profiles of blood in the arteries. A way to confirm this fact is to compare the different velocity profiles whenever steady and unsteady periodic conditions are applied to some district. Indeed, when the morphology of the fluid domain is simple, analytical solutions of equations (1.3.1.1) are available either for the steady and unsteady flows. More precisely, let us consider equations (1.3.1.1) for a Newtonian fluid. In this case, they read:

$$\begin{cases} \dfrac{\partial \mathbf{v}}{\partial t} + (\mathbf{v}\cdot\nabla)\mathbf{v} - \nu\Delta\mathbf{v} + \nabla p = \mathbf{f} \\ \nabla\cdot\mathbf{v} = 0 \end{cases}; \qquad (1.3.1.4)$$

for $\mathbf{x}\in\Omega$ and $t>0$. In (1.3.1.4), we set $p=P/\rho$ and $\nu=\mu/\rho$ (the so called kinematic viscosity). In the sequel, with a little abuse of language, p will be simply called pressure. Suppose, moreover, that Ω is an infinite cylindrical pipe, and denote by u, v, and w respectively the longitudinal, the radial and the circumferential components of the velocity. Z is the longitudinal coordinate, r the radial and θ the circumferential one. The walls of the pipe are supposed to be rigid and the velocity zero on them (non-slip conditions, see Sect. 1.3.1.1.3).

Let us consider two cases:

a) Hagen-Poiseuille flow: if the gradient of pressure in (1.3.1.4) is a vector with radial and circumferential components zero and the longitudinal one constant and equal to –C, see bellow:

$$\frac{\partial p}{\partial z} = -C, \frac{\partial \mathrm{p}}{\partial \mathrm{r}} = 0, \frac{\partial \mathrm{p}}{\partial \theta} = 0,$$

then the velocity profile is given by (see e.g. [White, 1986]):

$$u = \frac{C}{4\nu}(r_0^2 - r^2), \mathrm{v} = 0, \mathrm{w} = 0. \tag{1.3.1.5}$$

b) Womersley flow: in the case of a longitudinal pressure gradient changing periodically in time according to the law:

$$\frac{\partial p}{\partial z} = A\cos(\omega t), \frac{\partial \mathrm{p}}{\partial \mathrm{r}} = 0, \frac{\partial \mathrm{p}}{\partial \theta} = 0, \tag{1.3.1.6}$$

then the velocity profile is [Womersley, 1955]:

$$u = \Re\left(\frac{A}{i\omega}\left\{1 - \frac{J_0\left(i^{\frac{3}{2}}\sqrt{\frac{\omega}{\nu}}r\right)}{J_0\left(i^{\frac{3}{2}}\sqrt{\frac{\omega}{\nu}}r_0\right)}\right\}e^{i\omega t}\right), \mathrm{v} = 0, \mathrm{w} = 0. \tag{1.3.1.7}$$

In (1.3.1.7), J_0 denotes the Bessel function of order 0 with complex argument, i is the imaginary unit, $\Re(\cdot)$ is the real part. In this framework, the Womersley parameter α:

$$\alpha = r_0\sqrt{\frac{\omega}{\nu}}\ , \tag{1.3.1.8}$$

summarizes the information about the periodic regime of the fluid and its viscosity. Obviously, it changes in the arterial system on the basis of the vessel dimension. In men (about 70 heart beats per minute), α is equal to 20 in the aorta, 5 in the femoral artery, and decreases quickly in the capillaries. Figure 7: Main layers of a elastic artery and a vein

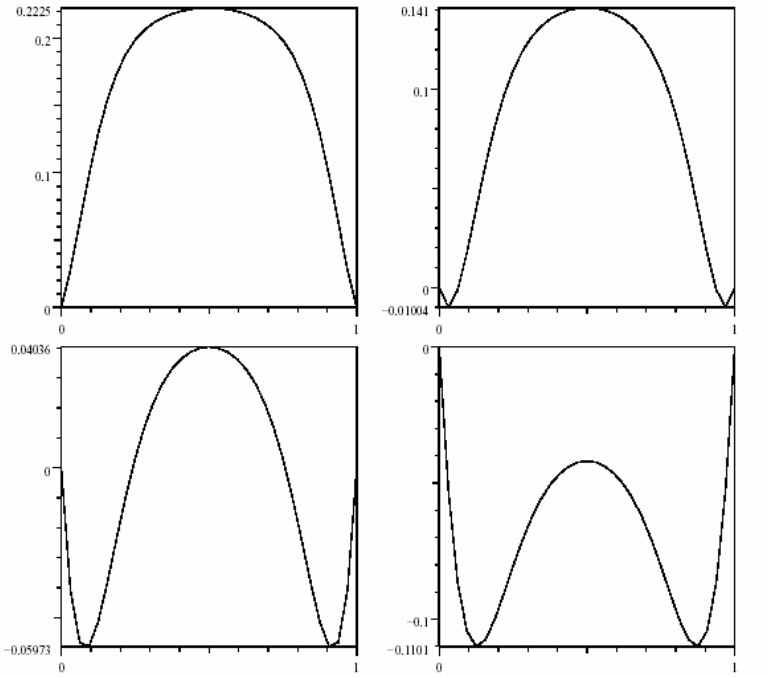

Figure 6: Velocity 2D profiles of Womersley unsteady flow at different instants. Along the x-axis the transversal (in 3D radial) coordinate is shown, on the y-axis the velocity

The Womersley flow can be considered the unsteady counterpart of the Poiseuille solution; it is indeed a fully developed unsteady flow in the case of a cylindrical right pipe. The time-dependence of the gradient pressure, for blood flow, is not expressed by a simple sinusoidal law (see Figure 5). Nonetheless, the Womersley solution may still be useful: indeed, since in the Womersley solution (as well as in the Poiseuille solution), the non-linear term of equation (1.3.1.4) actually vanishes, the problem at hand is linear. Therefore, it is possible to extract the different frequency components of the flow-rate waveform on the inflow boundary and correspondingly sum up the contribution at each frequency of the Womersley profiles associated (see [Hughes, 1998], [Taylor, 1996], [Taylor, Hughes et al., 1996]).

Another feature of blood flow in arteries is the presence in some specific districts and in some instants of the beat of turbulence phenomena, i.e. of irregular eddying motion, in which random, even chaotic, perturbations in time and space of the velocity and pressure fields occur about their mean values; the components of perturbation extend over a continuous hierarchy of scales or frequencies so that they must be characterized by statistical means (see [Nichols, 1990]). In particular, the experimental evidence, at least in the human system, shows the presence of disturbances in the ascending aorta (in the immediate neighbourhood of the aortic valve) and in the pulmonary artery: the phenomena are limited in the final part of the systolic phase, after the systolic peak (see [Nichols, 1990]). For a discussion about the reasons for and the consequences of these phenomena, see for instance [Pedley, 1980]. However, apart from the exceptions pointed out, blood flow can be assumed to be laminar. Indeed, in physiological conditions, the values of speed involved are low enough (see [Nichols, 1990]). Moreover, generally, the periodicity of the flow, accompanied by the shortness of vascular districts, does not give rise to fully developed turbulence. The disturbances, whenever present, are typically very spotty and localized, both in time and space and they do not have statistical properties that are featured by turbulent flows.

On the basis of the arguments developed so far, we will hereafter assume equations (1.3.1.4) for an incompressible Newtonian laminar fluid as an acceptable model to describe the blood flow in a specific arterial district.

9.1.1.3 Boundary treatment

In order to compute (analytically or numerically) the velocity and pressure fields of blood in a district Ω, equations (1.3.1.4) must be provided with initial conditions $\mathbf{v}=\mathbf{v}_0$ at time t_0 and suitable boundary conditions. The initial condition must essentially specify the velocity field at a given (arbitrary) starting time t_0; in the sequel, such an initial velocity field will be denoted by $\mathbf{v}_0$. For the later, on the one hand the prescribed data should correspond to physical data, which are actually measurable in practice. On the other hand, typical measures for boundary data do not provide enough information to make the associated mathematical problems well posed. Therefore, it is necessary to assess a specific treatment to supply the unavailable data with the further boundary conditions needed to obtain well posedness.

Three parts can essentially be distinguished on the boundary $\Gamma$of Ω. The first one, Γ_w, is the wall of the vessel. If it is supposed to be rigid, we impose homogeneous Dirichlet boundary conditions, $\mathbf{v}=\mathbf{0}$ for all $\mathbf{x}\in\Gamma_w$. Otherwise, when the compliance of the vascular tissue is accounted for, we will prescribe the continuity of the velocity field (see Sect. 1.3.3). In this section, we consider a rigid-wall problem.

Then, we identify two parts of Γ, Γ_{up} and Γ_{dw}, which can be composed of one or more simply connected sections. We will denote by Γ_{up} the upstream or proximal boundary. Then:

$$\int_0^T \int_{\Gamma_{up}} \mathbf{v} \cdot \mathbf{n} \, d\omega \, dt < 0 , \tag{1.3.1.9}$$

where T is the heartbeat duration and **n** the normal outward unit vector. Generally speaking, due to the presence of recirculation zones, it is not possible to suppose that $\mathbf{v} \cdot \mathbf{n}<0$, across a whole upstream section and for all $t \in (0,T]$. Similarly, the downstream or distal section is the one that satisfies the relation:

$$\int_0^T \int_{\Gamma_{dw}} \mathbf{v} \cdot \mathbf{n} \, d\omega \, dt > 0 , \tag{1.3.1.10}$$

Again, since in principle it is not true that $\mathbf{v} \cdot \mathbf{n}>0$, for all $\mathbf{x} \in \Gamma_{dw}$ and for all $t \in (0,T]$, strictly speaking Γ_{dw} is not an outflow boundary. Remark that both Γ_{up} and Γ_{dw} do not correspond to real boundaries, as they are introduced with the purpose of bounding the district at hand. Boundary conditions that are mathematically admissible for artificial sections have been extensively investigated. A choice often adopted in numerical computations consists of using the following set of equations:

$$\begin{cases} \mathbf{v} = \mathbf{g} \text{ on } \Gamma_{up} \\ -p\mathbf{n} + \nu \nabla \mathbf{v} \cdot \mathbf{n} = d\mathbf{n} \text{ on } \Gamma_{dw} \end{cases} \tag{1.3.1.11}$$

for all $t>0$, where g is an assigned velocity profile. The downstream condition in (1.3.1.11) results from prescribing the normal component of the stress tensor $\mathbf{T} \cdot \mathbf{n}$ (Neumann condition).

Conditions (1.3.1.11) provide a mathematically complete set of boundary data, in the sense that, prescribing three scalar conditions in a 3D problem (or two conditions in a 2D problem) at every point of the boundary, the associated differential problem can be well posed. It is possible to prove (see [Heywood, 1996], [Veneziani, 1998]) that the solution of the problem (1.3.1.1) with the boundary conditions (1.3.1.11) and the initial condition $\mathbf{v}=\mathbf{v}_0$ for $t=0$ (in two or three dimensions) exists for all $t \geq 0$ provided by a force term **f** and a boundary datum **g** that are smooth enough and with $\nabla \mathbf{v}_0$ sufficiently small with respect to ν. Moreover, if these quantities are sufficiently small, the solution is unique. Actually, the smallness of data is not a mandatory restriction for a 2D problem, provided that the downstream sections correspond exactly to the pointwise outflow sections ($\mathbf{v} \cdot \mathbf{n}>0$ on every point of the downstream sections). Unfortunately, as we have already pointed out, the presence of reversal zones in the vascular system makes this hypothesis seldom applicable in hemodynamics. Moreover, from the practical point of view, the prescription of pointwisse conditions can be troublesome. Indeed, measures of the velocity field on the whole upstream section are seldom available. For this reason, different strategies have been adopted.

A possibility consists of approximating the unavailable velocity inlet field g with a Poiseuille profile (1.3.1.5) in steady problems or a Womersley profile (1.3.1.7) in unsteady cases, assuming that the upstream vascular morphology could be approximately considered as being cylindrical (see [Hughes et al., 1998], [Perktold et al., 1991], [Taylor et al., 1996]). This is a reasonable approximation in order to fill in the gaps in information at the inlet, even if the complex vascular morphology seldom exhibits a cylindrical geometry, which allows for a fully developed flow (as Poiseuille and Womersley profiles are).

As far as the downstream conditions are concerned, a value of d can be assigned on the basis of previous considerations about the flow structure, as for the Dirichlet conditions (typically $d=0$). In any case, failing to fix the right value for a Neumann condition is by far less critical than for Dirichlet's. In principle, other boundary conditions than (1.3.1.11) can be considered if measurements are available. In this respect, on the upstream/downstream sections, it is possible,

for instance, to measure the blood flux; this means that on every section we prescribe the condition:

$$\int_{\Gamma_i} v \cdot n \, d\gamma = F_i(t) \;\; i = 1,...n \tag{1.3.1.12}$$

where n denotes the number of upstream/downstream sections. Indeed, different techniques can be set up in order to measure $F_i(t)$. Among others, one of the most common is based on the measurements at different sites of the concentration of a tracer material injected into the vasculature. If the injected concentration is known, it is possible to deduce the flow rate from the concentration measured downstream. Other methods are based on Ultrasound Techniques (whose performance can be in turn supported by numerical computations – see [Pennati et al., 1998]).

9.2 Blood vessels simulation module

Biological soft tissues sustain large deformations, rotations and displacements, have a highly non-linear behaviour and anisotropic mechanical properties and show a clear time and strain-rate dependency. Their typical anisotropic behaviour is caused by several collagen fiber families (usually one or two fibers coincide at each point) that are arranged in a matrix of soft material named ground substance [Holzapfel, 2000]. Typical examples of fibered soft biological tissues are blood vessels, tendons, ligaments, cornea and cartilage. The time-rate dependent material behaviour of this kind of tissues has been well documented and quantified in the literature. This includes works on ligaments [Puso, 1998], tendons [Johnson, 1996], blood vessels (Humphrey, 1995), cornea and articular cartilage. This behaviour can arise from the fluid flow inside the tissue, from the inherent viscoelasticity of the solid phase, or from viscous interactions between the tissue phases.

9.2.1 Structure of arterial vessels

Arteries are frequently subdivided in two types: elastic and muscular. Elastic arteries have larger diameters and are located close to the heart (i.e., aorta and iliac arteries), while muscular arteries are found at the periphery of the body (i.e., femoral artery). However, there are arteries that show a morphologic structure of both types. Focusing now in their microscopic structure, arterial walls are composed from in to out in three layers: the intima (tunica intima), the media (tunica media), and the adventitia (tunica externa) as shown in Figure 7: Main layers of a elastic artery and a vein

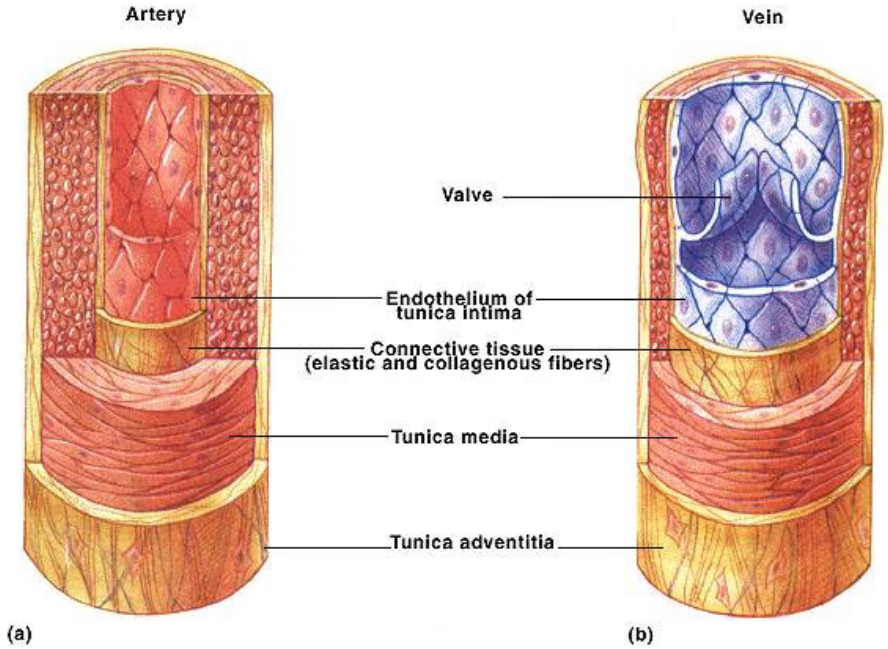

Figure 7: Main layers of a elastic artery and a vein

The intima is the innermost layer of the artery. It is composed of a single layer of endothelial cells lining the arterial wall. There is also a subendothelial layer which thickness varies according to the blood vessel, age and disease (for young and healthy muscular arteries the subendothelial layer is almost inexistent). The contribution of this layer to the mechanical properties of young and healthy arteries is neglectable due to its small thickness.

The intermediate layer in arteries is the media, separated form the intima and the adventitia by the so called inner and outer elastic laminae respectively. This layer consists of a complex three dimensional network of smooth muscle cells, collagen fibres and elastin. Smooth muscle cells appear to play an important role in the atherosclerosis, trapping lipids which are later deposited in the subendothelial layer resulting in a artherosclerotic plaque. On the other hand, the orientation and close interconnection between elastin and collagen fibres, elastic laminae and smooth muscle cells lead to a continuous fibrous helix running almost circumferential. This structural arrangement gives the media a great load bearing capacity in both longitudinal and circumferential directions. From a mechanical point of view, the media is the most important layer in healthy arteries.

The adventitia is the outermost layer of the artery and consists mainly of thick bundles of collagen fibres. The thickness of this layer strongly depends of the type of artery, its physiological function, and location within the vascular system. This layer is surrounded of loose connective tissue which deliver nutrients to the artery. Within this layer, collagen fibres are wavy and arranged in helical structures. They offer little stiffness to the artery for low pressures as compared with the media, however, this layer gives stability and strength to the artery at high pressures or when the media has been damaged by the atherosclerotic process.

The arterial system is the higher-pressure portion of the blood system. Since the heart output is pulsatile, arterial pressure varies between systolic, the peak pressure during heart contraction, and diastolic, the minimum pressure between heart contractions, values with each heart cycle. This pressure and blood volume variation within the artery produces the pulse which is palpable in any artery, reflecting the heart action.

The systemic arterial pressures, e.g 120/80 mmHg, are generated by the forceful contractions of the heart's left ventricle. Similarly, the pulmonary arterial pressures, e.g 25/6 mmHg, are generated by the contractions of the heart's right ventricle.

Healthy resting arterial pressures, compared to many man-engineered system are relatively low, mean systemic pressures typically being under 100 mmHg, about 1.8 lbf/in^2, above surrounding atmospheric pressure (about 760 mmHg or 14.7 lbf/in^2 at sea level).

9.2.2 Structure of the Heart

In the human body, the heart is normally situated slightly to the left of the middle of the thorax, underneath the sternum (breastbone). It is enclosed by a sac known as the pericardium and is surrounded by the lungs. In adults, it weighs about 300-350 g. It consists of four chambers, the two upper atria (singular: atrium) and the two lower ventricles.

A thick muscular wall, the septum, divides the right atrium and ventricle from the left atrium and ventricle, preventing blood from passing between them. Valves between the atria and ventricles (atrioventricular valves) maintain coordinated unidirectional flow of blood from the atria to the ventricles.

The left ventricle pumps blood throughout the body's arteries and veins; the right ventricle pumps blood to the lungs. Compared with the walls of the atria, the ventricle walls are thicker.
Oxygen-depleted or deoxygenated blood from the body enters the right atrium through two great veins, the superior vena cava, which drains the upper part of the body, and the inferior vena cava that drains the lower part. The blood then passes through the tricuspid valve to the right ventricle. The right ventricle pumps the deoxygenated blood to the lungs, through the pulmonary artery. In the lungs gaseous exchange takes places and the blood releases carbon dioxide into the lung cavity and picks up oxygen. The oxygenated blood then flows through pulmonary veins to the left atrium. From the left atrium this newly oxygenated blood passes through the mitral valve to enter the left ventricle. The left ventricle then pumps the blood through the aorta to the entire body except the lungs.
The left ventricle is much more muscular than the right as it has to pump blood around the entire body, which involves exerting a considerable force to overcome the vascular pressure. As the right ventricle needs to pump blood only to the lungs, it requires less muscle.
Even though the ventricles lie below the atria, the two vessels through which the blood exits the heart (the pulmonary artery and the aorta) leave the heart at its top side.

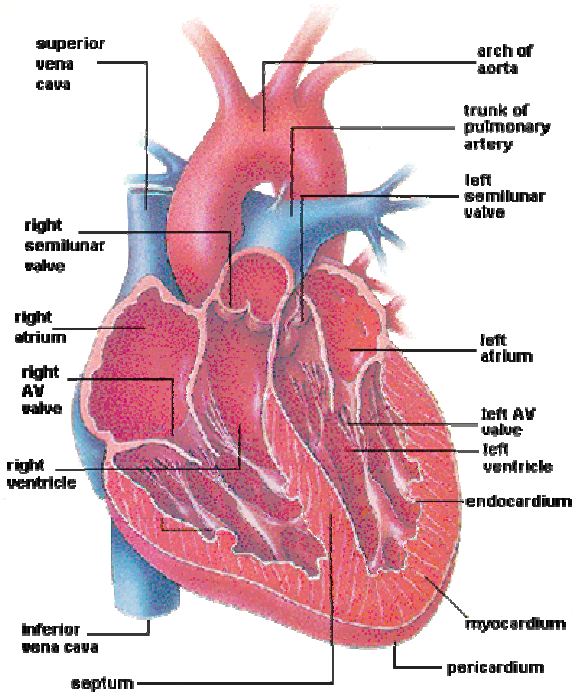

Figure 8: Structure of the heart

The contractile nature of the heart is due to the presence of cardiac muscle in its wall which can work continuously without fatigue. The heart wall is made of three distinct layers. The first is the outer epicardium, which is composed of a layer of flattened epithelial cells and connective tissue. Beneath this is a much thicker myocardium made up of cardiac muscle. The endocardium is a further layer of flattened epithelial cells and connective tissue, which lines the chambers of the heart.
The blood supply to the heart itself is supplied by the left and right coronary arteries, which branch off from the aorta

1.1.1 Finite Elasticity for heart and blood vessel

The blood supply to the heart itself is supplied by the left and right coronary arteries, which branch off from the aorta
As a first step towards the development of a nonlinear anisotropic hyper elastic model, we consider the formulation of finite strain hyper elasticity in terms of invariants with uncoupled volumetric-deviatoric responses, first suggested in [Flory, 1961] and [Spencer, 1954], generalized in [Simo y Taylor, 1991] and employed for anisotropic soft biological tissues in [Weiss, 1996] and [Holzapfel, 2000].

Let $\boldsymbol{x} = (\boldsymbol{X}, t) : \Omega_0 \times \Re \to \Re^3$ denote the motion mapping and let $\boldsymbol{F}$ be the associated deformation gradient. Here X and x define the respective positions of a particle in the reference Ω_0 and current Ω configurations such as $\boldsymbol{F} = \frac{d\boldsymbol{x}}{d\boldsymbol{X}}$. Further, let $\boldsymbol{J}$= *det* $\boldsymbol{F}$ be the Jacobean of the motion. To properly define volumetric and deviatoric responses in the nonlinear range, we introduce the following cinematic decomposition:

$$\boldsymbol{F} = J^{\frac{1}{3}}\boldsymbol{F}, \qquad \overline{\boldsymbol{F}} = J^{-\frac{1}{3}}\boldsymbol{F}$$

$$\boldsymbol{C} = \boldsymbol{F}^T\boldsymbol{F}, \qquad \overline{\boldsymbol{C}} = J^{-\frac{2}{3}}\boldsymbol{C}$$

The term $\mathrm{J}^{\frac{1}{3}}\boldsymbol{I}$ is associated with volume-changing deformations, while $\overline{\boldsymbol{F}}$ is associated with volume-preserving deformations. We shall call $\overline{\boldsymbol{F}}$ and $\overline{\boldsymbol{C}}$ the modified deformation gradient and the modified right Cauchy-Green tensors, respectively.

The direction of a fiber at a point $X \in \Omega_0$ is defined by a unit vector field $m_0(X)$, $|m_0|=1$. It is usually assumed that, under deformation, the fiber moves with the material points of the continuum body. Therefore, the stretch λ of the fiber defined as the ratio between its lengths at the deformed and reference configurations can be expressed as

$$\lambda \boldsymbol{m}(\mathbf{x},t)=\boldsymbol{F}(\mathrm{X},t)\boldsymbol{m}_0(\boldsymbol{X}) \qquad \lambda^2=\boldsymbol{m}_0.\boldsymbol{F}^T\boldsymbol{F}.\boldsymbol{m}_0=\boldsymbol{m}_0.\boldsymbol{C}.\boldsymbol{m}_0$$

where *m* is the unit vector of the fiber in the deformed configuration.

The introduced kinematics for one family of fibers may be applied to other in an analogous manner. We will denote the second preferred direction by the unit vector field $n_0(X)$.

To characterize isothermal processes, we postulate the existence of a unique decoupled representation of the strain-energy density function Ψ. Based on the cinematic assumption and following [Spencer, 1954] it can be shown that eight modified invariants are necessary to form the

integrity bases of the tensors $\overline{\boldsymbol{C}}, \boldsymbol{m}_0 \otimes \boldsymbol{m}_0, \boldsymbol{n}_0 \otimes \boldsymbol{n}_0$. Then, the free energy can be written in a decoupled form as:

$$\Psi = \Psi_{vol}(J) + \Psi_{iso}\left(\overline{\boldsymbol{C}}, \boldsymbol{m}_0 \cdot \boldsymbol{m}_0, \boldsymbol{n}_0 \cdot \boldsymbol{n}_0\right)$$
$$\Psi = \Psi_{vol}(J) + \Psi_{iso}\left(\overline{\boldsymbol{I}}_1, \overline{\boldsymbol{I}}_2, \overline{\boldsymbol{I}}_4, \overline{\boldsymbol{I}}_5, \overline{\boldsymbol{I}}_6, \overline{\boldsymbol{I}}_7, \overline{\boldsymbol{I}}_8, \overline{\boldsymbol{I}}_9\right)$$

with

$$\overline{I}_1 = \mathrm{tr}\overline{\boldsymbol{C}}, \overline{I}_2 = \frac{1}{2}((\mathrm{tr}(\overline{\boldsymbol{C}})^2 - \mathrm{tr}\overline{\boldsymbol{C}}^2)$$
$$\overline{I}_4 = \boldsymbol{m}_0 \overline{\boldsymbol{C}} \boldsymbol{m}_0, \overline{I}_5 = \boldsymbol{m}_0 \overline{\boldsymbol{C}}^2 \boldsymbol{m}_0, \overline{I}_6 = \boldsymbol{n}_0 \overline{\boldsymbol{C}} \boldsymbol{n}_0$$
$$\overline{I}_7 = \boldsymbol{n}_0 \overline{\boldsymbol{C}}^2 \boldsymbol{n}_0, \overline{I}_8 = \boldsymbol{m}_0 \overline{\boldsymbol{C}} \boldsymbol{n}_0, \overline{I}_9 = (\boldsymbol{n}_0 \boldsymbol{m}_0)^2$$

with $\overline{I}_1$ and $\overline{I}_2$ the first two strain invariants of the symmetric modified Cauchy-Green tensor and the pseudo-invariants. $\overline{I}_4 \ldots \overline{I}_9$ characterize the anisotropy constitutive response of the fibers, $\overline{I}_4$ and $\overline{I}_6$ have a clear physical meaning since they are the squares of the stretches along the two families of fibers. In order to reduce the number of material parameters and to work with physically motivated invariants, we shall omit the dependency of the free energy Ψ on $\overline{I}_5$, $\overline{I}_7$, $\overline{I}_8$ and $\overline{I}_9$. This hypothesis is usually used in biomechanical modelling.

The stress response is then obtained from the derivatives of the stored-energy function, getting

$$\boldsymbol{S} = 2\frac{\partial \psi}{\partial \boldsymbol{C}} = \boldsymbol{S}_{\mathrm{vol}} + \otimes \boldsymbol{S}_{\mathrm{iso}} = Jp\boldsymbol{C}^{-1} + J^{-2/3}(\mathbf{I} - 1/3\boldsymbol{C}^{-1} \otimes \boldsymbol{C}) : \overline{\boldsymbol{S}}$$

where p is the hydrostatic pressure and $\overline{\boldsymbol{S}}$ the modified second Piola-Kirchhoff stress tensor.

$$p = \frac{\partial \psi_{vol}(J)}{\partial J}$$
$$\overline{\boldsymbol{S}} = 2\frac{\partial \psi_{iso}\left(\overline{\boldsymbol{C}}, \boldsymbol{m}_0, \boldsymbol{n}_0\right)}{\partial \overline{\boldsymbol{C}}}$$

The Cauchy stress tensor σ is $1/J$ times the push-forward of $\boldsymbol{S}\left(\boldsymbol{\sigma} = J^{-1}\chi_*(\boldsymbol{S})\right)$, that is, $\sigma_{ij} = J^{-1}F_{iI}F_{jJ}S_{IJ}$ so, we obtain

$$\boldsymbol{\sigma} = p\mathbf{1} + \frac{2}{p}dev\left[\overline{\boldsymbol{F}}\frac{\partial \psi_{iso}\left(\overline{\boldsymbol{C}}, \boldsymbol{m}_0, \boldsymbol{n}_0\right)}{\partial \overline{\boldsymbol{C}}}\overline{\boldsymbol{F}}^T\right]$$

We conclude our development of uncoupled volumetric/deviatoric finite deformation elasticity with two families of fibers by recording the explicit expressions for the elastic tangent moduli. Consider the nonlinear second Piola-Kirchhoff stress tensor S at a certain point. Its variation with respect to the right Cauchy-Green tensor C is the *elasticity tensor* in the material description or the *referential tensor* of *elasticities* and may be written as

$$\mathbf{C} = 2\frac{\partial \mathbf{S}(\mathbf{C})}{\partial \mathbf{C}} = \mathbf{C}_{vol} + \mathbf{C}_{iso} = 2\frac{\partial \mathbf{S}_{vol}}{\partial \mathbf{C}} + 2\frac{\partial \mathbf{S}_{iso}}{\partial \mathbf{C}}$$

where $\boldsymbol{C}_{vol}$ and $\boldsymbol{C}_{iso}$ may be written as

$$\begin{aligned}\mathbf{C}_{vol} &= 2\mathbf{C}^{-1} \otimes (p\frac{\partial J}{\partial \mathbf{C}} + J\frac{\partial p}{\partial \mathbf{C}} + 2Jp\frac{\partial \mathbf{C}^{-1}}{\partial \mathbf{C}}) \\ &= J\tilde{p}\mathbf{C}^{-1} \otimes \mathbf{C}^{-1} - 2Jp\mathbf{C}^{-1} \odot \mathbf{C}^{-1}\end{aligned}$$

$$\begin{aligned}\mathbf{C}_{iso} = &-\frac{4}{3}J^{-\frac{4}{3}}(\frac{\partial \Psi_{iso}}{\partial \bar{\mathbf{C}}} \otimes \bar{\mathbf{C}}^{-1} + \bar{\mathbf{C}}^{-1} \otimes \frac{\partial \Psi_{iso}}{\partial \bar{\mathbf{C}}}) + \\ &+\frac{4}{3}J^{-\frac{4}{3}}(\frac{\partial \Psi_{iso}}{\partial \bar{\mathbf{C}}} : \bar{\mathbf{C}})(\mathbb{I}_{\boldsymbol{C}}^{-1} - \frac{1}{3}\bar{\mathbf{C}}^{-1} \otimes \bar{\mathbf{C}}^{-1}) + J^{-\frac{4}{3}}\bar{\mathbf{C}}_{\bar{w}}\end{aligned}$$

$$\begin{aligned}\bar{\mathbf{C}}_{\bar{w}} = &4\frac{\partial^2 \Psi_{iso}}{\partial \bar{\mathbf{C}} \partial \bar{\mathbf{C}}} - \frac{4}{3}[(\frac{\partial^2 \Psi_{iso}}{\partial \bar{\mathbf{C}} \partial \bar{\mathbf{C}}} : \bar{\mathbf{C}}) \otimes \bar{\mathbf{C}}^{-1} + \bar{\mathbf{C}}^{-1} \otimes (\frac{\partial^2 \Psi_{iso}}{\partial \bar{\mathbf{C}} \partial \bar{\mathbf{C}}} : \bar{\mathbf{C}})] \\ &+\frac{4}{9}(\bar{\mathbf{C}} : \frac{\partial^2 \Psi_{iso}}{\partial \bar{\mathbf{C}} \partial \bar{\mathbf{C}}} : \bar{\mathbf{C}})\bar{\mathbf{C}}^{-1} \otimes \bar{\mathbf{C}}^{-1}\end{aligned}$$

with

$$\mathbb{I}_{C^{-1}} = \frac{\partial \mathbf{C}^{-1}}{\partial \mathbf{C}} = -\mathbf{C}^{-1} \odot \mathbf{C}^{-1} = -\frac{1}{2}(C_{IK}^{-1}C_{JL}^{-1} + C_{IL}^{-1}C_{JK}^{-1})$$

For convenience, we have introduced the scalar function, defined by

$$\tilde{p} = p + J\frac{dp}{dJ}$$

The elasticity tensor in the spatial description or the spatial tensor of *elasticities*, denoted by c, is defined as the push-forward of C times a factor J^{-1}, so that

$$\mathbf{c} = J^{-1}\chi_*(\mathbf{C}) = \mathbf{c}_{vol} + \mathbf{c}_{iso}$$

9.2.4 Material Behaviour for blood vessel

Some of the energy deformation density functions for isotropic materials were proposed by Weiss, Almeida and Holzapfel

- Weiss:

$$W = \frac{K}{2}\log^2 J + c_1(\bar{I}_1 - 3) + c_2(\bar{I}_2 - 3) + c_4(\exp(\bar{I}_4 - 1) - \bar{I}_4)$$

- Weiss for ligaments:

$$\psi(\mathbf{C}) = \psi(J) + \psi_{iso}^{m}(\bar{\mathbf{C}}) + \psi_{iso}^{f}(\bar{\mathbf{C}}, \mathbf{a} \otimes \mathbf{a})$$

$$\psi_{vol} = \frac{1}{D}\ln^2 J \qquad \psi_{m}^{iso} = C_1(\bar{I}_1 - 3)$$

$$\lambda \frac{\partial \psi_\lambda}{\partial \lambda} = 0 \qquad \lambda < 1$$

$$\lambda \frac{\partial \psi_\lambda}{\partial \lambda} = C_3(\exp(C_4(\lambda - 1)) - 1) \qquad \lambda < \lambda^*$$

$$\lambda \frac{\partial \psi_\lambda}{\partial \lambda} = C_5 \cdot \lambda + C_6 \qquad \lambda > \lambda^*$$

- Almeida:

$$W = a_0 \exp(\phi - n \log I_3)$$

where:

$$\begin{aligned} \phi \quad = \quad & a_1(I_1 - 3) + a_2(I_2 - 3) + a_3(I_1 - 3)^2 + a_4(I_4 - 1) + a_5(I_4 - 1)^2 \\ & + a_6(I_1 - 3)(I_4 - 1) + a_7(I_5 - 1) \end{aligned}$$

- Holzapfel:

Several material models have been proposed for hyperelastic two family fibre reinforced materials. The one developed by Holzapfel and Gasser was specially designed for modelling the arterial walls. Its deformation energy density function is written as follows

$$W = \frac{K}{2} \log^2 J + \frac{c}{2}(\bar{I}_1 - 3) + \frac{k_1}{2k_2} \sum_{a=4,6} \left(\exp(k_2(\bar{I}_a - 1)^2 - 1 \right)$$

- Fung:

Material models including anisotropic behaviour with three preferred directions have been developed and applied in biological soft tissues modelling. One of the most commonly used is Fung's model:

$$W = b \exp\left(Q(\boldsymbol{E})\right)$$

where $Q(\boldsymbol{E}) = b_1 E_{11}^2 + b_2 E_2^2 + b_3 E_{33}^2 + b_4 E_{11} E_{22} + b_5 E_{11} E_{33} + b_6 E_{22} E_{33}$, and E_{AB} the components of the Green tensor

9.2.5 Material Behaviour for heart

In order to model the cardiac cycle, the material model must contemplate the active behaviour of the tissue ant the same time that it accounts for the anisotropy of the underlying material. The activation of the muscle fibres changes the properties of the material at the same time that contracts the muscle itself. Therefore, most models of activation consider two transformations. The first one changing the material properties without changing the geometry, and the second one, contracting

the muscle without changing the geometry. Bourdarias et al. 2003 have proposed a model for the myocardium based on the model by Lin and Yin, 1998. The strain energy function has the form

$$W(\mathbf{C},t) = W_{pas}(\mathbf{C}) + \beta(t) W_{act}^{f}(\mathbf{C}),$$

where C is the right Cauchy-Green tensor, W_{pas} represents the contribution of the surrounding collagen matrix and the passive component of the fibres, W_{act}^{f} is the active component of the embedded muscle fibres. In the definition of W_{act}^{f} is where the models of Bourdarias et al, 2003 and Lin and Yin, 1998 differ. Bourdarias et al, consider W_{act}^{f} to affect only the mechanical properties of the muscle fibres during activation. The active contraction is introduced in their model by means of an active fibre stress $T^{(0)}$ applied in the deformed fibre direction a. Therefore, the Cauchy stress tensor is

$$\sigma(\mathbf{C},t) = -p\mathbf{I} + \bar{\sigma}(\mathbf{C},t) + \beta(t) T^{(0)} \mathbf{a} \otimes \mathbf{a},$$

where p is the hydrostatic pressure resulting from the incompressibility of the material, $\bar{\sigma}$ is the deviatoric component of σ, and $\otimes$ denotes the tensor product.

In the model proposed by Lin and Yin, W_{act}^{f} considers both, the variation in the mechanical properties of the fibre muscle during activation, and the active contraction of the muscle. Doing this, the expression for the Cauchy stress is

$$\sigma(\mathbf{C},t) = -p\mathbf{I} + \bar{\sigma}(\mathbf{C},t) + \beta(t) T^{(0)*} \lambda^2 \mathbf{a} \otimes \mathbf{a},$$

where β is the actual elongation of the muscle fibre and $T^{(0)*}$ is a constant related to $T^{(0)}$. The form of W_{pas} proposed in both model is

$$W_{pas}(\mathbf{C}) = a_0 \left(e^{Q} - 1\right),$$

with

$$Q = a_1 (I_1 - 3)^2 + a_2 (I_1 - 3)(I_4 - 1) + a_3 (I_4 - 1)^2.$$

The active component of the strain energy density function, W_{act}^{f}, has been defined for Bourdarias et al. as

$$W_{act}^{f} = a_1^a (I_1 - 3)(I_4 - 1) + a_2^a (I_1 - 3)^2 + a_3^a (I_4 - 1)^2.$$

For Lin and Yin, W_{act}^{f} is given as

$$W_{act}^{f} = a_1^a (I_1 - 3)(I_4 - 1) + a_2^a (I_1 - 3)^2 + a_3^a (I_4 - 1)^2 + a_4^a (I_4 - 1).$$

9.3 Interaction between blood and vessels

Blood and vascular tissue interact in different ways. There is a biochemical interaction: substances soluted in blood are absorbed through the endothelium layer and, in some cases this process could

lead to thickening. Biochemical interaction has been numerically considered in [Perktold, 1998] and [Rappitsch, 1996], where the Navier-Stockes equations are supplemented by linear advection diffusion equations describing the concentration of solutes in blood. The boundary conditions for the latter equation model the filtration process through the walls as a function of the shear stress induced by the blood on the vessel.

Another interaction between the blood and the fluid which will be considered in the present section is the mechanical one. The pulsatile character of blood flow is responsible for the strong interaction between the flow motion and the vascular wall movement. According to the Windkessel model (see [Nichols, 1990]), during the systolic phase (blood ejection), the wall deformation accumulates part of the mechanical energy, which will afterwards be returned back to the fluid during the diastolic phase. Such a mechanism actually guarantees almost uniform velocity and pressure at capillary level.

The wall interacts mechanically with the flow field. This aspect is relevant for relatively large vessels. In the aorta, for example, the radius may vary in a range of 5 to 10% between diastole and systole. This is quite a large displacement, which affects the flow field. The fluid-structure interaction problem is the responsible for the propagation of pulse pressure waves. Indeed, no propagative phenomena would otherwise occur in an incompressible fluid like blood. The interaction problem is a rather complex one, since the time scales associated to the interaction phenomena are two orders of magnitude greater than those associated to the bulk flow field. In arterioles and capillaries the movement of the wall may be considered negligible.

The correct understanding of this interaction, besides being of primary interest for the analysis of the flow field, may help to simulate tissue-tearing phenomena or atherogenesi which eventually lead to aneurisms or stenoses. From the mathematical and numerical point of view, the problems arising from this mechanical interaction are very challenging due to their strongly nonlinear nature. In this section, we will investigate some issues concerned with these problems.

9.3.1 Mathematical models of the coupled problem

A coupled approach is based on interacting two different models, one for fluids, and the other for structures, through suitable matching conditions, which play the role of boundary conditions for the sub-models. As previously pointed out, the fluid model adopted here is based on Navier-Stockes equations, in particular (but not necessarily) for a Newtonian fluid. The model for the description of vascular wall dynamics has been presented in Sect. 1.3.2. This approach enables the splitting of the global computation into a sequence of separate computations for the fluid and the vascular wall, therefore yielding a considerable reduction of the computational complexity. On the other hand, maintaining physical and numerical consistency in the splitting approach may not be easy. Indeed, several issues have to be addressed in this regard:

a) The matching conditions between fluid and structure must be physically consistent on the one hand; on the other hand, they should provide the model with boundary conditions that are mathematically admissible for its well posedness;
b) Although each sub-model, with the provided boundary condition, yields a stable problem, it is by no means guaranteed that the global problem is stable too;
c) The flow model is naturally written in Eulerian coordinates, while the wall is expressed in Lagrangian coordinates. The interaction between these two heterogeneous frames demands a suitable approach, in order to set up a numerical device for the analysis of the coupled "moving boundary" problem.

In Sect. 1.3.3.1.1, we focus on some issues relevant to point a) and b). The third issue is faced in Sect. 1.3.4.1.1.

9.3.1.1 The coupled problem

To consider the problem arising when coupling fluid and structure models, let us restrict our analysis to a domain Ω. The boundary Γ is composed of a portion Γ_C, which is assumed to be compliant, and a part Γ_F, which is assumed to be fixed. As a model for the blood flow, we adopt the Navier-Stockes equations (1.3.1.4). The fluid problem is therefore described by the system:

$$\begin{cases} \dfrac{\partial \mathbf{v}}{\partial t} + (\mathbf{v}\cdot\nabla)\mathbf{v} - \nu\Delta\mathbf{v} + \nabla p = \mathbf{f} \\ \nabla\cdot\mathbf{v} = 0 \end{cases}; \qquad (1.3.3.1)$$

together with initial condition at t=0 for v and suitable boundary conditions. For the sake of simplicity we consider the boundary conditions (1.3.1.11) with d=0 on Γ_F, while the conditions on Γ_C will be specified bellow, as matching relations between the fluid and the structure.

Let us consider the interface conditions between the fluid and the structure. The first condition ensures the continuity of the velocity field, and reads:

$$\mathbf{v} = \dot{\boldsymbol{\eta}} \quad x \in \Gamma_C, \qquad (1.3.3.2)$$

where $\dot{\boldsymbol{\eta}}$ is the velocity field of the vessel.

The fluid exerts a surface force field over the vessel (we will neglect the possible stresses excreted by the surrounding organs in our analysis). These forces must be treated as a (Neumann) boundary data for the structure problem:

$$\boldsymbol{\Phi} = -P\mathbf{n} + \mathbf{nS} \quad \mathbf{x} \in \Gamma_C; \qquad (1.3.3.3)$$

where $\boldsymbol{\Phi}$ is the forces field vector applied in the vessel due to the blood flow.

The fluid-structure interaction problem we deal with is therefore specified by (1.3.3.1), (1.3.3.2), (1.3.3.3) and the governing equations of the vessel model. In view of its numerical solution, the coupled problem ought to be split at each time step into two sub-problems, one in Ω, the other on Ω_s (the vessel domain), communicating to one another through the matching conditions (1.3.3.2) and (1.3.3.3). In particular, the structure problem provides the boundary data for the fluid problem; vice-versa, the fluid problem provides the forcing term for the structure.

9.4 Numerical methods

Although many (reasonable) simplifications have been adopted for the definition of the coupled problem (1.3.3.1, 1.3.1.11, 1.3.3.2, 1.3.3.3 and the governing equations of the vessel model and its boundary conditions), it is impossible to obtain an analytical solution, especially when real human vascular morphologies are considered. Therefore, we need to approximate conveniently the problems at hand in order to obtain a numerical solution. This means that we have to discretize both the space and time derivatives, replacing the differential operators with algebraic ones.

As already pointed out, a distinctive feature of the fluid-structure problem at hand is the coupling of two different sub-problems, the first referring to the fluid (whose solution is characterized by the velocity and pressure fields of the blood) and the second to the structure (whose unknown variable is the displacement field of the vascular wall). In the previous section, we remarked that the coupled problem is non-linear, since fluid and structure influence themselves according to the matching relations (1.3.3.2) and (1.3.3.3). The approach we adopt for the numerical study of this problem consists of solving the two sub-problems separately, accounting for the reciprocal influence through a suitable approximation of the matching relations. Hence, in the following sections, we consider the approximation of the fluid and the structure problems separately and then we illustrate a simple (explicit) algorithm for the coupling of the two solvers.

9.4.1 Numerical study of the fluid problem

The space discretization of the Navier-Stockes equations (1.3.1.4) can be performed according to many approaches. In the problem at hand, a relevant feature refers to the complex morphologies characterizing the domain where the blood flows. The space discretization method, which is probably the most suitable for problems involving such complex geometries, is the Finite Element Method (FEM). The basic idea is to subdivide the domain into many regions (elements), which are typically tetrahedral or prismatic, and then approximate the solution with a piecewise polynomial (with respect to the space variables). The interesting feature of this method is that the subdivision (called mesh) can be unstructured, i.e. it does not necessarily follow preferential directions, as it is required by the finite different discretization. For this reason, it turns out really suitable for treating complex domains.

We will use the Tdyn code for the numerical solution of the fluid problem. *Tdyn* is a fluid dynamic (CFD) simulation environment based on the stabilized Finite Element Method. *Tdyn* works with number of different turbulence models and sophisticated tools for simulating problems of species advection, heat transfer in fluids and solids, as well as free surface among others. *Tdyn* also includes fully integrated pre/post-processing modules. *Tdyn* is highly flexible in defining physical properties of the model, boundary conditions, through user-defined functions that can make *Tdyn* a tool with large variety of applications, and will allow achieving the coupling between the fluid and the vessel models.

9.4.1.1 The Arbitrary Lagrangian Eulerian (ALE) formulation of fluid motion in moving domains

Since the fluid domain is moving, the nodes where the solution is evaluated change their position at every time instant on the boundary and consequently in the inner domain. A specific treatment of this problem is therefore required. A possible strategy is given by the Abitrary Lagrangian Eulerian method (ALE), which is often used as an alternative to the more classical Lagrangian and Eulerian approaches. In the particular case where the moving domain encompasses the coupling of two heterogeneous media, such as a fluid and solid structure, this formulation becomes especially attractive, as it allows the simultaneous use of the Eulerian frame in the fluid domain and the Lagrangian one in the wall structural.

9.4.2 Numerical study of the structure problem

The problem of the behaviour of blood vessels and cardiac mechanics correspond to a finite deformation formulation in the field of continuum mechanics. For the case of complex geometries it is necessary to use a numerical method. The finite element method (FEM) is the most extended method for this type of problems. In this section a brief overview of the theory is presented. The expression of the variational description of the problem, and the finite element approximation and linearization of the previous expression are showed.

9.4.2.1 Variational Description

A variational structure is based in a scalar functional depending of one or more unknown variables, generally displacement and usually us expressed in an integral form. The finite element formulation is based in a variational theorem that describes the total energy of the system, so the solution of the elastic problem minimizes the functional.

The functional $\prod$ is defined as a function of the displacements:

$$\prod(\boldsymbol{u}) = \int_{\Omega} \{\Psi(\boldsymbol{X}, (\boldsymbol{C}(\boldsymbol{u})))\} dV + \prod_{ext}(\boldsymbol{u})$$

where $\prod_{ext}$ is the potential energy due to the external load in the reference configuration, and for load non-dependent of the motion is expressed as:

$$\prod_{ext}(\boldsymbol{u}) = -\int_{\Omega} \rho_0 \boldsymbol{B} \cdot \boldsymbol{u} dV + -\int_{\partial_t \Omega} \bar{\boldsymbol{t}} \cdot \boldsymbol{u} dA$$

In this equation ρ_0 is the material density in the reference configuration, $\boldsymbol{B}$ are the volumetric forces and $\bar{\boldsymbol{t}}$ are the specified traction defined in the boundary $\partial\Omega_t$.
The first variation of the functional $\prod$ respect $\boldsymbol{u}$ in the direction η is expressed as:

$$D_{\boldsymbol{u}} \prod(\boldsymbol{u}) \cdot \eta = \int_{\varphi(\Omega)} [\sigma : \nabla \eta - g_{ext}(\eta)] dV$$

where $g_{ext}(\eta)$ is the virtual work due to the external load in the spatial configuration.

9.4.2.2 Finite Element approximation and Linearization

In non-linear problems, the problem solution is obtained in an incremental way, so the new unknown variable is $\Delta\boldsymbol{u}$ in the continuum form and $\Delta\boldsymbol{u}^h$ for a finite element interpolation so:

$$\begin{aligned} \Delta\boldsymbol{u}^h &= N_I(\xi) \Delta\boldsymbol{u}^I(t) \\ \boldsymbol{u}^h &= N_I(\xi) \boldsymbol{u}^I(t) \\ \eta^h &= N_I(\xi) \mu^I(t) \end{aligned}$$

$$\boldsymbol{x}^h = N_I(\xi)\boldsymbol{x}^I(t)$$

In non-linear problems, the solution $\boldsymbol{u}_n$ in the time instant t_n is supposed as known and the solution $\boldsymbol{u}_n + \Delta\boldsymbol{u}_{n+1}$ at the end of the time increment is search t_{n+1}. A popular scheme to solve this type of problem is Newton´s method, which linearization is obtained as:

$$L_{\boldsymbol{u}_n} G_e(\boldsymbol{u}_n)\cdot\eta = G_e(\boldsymbol{u}_n) + DG_e(\boldsymbol{u}_n)\cdot(\Delta\boldsymbol{u}_{n+1})$$

The solution for $\Delta\boldsymbol{u}_{n+1}$ is computed iteratively using the Newton´s method and updated in the successive iterations as:

$$\Delta\boldsymbol{u}_{n+1}^{(k+1)} = \Delta\boldsymbol{u}_{n+1}^{(k)} + \Delta(\Delta\boldsymbol{u})_{n+1}^{(k+1)}$$

where $\Delta(\Delta\boldsymbol{u})_{n+1}^{(k+1)}$ is the correction of the increment of displacement $\Delta\boldsymbol{u}_{n+1}^{(k+1)}$ in the iteration $k+1$.
The linearization respect $\Delta\boldsymbol{u}$ of the earlier expression of the variational theorem is:

$$\begin{aligned} DG_e\cdot\Delta\boldsymbol{u}^h = &\int_{V_{ref}} \{[\nabla(\Delta\boldsymbol{u})\boldsymbol{\sigma}] : \nabla\boldsymbol{\eta}\} J_e j_\xi d\boldsymbol{\xi} \\ &+ \int_{V_{ref}} \nabla^s(\Delta\boldsymbol{u}) : [p(\mathbf{1}\otimes\mathbf{1} - 2\mathbb{I}) + \tilde{\mathbb{C}}] : (\nabla^s\boldsymbol{\eta}) J_e j_\xi d\boldsymbol{\xi} \end{aligned}$$

where j_ξ is the jacobian of the geometric transformation and J_e is the jacobian of the deformation map.
The reference configuration for the linearization will be $\boldsymbol{u}_{n+1}^{(k+1)}$, while the unkown variable will be the correction of this variable in the corresponding iteration $\Delta(\Delta\boldsymbol{u})_{n+1}^{(k+1)}$, so the update strategy can be rewritten as:

$$\boldsymbol{u}_{n+1}^{k+1} = \boldsymbol{u}_n + \Delta\boldsymbol{u}_{n+1}^{k+1} = \boldsymbol{u}_n + \Delta\boldsymbol{u}_{n+1}^{k} + \Delta(\Delta\boldsymbol{u}_{n+1}^{k+1}) = \boldsymbol{u}_{n+1}^{k} + \Delta(\Delta\boldsymbol{u}_{n+1}^{k+1})$$

In a matricial form, the former expression is written as:

$$(\boldsymbol{K}^M(\boldsymbol{u}_n^k) + \boldsymbol{K}^G(\boldsymbol{u}_{n+1}^k))(\Delta(\Delta\boldsymbol{u}_{n+1}^{k+1}) = (\boldsymbol{F}^{ext} - \boldsymbol{F}^{int}(\boldsymbol{u}_{n+1}^k))$$

where the term $\boldsymbol{K}^M$ represents the material tangent matrix, $\boldsymbol{K}^G$ the geometric stiffness matrix, $\Delta\boldsymbol{u}$ the initial prediction of the unknown displacement in the current time increment $\boldsymbol{u}_{n+1}$. Solving $\Delta\boldsymbol{u}$, the displacement in each Newton´s iteration is updated as

$$\boldsymbol{u}_{n+1}^{(k+1)} = \boldsymbol{u}_n^{(k)} + \Delta\boldsymbol{u}_{n+1}^{(k+1)}$$

Rewriting the previous expression in as symbolic way

$$\boldsymbol{K}(\boldsymbol{u}_n)\cdot\Delta\boldsymbol{u}_n = \boldsymbol{F}_{ext} - \boldsymbol{F}_{\text{int}}(\boldsymbol{u}_n)$$

The part corresponding to the geometric stiffness can be written as:

$$\int_{V_{ref}} \{[\nabla(\Delta \boldsymbol{u})\boldsymbol{\sigma}] : \nabla\boldsymbol{\eta}\} J_e j_\xi d\boldsymbol{\xi} = \sum_{i=1}^{N_{nodos}} \sum_{j=1}^{N_{nodos}} \boldsymbol{\eta}_i^T \boldsymbol{K}_{ij}^G \Delta \boldsymbol{u}_j$$

where $\boldsymbol{K}^G$, the geometric stiffness matrix is defined as:

$$\boldsymbol{K}_{ij}^G = \int_{V_{ref}} \widehat{\boldsymbol{B}}_i^T \widehat{\boldsymbol{\sigma}}_e \widehat{\boldsymbol{B}}_j J_e j_\xi d\boldsymbol{\xi}$$

In a analogous way, the part of the linearization process corresponding to the material tangent matrix is obtained

$$\int_{V_{ref}} \{[\nabla^s(\Delta \boldsymbol{u}) : [p(\mathbf{1}\otimes\mathbf{1} - 2\mathbb{I}) + \widetilde{\mathbb{C}}] : (\nabla^s \boldsymbol{\eta})\} J_e j_\xi d\boldsymbol{\xi} = \sum_{i=1}^{N_{nodos}} \sum_{j=1}^{N_{nodos}} \boldsymbol{\eta}_i^T \boldsymbol{K}_{ij}^M \Delta \boldsymbol{u}_j$$

where $\boldsymbol{K}^M$, the geometric stiffness matrix is defined as:

$$\boldsymbol{K}_{ij}^M = \int_{V_{ref}} \widehat{\boldsymbol{B}}_i^T [p(\mathbf{1}\otimes\mathbf{1} - 2\mathbb{I}) + \widetilde{\mathbb{C}}] \widehat{\boldsymbol{B}}_j J_e j_\xi d\boldsymbol{\xi}$$

In a three-dimensional case, each one of the matrices is expressed as:

$$\boldsymbol{\eta} = \begin{bmatrix} \eta_x & \eta_y & \eta_z \end{bmatrix}^T, \qquad \boldsymbol{B}_k = \begin{bmatrix} N_{k,x} & 0 & 0 \\ 0 & N_{k,y} & 0 \\ 0 & 0 & N_{k,z} \\ N_{k,y} & N_{k,x} & 0 \\ 0 & N_{k,z} & N_{k,y} \\ N_{k,z} & 0 & N_{k,x} \end{bmatrix}$$

$$\nabla^s \boldsymbol{\eta} = \sum_{k=1}^{N_{nodos}} \boldsymbol{B}_k \boldsymbol{\eta}_k$$
$$= \begin{bmatrix} \eta_{x,x} & \eta_{y,y} & \eta_{z,z} & \eta_{x,y} + \eta_{y,x} & \eta_{y,z} + \eta_{z,y} & \eta_{x,z} + \eta_{z,x} \end{bmatrix}^T$$

$$\boldsymbol{\sigma} = \begin{bmatrix} \sigma_{xx} & \sigma_{yy} & \sigma_{zz} & \sigma_{xy} & \sigma_{xz} & \sigma_{yz} \end{bmatrix}^T$$

But, in order to rewrite them in a more efficient way it is possible to express as:

$$\widehat{\boldsymbol{B}}_k = \begin{bmatrix} N_{k,x} & 0 & 0 \\ N_{k,y} & 0 & 0 \\ N_{k,z} & 0 & 0 \\ 0 & N_{k,x} & 0 \\ 0 & N_{k,y} & 0 \\ 0 & N_{k,z} & 0 \\ 0 & 0 & N_{k,x} \\ 0 & 0 & N_{k,y} \\ 0 & 0 & N_{k,z} \end{bmatrix}$$

$$\begin{aligned} \nabla^s \boldsymbol{\eta} &= \sum_{k=1}^{N_{nodos}} \boldsymbol{B}_k \boldsymbol{\eta}_k \\ &= \begin{bmatrix} \eta_{x,x} & \eta_{x,y} & \eta_{x,z} & \eta_{y,y} & \eta_{y,z} & \eta_{y,x} & \eta_{z,z} & \eta_{z,y} & \eta_{z,x} \end{bmatrix}^T \end{aligned}$$

$$\widehat{\boldsymbol{\sigma}} = \begin{bmatrix} \sigma_{xx} & \sigma_{xy} & \sigma_{xz} & 0 & 0 & 0 & 0 & 0 & 0 \\ \sigma_{yx} & \sigma_{yy} & \sigma_{yz} & 0 & 0 & 0 & 0 & 0 & 0 \\ \sigma_{zx} & \sigma_{zy} & \sigma_{zz} & 0 & 0 & 0 & 0 & 0 & 0 \\ 0 & 0 & 0 & \sigma_{xx} & \sigma_{xy} & \sigma_{xz} & 0 & 0 & 0 \\ 0 & 0 & 0 & \sigma_{yx} & \sigma_{yy} & \sigma_{yz} & 0 & 0 & 0 \\ 0 & 0 & 0 & \sigma_{zx} & \sigma_{zy} & \sigma_{zz} & 0 & 0 & 0 \\ 0 & 0 & 0 & 0 & 0 & 0 & \sigma_{xx} & \sigma_{xy} & \sigma_{xz} \\ 0 & 0 & 0 & 0 & 0 & 0 & \sigma_{yx} & \sigma_{yy} & \sigma_{yz} \\ 0 & 0 & 0 & 0 & 0 & 0 & \sigma_{zx} & \sigma_{zy} & \sigma_{zz} \end{bmatrix}$$

9.4.3 Numerical study of the coupled fluid-structure problem

So far, we have illustrated the features of the schemes used for the fluid and the structure problems separately. To match the two solvers, we can proceed in many different ways. Similarly, different strategies can be considered for the computation of the grid velocity in the ALE perspective. In this section, we illustrate, in particular, an explicit algorithm for the coupling of fluid and structure.

The original coupled problem (1.3.3.1, 1.3.1.11, 1.3.3.2, 1.3.3.3 and the governing equations of the vessel model and its boundary conditions) is split at each time into a structure and a fluid problem, communicating with one another through boundary terms: a forces field boundary term in the vessel due to the fluid and a velocity restriction of the boundary Γ_C of the fluid. Figure 9 shows the basic steps of the algorithm which we are going to illustrate for advancing from time level n to time level n+1.

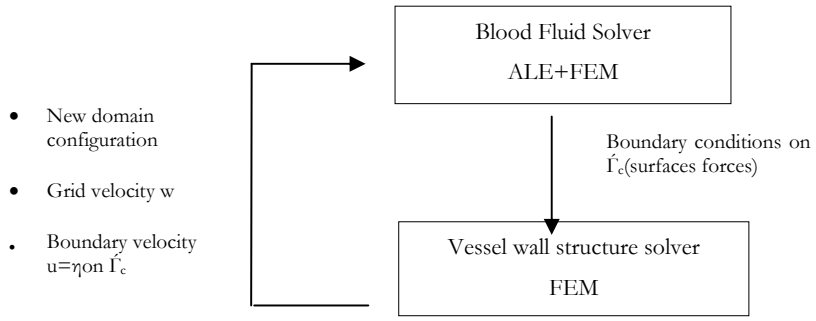

Figure 9: Representation of the splitting in two sub-problem for our approach (coupled solver)

V and P respectively as usual will denote the unknowns referring to the velocity and pressure, while the ones relative to the structure are denoted by **H**.

The algorithm iteration process for each time step can be resumed as follows:

- Solving the structure problem (vessel wall) with the boundary terms due to the blood flow. At the first time level, the scheme is suitable modified, taking into account the initial data on the position and the velocity at time t=0.

- Updating domain configuration and boundary conditions for the fluid solver: Once $\mathbf{H}^{n+1}$ is known, we can compute the domain deformations and the movement of the nodes of the grid for the fluid. The new position of the boundary Γ_C is computed through the relation:

$$\mathbf{x}_i^{n+1} = \mathbf{x}_i^0 + \boldsymbol{\eta}_i^{n+1}.$$

  The displacement of the nodes of the grid for the fluid is obtained as a diffused into the fluid domain of the boundary displacement. Diffusion process is based on an arrangement by levels of the mesh nodes, where level 0 corresponds to the mesh nodes on the ship surface, level 1 to the nodes connected to level 0 nodes, and so on.

  We compute the mesh velocity **w** by the equation:

$$\mathbf{w}^{n+1} = \frac{1}{\Delta t}(\mathbf{x}^{n+1} - \mathbf{x}^n).$$

The idea underlying this approach is to take advantage of the regularization due to the inversion of the Laplace operator in order to have an acceptable mesh. From time to time, however, it could be necessary to remesh the whole domain, if the grid is too distorted after a certain number of steps.

Another strategy consists of computing the velocity mesh as the solution of the problem:

$$\begin{cases} -\Delta \mathbf{w}^{n+1} = 0 & \text{in } \Omega \\ \mathbf{w}^{n+1} = \dot{\boldsymbol{\eta}}^{n+1} & \text{on } \Gamma_C \\ \mathbf{w}^{n+1} = 0 & \text{on } \Gamma_F \end{cases}.$$

Finally, the mesh update is obtained by:

$$\mathbf{x}^{n+1} = \mathbf{x}^n + \Delta t \mathbf{w}^{n+1}.$$

For a comparison of the two strategies, see [Nobile, 1998].

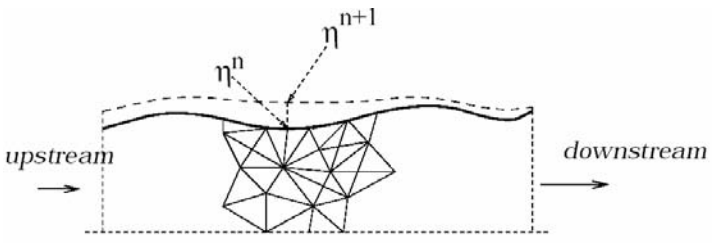

Figure 10: Updating of the mesh

- Solving the blood flow problem
  The ALE formulation of the Navier-Stockes equations (1.3.1.1) is solved by implicit 2nd order accurate projection schemes. The choice of the time-advancing method satisfies the Geometric Conservation Laws.

- Computing the force field applied as a boundary condition in the structure problem due to the fluid.

When the boundary nodes of the structure and the fluid are not coincident is necessary to make an interpolation of the nodal quantities during the interaction algorithm. The methodology used for this interpolation is based on an octtree search algorithm of elements and standard finite element techniques.

This algorithm performs a staggered coupling between the fluid and the structure problems; therefore, it should generally undergo stability limitations on the time step. These limitations could turn out to be restrictive in practical computations. In such cases, different implicit strategies for the coupling have to be investigated (see [Nobile, 1998]).

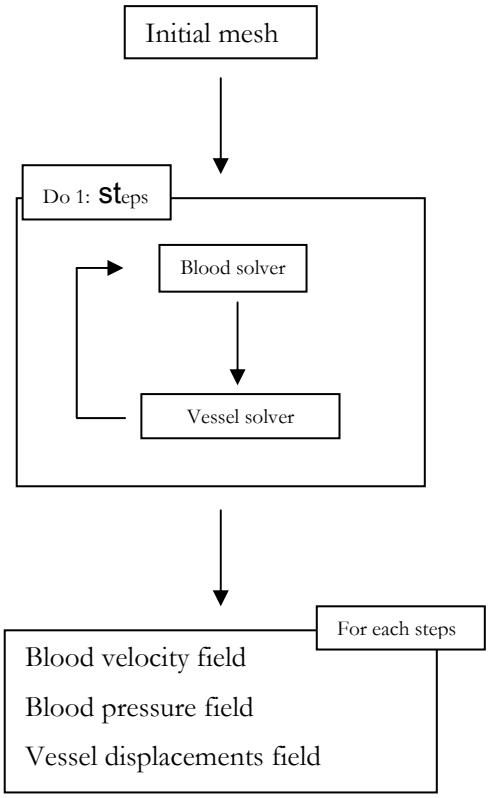

Figure 11: Simulation process

10 DATA PRE AND POST PROCESSING FOR THE SIMULATION MODULES

The suitable treatment of clinical data is crucial for the definition of a real (i.e. taken from a patient) geometrical model, which is of utmost importance for the meaningfulness of numerical results. This aspect demands geometrical reconstruction algorithms in order to achieve simulation in real vascular morphologies. This geometric reconstruction of the real vascular morphology will be done with the image treatment program developed by I3A (for a more detailed explanation see deliverable D2.2). The geometry created will be exported and read with the pre and post processor GiD.

Based on the geometrical model, we will assign material properties to each material, boundary conditions and loads and we will create a mesh with a user-defined degree of refinement. All this process will be done with the pre and post processor GiD, developed in CIMNE and commercialised by Compass and adapted for this project. The results obtained from the different simulation modules will be also visualized in the new customized GiD for the DISHEART system.

Compass have a great expertise in the development of methods for mesh generation, the pre-processing of the data needed for the simulations and the post- processing of the results obtained, with different tools for an easy visualization of the results. All this experiences have been integrated in the pre and post-processing program GiD.

10.1 GiD

GiD is a graphical environment for pre/post-processing complex geometrical models, generating a mesh and other data necessary for the FEM analysis. GiD also displays the results of the analysis using several graphical techniques. GiD will be customized for the development of the integral DISHEART system.

The segmented image obtained by means of the image treatment program will be imported to GiD through *dxf, *parasolid, *iges, *acis or *vda formats or *stl meshes, among others.

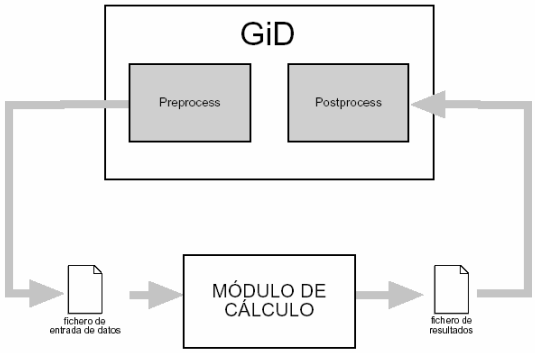

Figure 12: GiD

Next, we will list some of the GiD characteristics:

- Fast and easy understandable, intuitive user interface
- Triangular, quadratic, tetrahedronal and hexahedronal mesh generation with ability to generate more then one million elements on a standard PC
- Boundary conditions, materials and other data integrated the way, that they can be defined directly in the geometry
- Post-processing optimized for large dimensional models (hundreds of thousands or millions of elements) with number of display techniques

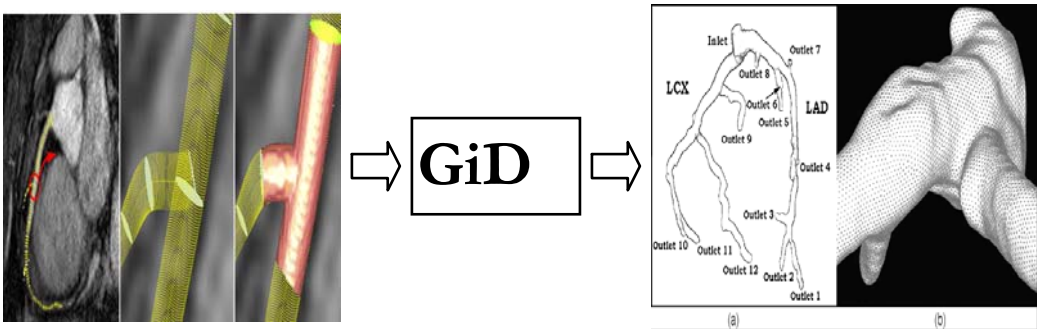

Figure 13: Meshing GiD

More information about GiD can be found in: http://www.gidhome.com.

10.2 GiD integration with the simulation modules

The different simulation modules will be integrated in GiD by the creation of a Problem Type for each one.

When GiD is to be used for a particular type of analysis (or simulation), it is necessary to predefine all the information required from the user and to define the way the final information is given to the solver module. To do so, some files are used to describe conditions, materials, general data, units systems, symbols and the format of the input file for the solver. We call Problem Type to this this collection of files used to configure GiD for a particular type of analysis.

Due to the vocation of GiD as general-purpose pre and post processor, the configuration for the different analysis must be performed according to the particular specifications of every solver. This implies the necessity of creating specific data input files for every solver. However, GiD allows to perform this configuration process inside itself without any change in the solver and without having to program any independent utility.

To configure these files means to define the data that must be input by the user, as well as the materials to be implemented and other geometrical and time-dependent conditions. It is also possible to add some symbols or drawings to represent the defined conditions. GiD gives the oportunity of working whith units when defining the properties of the mentioned data, but there must be a configuration file where it could be found the definition of the units systems. It must be also defined the way that all this data must be written inside a file that will be the input file to be read by the corresponding solver.

The creation of a Problem Type implies the creation of a directory with the Problem's Type name and the extension .gid. This directory can be located in the current working directory or in the main GiD executable directory. The first case, the creation inside the current working directory, can be useful during the development of the project. Once it is finished, it can be advisable to move the directory to the one where GiD is stored; like this, your Problem Type will be added to those included in the system and it will appear in the GiD menu. In both cases, the series of files must be inside the problem type directory. The name for most of them will be composed by the same problem type's name and an extension referring to their function. Considering problem_type_name to be the name of the Problem Type and project_name the name of the project, the diagram of the file configuration is the following:

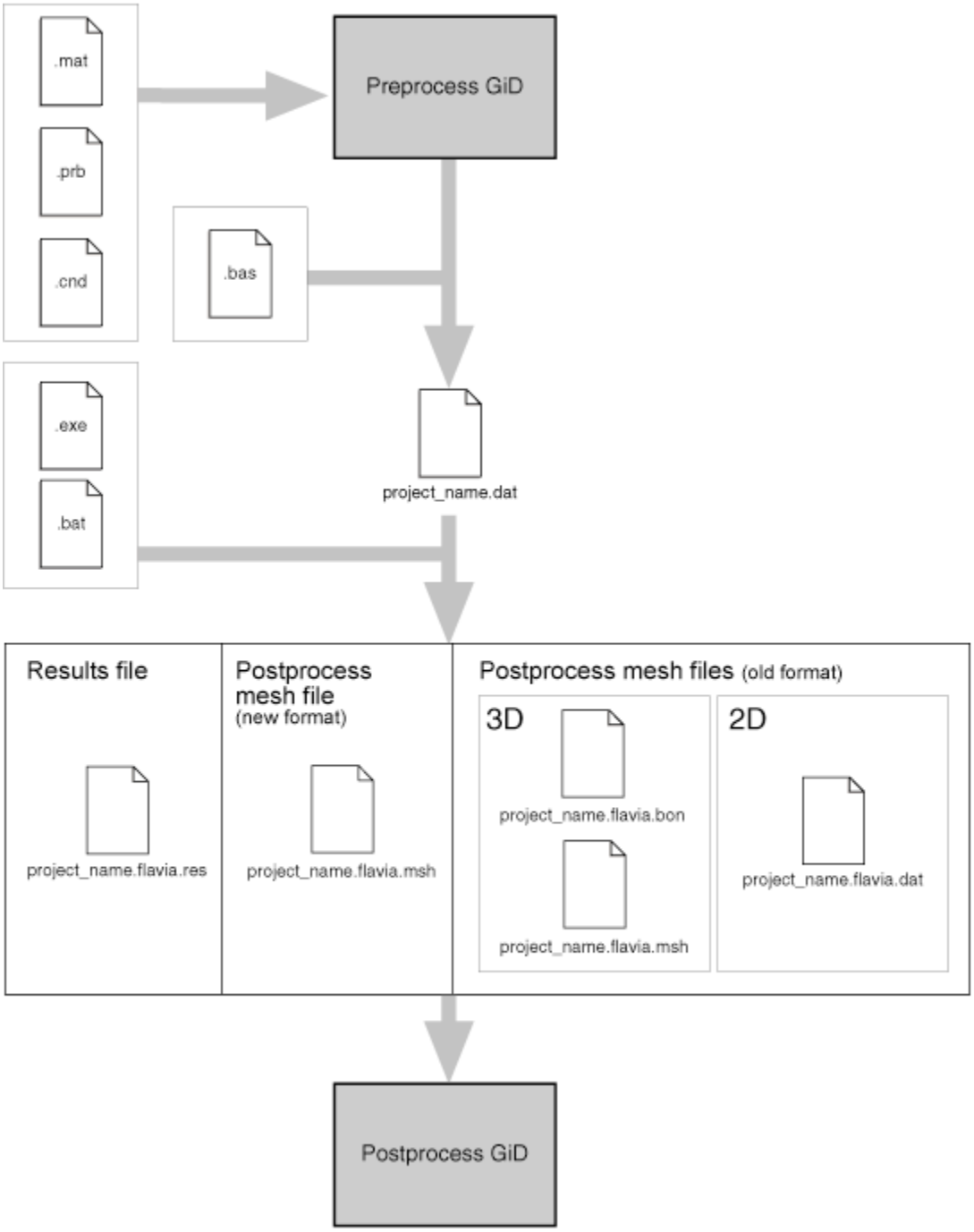

Figure 14: GiD files

Once all the files of the problem type are finished (.cnd, .mat, .prb, .sim, .bas files), you are able to run the solver. It may be interesting to run it directly from inside GiD. To do so, it is necessary to create the file problem_type_name.bat in the problem type directory. This must be a shell script that can contain any type of information and that will be different for every operating system. When the user selects the option CALCULATE in the GiD preprocess this shell script is executed

Detailed information about the Problem Type creation can be found in the web page: http://www.gidhome.com/support.

11 SIMULATION ENVIRONMENT

The new customized GiD with all the simulation modules, as Problem Types, integrated on it will constitute the simulation environment.

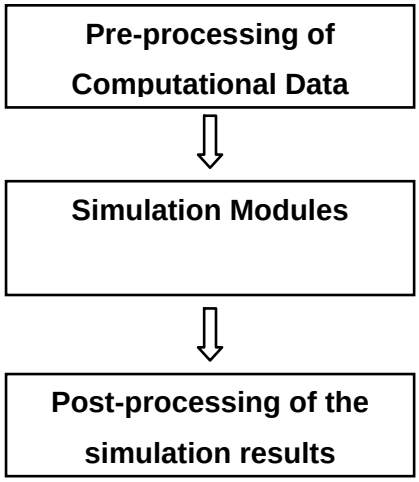

Figure 15:Simulation Process

12 BUILT AND TRAINING OF THE NEURAL NETWORK

12.1 Introduction

The goal that we want to achieve by building and training a neural network is to obtain results very quickly, almost in real time. This makes possible to use our simulations for supporting the clinicians when they must take decisions for prevention, diagnosis, surgical intervention, etc and learning

We are going to build an ANN for each one of the two intelligent modules that we will integrate in the DISHEART system:

- Study the mechanical factors that may be important in triggering the rupture of aneurysms;
- Determine mechanical risk factors for plaque rupture and stability.

12.2 Artificial Neural Networks (ANN)

The artificial neural networks (ANN) are massively interconnected networks in parallel of simple elements denoted by neurons with a hierarchical organization, which interacts with the real world, as the biological nervous systems do. Drawing an analogy between the synaptic activity and the ANN, we can fix the following concepts:

- The signals arriving at the synapses are the entries for the neuron
- This entries are weighted through a parameter denoted weight, which is associated with a specific synapse
- This signals can excite or inhibit the neurons (positive or negative weights)
- The effect on the neuron results from the addition of all the entries

If the addition of all the entries is greater or equal to the neuron threshold, the neuron is activated and gives a response.

The structure of the artificial neural networks (ANN) consists of three levels or neuron layers: the input level, the level of hidden layers and the output level. The network adapts the different weights during its learning process. The changes during the learning process are: the destruction, modification and creation of connections between neurons. In the biologic systems exists a continuous process of creation and destruction of connections between neurons. In ANN a creation of a connection is equivalent to give to its weight a value different from cero. When a weight with a no null value is substituted with a cero a connection is destroyed. A ANN can be implemented in different ways:

1. Simulation of the network with a conventional computer by a specific software
2. Creation of an ANN through architectures oriented to processes with a high grade of parallelism, as transposed networks or systolic architectures
3. Creation of an ANN by means of its implementation by one or several specific integrated circuits

The artificial neural networks for the DISHEART decision modules will be implemented using several specific integrated circuits.

The problem of building a neural network can be, in short, formulated as follows: Given a set of input data with dimension n within a domain D_{in} and a set of output data with dimension m within a domain D_{out}, a neural network is a function:

$$f^{n} : D_{in} \rightarrow D_{out}$$

in such a way that an error function is minimum for that training data set. We aim to create a non-linear functional mapping between spaces of many dimensions.

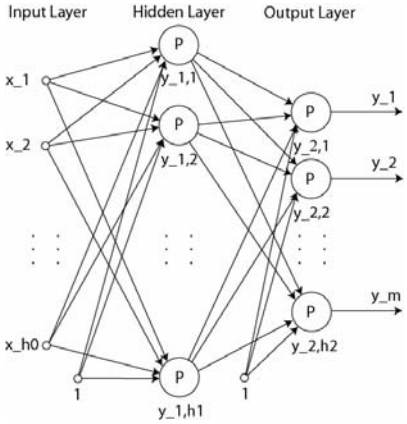

Figure 16: ANN representation.

12.3 Building of a neural network for the decision modules

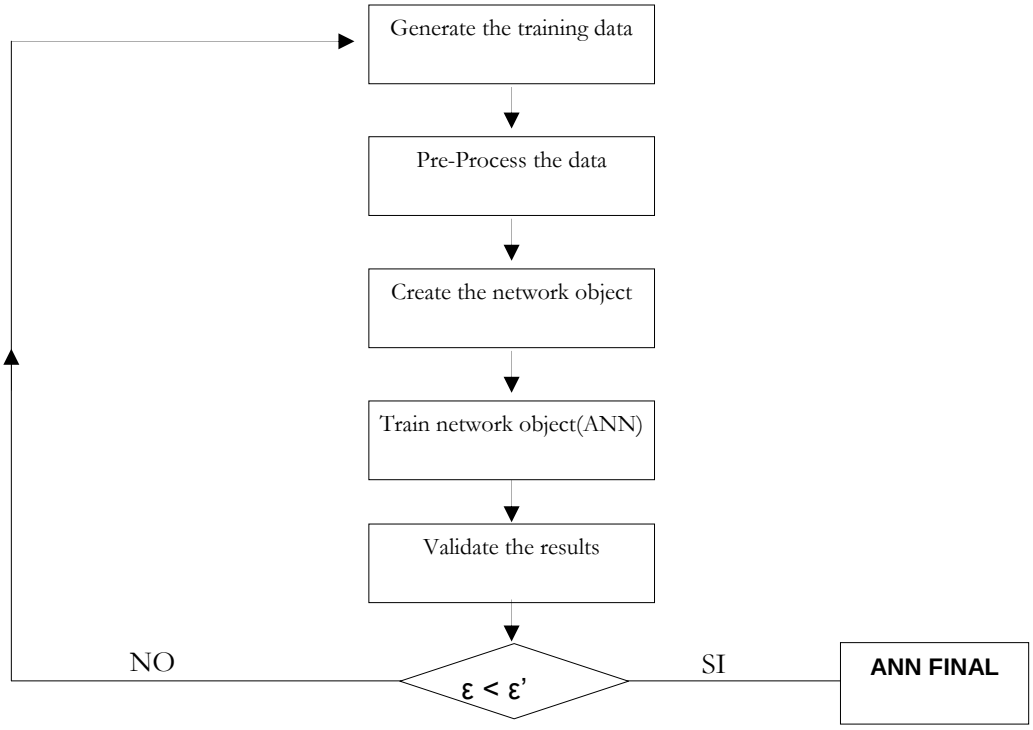

Figure 17: Obtaining ANN-Final

To build a neural network for the decision modules is necessary to follow these steps:

1. Generate the training data
2. Pre-process the data
3. Create the network object
4. Train the network
5. Validate the results

12.3.1 Generation of the training data

The training data set must contain all the relevant information about the process simulated in the inteligent module.

There are four steps in the training data generation process:

- Assign random values for the input variables. This step is associated with the data selection problem, i.e., choosing which data provides the most important information
- Call the simulation process with that input values and select the output values
- Collect the instance obtained with the input and output values in a data file
- Repeat steps 1, 2 and 3 until the size of the training data set is enough to map the simulation process with a set accuracy. The size of the training data set is an important issue here, since the simulation process seems to take quite a long time to compute. To overcome this problem there might be the possibility of using a mainframe computer

12.3.2 Pre-Processing of the data

In practice it is always advantageous to apply pre-processing transformations to the input data before it is presented to the network. Similarly, the outputs of the network are then post-processed to give the required output values. One of the most common forms of pre-processing consists of a simple linear rescaling of the data. An approach for scaling network inputs and targets is to normalize the mean and the standard deviation of the training set so that they will have zero mean and unity standard deviation. This sort of pre-processing forces the input variables to have similar ranges, which makes easier the network training.

12.3.3 Creation of the network

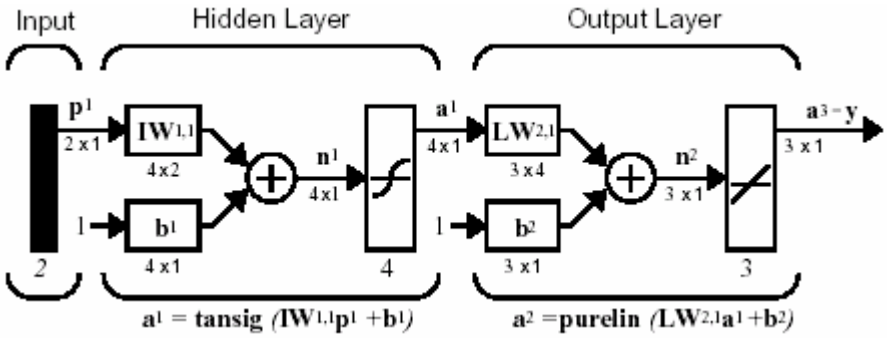

Figure 18: Graphical representation of a typical multi-layer perception. This network can be used as a general function approximated.

To find the network having the best performance on new data, different networks must be compared. The best performance for similar applications has been found in a classical multi-layer perception with hyperbolic tangent sigmoid neurons in the hidden layer and linear neurons in the output layer. The number of neurons in the hidden layer depends on the complexity of the function to map. The number of neurons in the output layer must be set in function of the output variables.

12.3.4 Training of the network

There are many different training algorithms. They have a variety of different computation and storage requirements, and no one is best suited to all locations. The Levenberg-Marquardt back-propagation algorithm is the fastest training algorithm for networks of moderate size. Note that we need to train many small networks rather than a big one.

One of the problems that occur during neural network training is called over-fitting. The error in the training set is driven to a very small value, but when new data is presented to the network the error is large. The network has memorized the training examples, but it has not learned to generalize to new situations.

One method for improving network generalization is to use a network that is just large enough to provide an adequate fit. The larger a network you use, the more complex the functions the network can create. If we use a small enough network, it will not have enough power to over-fit the data.

Unfortunately, it is difficult to know beforehand how large a network should be for a specific application. A method for improving generalization is called regularization. This involves modifying the performance function, which is normally chosen to be the sum of squares of the network errors on the training set, by adding a term that consists of the mean of the sum of squares of the network weights and biases. Using this performance function will cause the network to have smaller weights and biases, and this will force the network response to be smoother and less likely to over-fit.

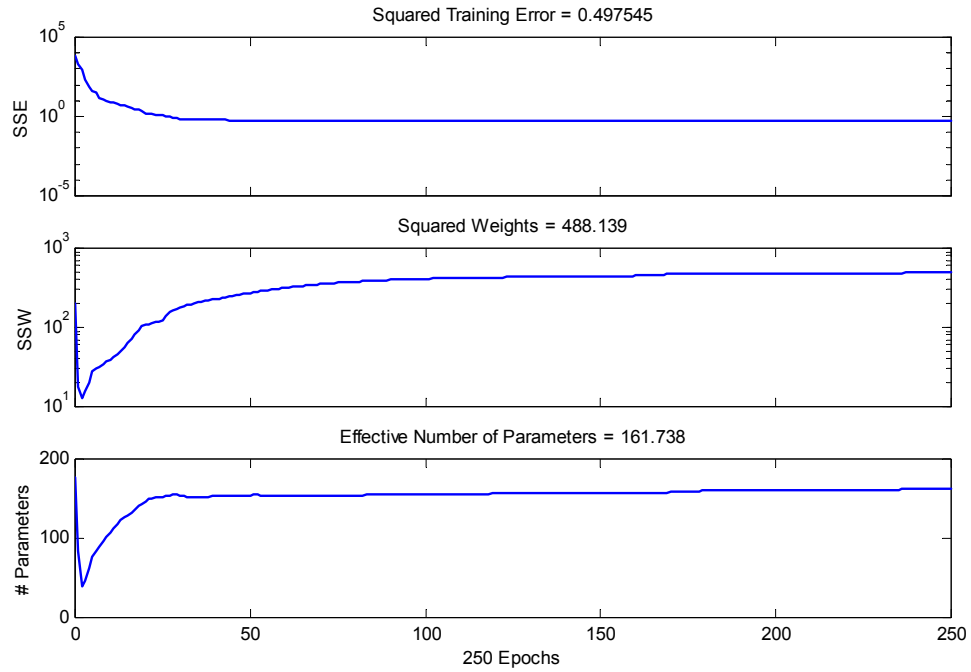

Figure 19: Typical training session with regularization. The figures represent the behaviour of sum squared error, sum squared weights and effective number of parameters during the training session, as a function of the iteration step.

12.3.5 Validation of the results.

The objective of forecasting validation is to determine its quality. To validate a forecasting technique we need to compare the values provided by this technique to the actually observed values.

The performance of a trained network can be measured to some extent by the error on the training set, but it is often useful to investigate the network response in more detail. One option is to perform a regression analysis between the network response and the corresponding targets for an independent test set.

This analysis leads to the get of 3 parameters. The first two, m and b, correspond to the slope and the y-intercept of the best linear regression relating targets to network outputs. If we had a perfect fit (outputs exactly equal to targets), the slope would be 1, and the y-intercept would be 0. The third parameter got is the correlation coefficient (R-value) between the outputs and targets. If this number is equal to 1, then there is perfect correlation between targets and outputs.

To perform this analysis of the network response we put a test data set through the network and perform a linear regression between the network outputs and the corresponding targets.

The following figures illustrate a graphical output provided by this post-training analysis. The network outputs are plotted versus the targets as open circles. A dashed line indicates the best linear fit. A solid line indicates the perfect fit (output equal to targets).

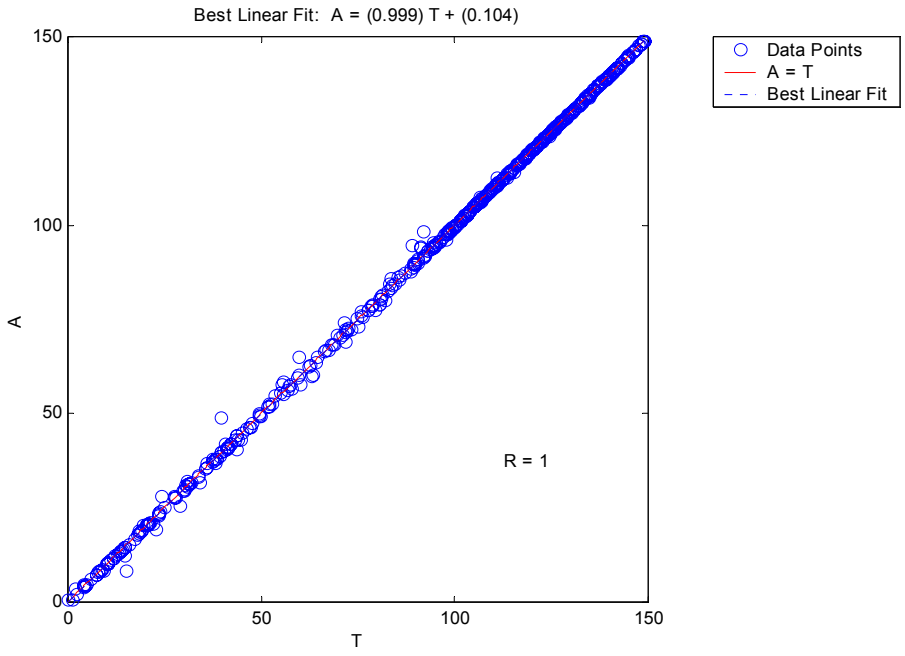

Figure 20: Typical regression analysis. The figure represents network outputs versus targets.

13 DECISION MODULE

The tool created for the support of the decision making process will consider three basic elements: clinical experiences, medical images and an intelligent module based on ANN.

There will be three support degrees for the decision making process:

- Information: This is the first support degree. The user could access to all the information stored in the database of images, materials and simulations (graphs, animations, tables, etc)
- Technical support: This is the second support degree. The user can access to the simulation modules to visualize results stored or generate new simulation processes
- Decision support: This is the third support degree. The user can access to the previous results of the intelligent module stored or ask for the decision support in a new study case

14 MULTIUSER INTERFACE

14.1 User interface

The Dishearth DSS system is initiated through the download and execution of an executable file that can be obtained in the restricted area of the project web page (www.cimne.upc.es/disheart). Immediately after that, the system shows the next window requiring the user's login and password. This will allow the connection to the database server, that is located on CIMNE's premises.

Figure 21 DISHEART DSS

In this way, any partner of the project or new stakeholder cooperating in it can access the database from any workstation connected to the internet, and will be able to share information stored on the Disheart DSS system.

Figure 22 Disheart Server

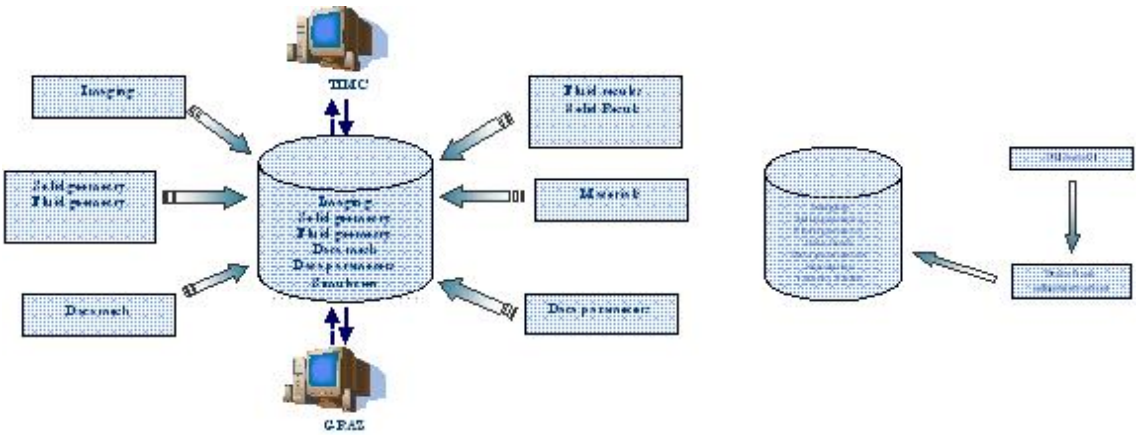

Figure 23 Management/Share database

Once validated through user login and password, the principal window of the Disheart DSS system is shown as in the following figure. From this interface the user, depending on the permission level assigned (see Deliverable 1ST) will be able to use the features of the system. Disheart allows the access to its functionalities through different ways: the menu system, the tool bars and a tree menu in a fast and trusty way.

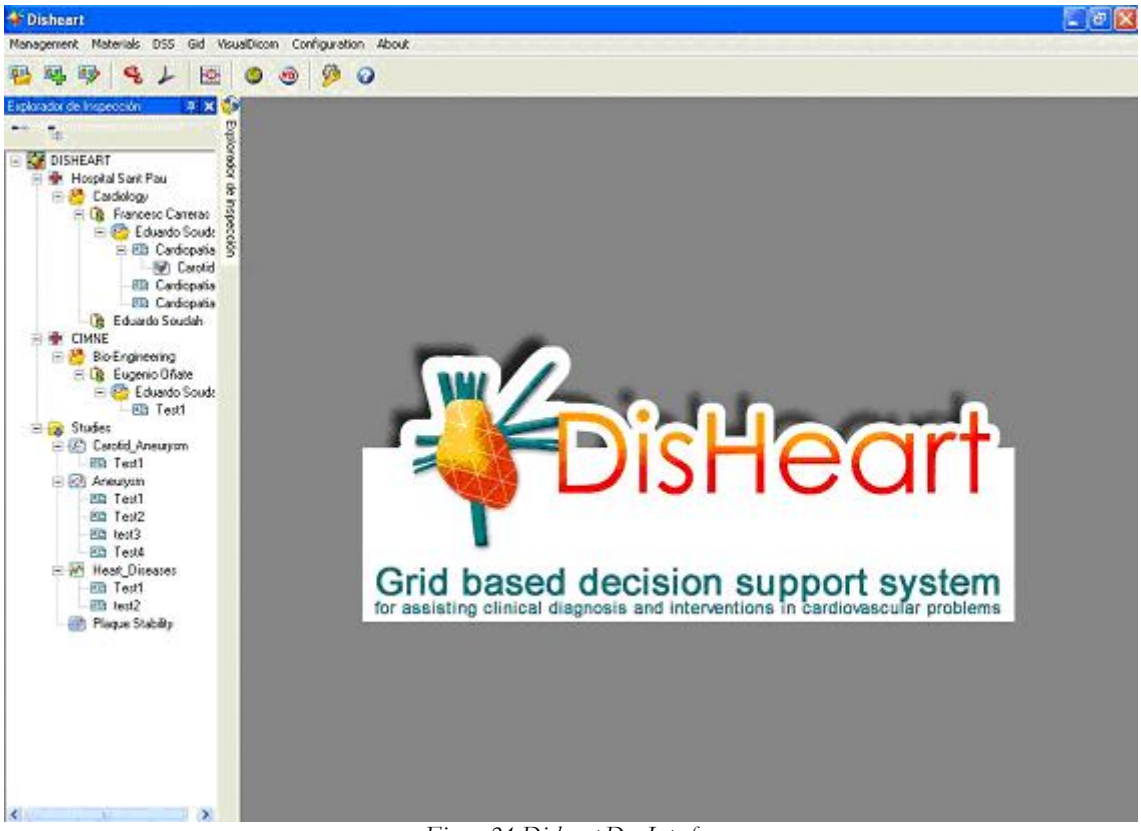

Figure 24 Disheart.Dss Interface

For those users familiarized with the Microsoft Windows platform, it will be simple to work with Disheart DSS. As in Windows, the user can for example move a window by placing the mouse cursor on the title bar and dragging it to a new position. The buttons and the elements from the menu that are not available appear tenuous or grey, but the user can see what are the options offered with each menu and button just by placing the cursor on it.

On the other hand, the DISHEART DSS environment has some special characteristics: it includes several special windows that will be available in certain circumstances. For example, the decision module window will only be active when the whole training process of the neural network has been completed.

Finally, from the menu or from the tool bar or tree menu, the user can move along the process of creation of a medical report in an intuitive manner.

14.1.1 Description of the Disheart Icons.

 Open patient files, all the patient are showed.

 Insert new patient.

 Modify patient. Modify the patient information inserted.

 Fluid materials, all the fluid materials of Disheart.DSS are showed.

 Solid materials, all the Solid materials of Disheart.DSS are showed.

 ANN, Artificial Neural Networks.

 Gid, Pre-post processor of Disheart.DSS.

 Visual Dicom, Segmetation program used in Disheart.DSS.

 System preferences of Disheart.DSS.

 Help of Disheart.DSS.

14.1.2 Description of the Tree Menu Disheart Icons.

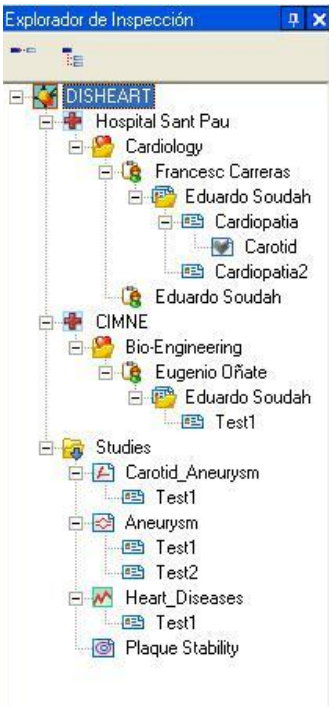

Figure 25 Disheart.Dss Tree

 Open tree files, all the hospitals, departments, doctors ,patients, tests and reports are showed.

 Close tree files.

 Disheart Main

 All the Hospital of the system are showed.

 All the department of the hospital are showed.

 All the Doctors of the department are showed.

 Patient Information.

Test relation of the Patient.

Report of the Patient.

Studies Neural Network.

Aneurism Artificial Neural Network.

Carotid Artificial Neural Network.

Heart Diseases Artificial Neural Network.

Plaque Stability.

14.2 Medical report creation

As it was specified on the system requirements (see Appendix 1), there exist 3 different management levels (System manager, Experts and User). To create a medical report, the expert user will need to have previously registered a Hospital, a department and a doctor (user), having the possibility to create a relation of hospitals of an area, an association of departments pertaining to a hospital or a group of doctors that integrate a department. The tree menu is updated every time a new item is inserted by the user. Once created, the user can then create a medical report.

In the following illustrations we show the window to register a hospital, a department inside such a hospital, and a user or doctor. These tasks only can be carrying out by the System Manager.

14.3 Hospital Management.

The System manager is the administrator of the hospitals management added to the system. He can create a new Hospital, modify the information about hospital added and delete hospital.

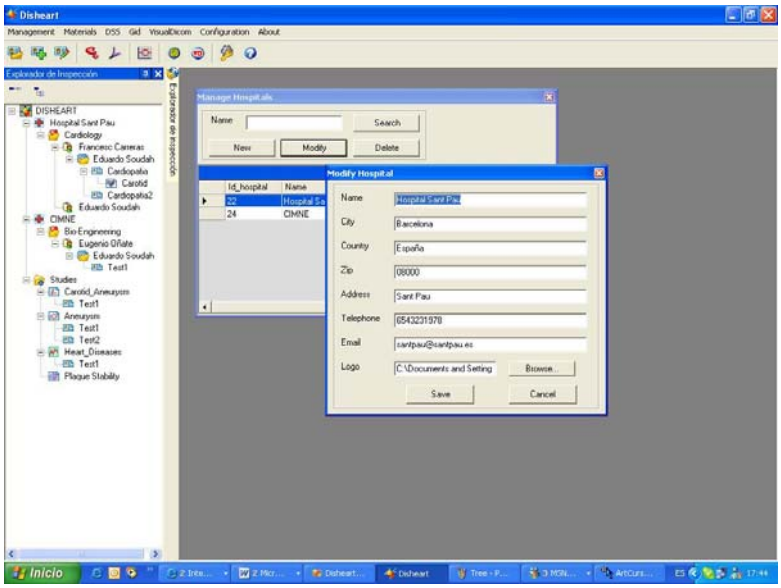

Figure 26 New Hospital

The available user-actions are:

- *Creation of a new Hospital.*
- *Correction and modification of a Hospital Added.*
- *Delete Hospital*
- *Search Hospital data*

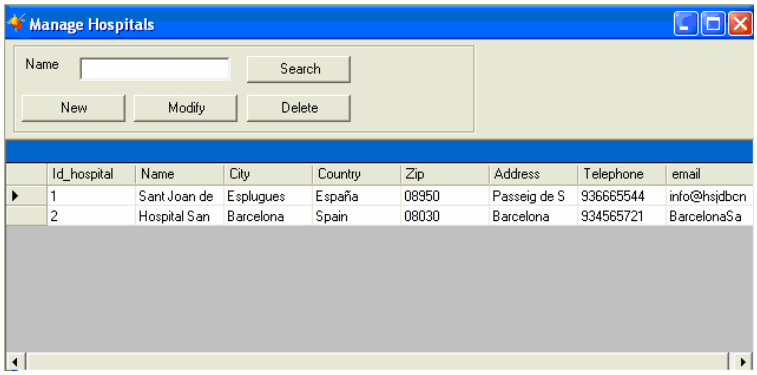

Figure 27 Hospitals list

The following picture shows us the presentation of a group of hospitals ordered by the Key_Field Id_hospital, this attribute of the table used allow us to enumerate the nosocomious present in our database.

In the insertion window are present some fields that the user has to fill completely:

- *The hospital NAME*
- *The CITY where the hospital is situated.*
- *The COUNTRY where the hospital is situated.*
- *The ZIP code of the hospital zone*
- *The ADDRESS of the hospital.*
- *The TELEPHONE number associated to the hospital*
- *And finally an EMAIL or Web-page of the Hospital.*

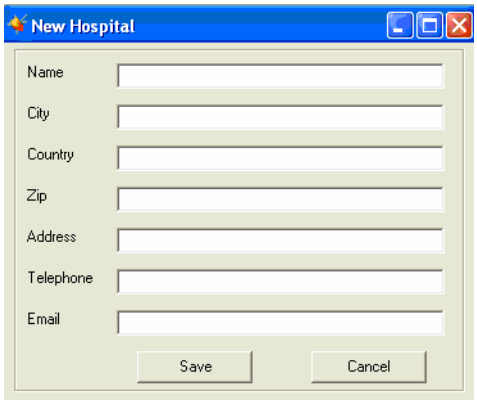

Figure 28 New Hospital insertion window.

To modify some information of the hospital, solely change the wrong information in the next window (Figure 29) and save the new information.

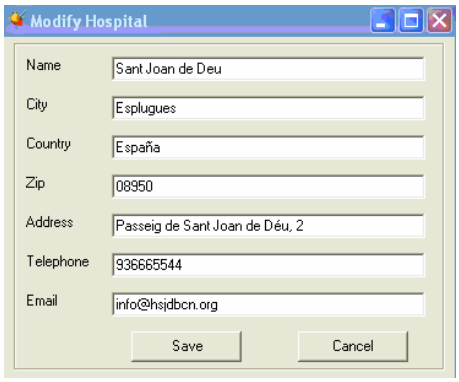

Figure 29 Correction of a wrong data

14.4 Department Management

In this section is described how the department management tool is used. The main window for administrator is the follow.

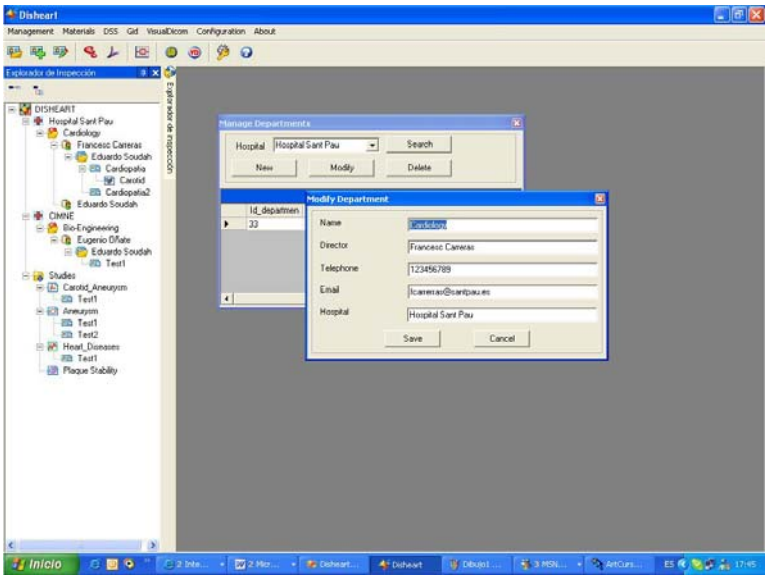

Figure 30 New Department

Through this window is possible to manage the data of the departments created into the hospital. The *available actions are:*

- *Add New department.*
- *Search a department.*
- *Modify information of the one department.*
- *Delete a department.*

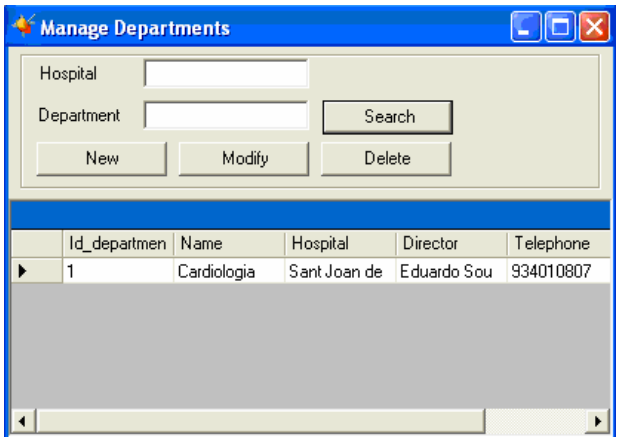

Figure 31 Search of a Department

The tool allows looking for a department, shows the name of the Hospital which it belongs, the department Director and visualizes the e-mail and telephone number associated with the department.

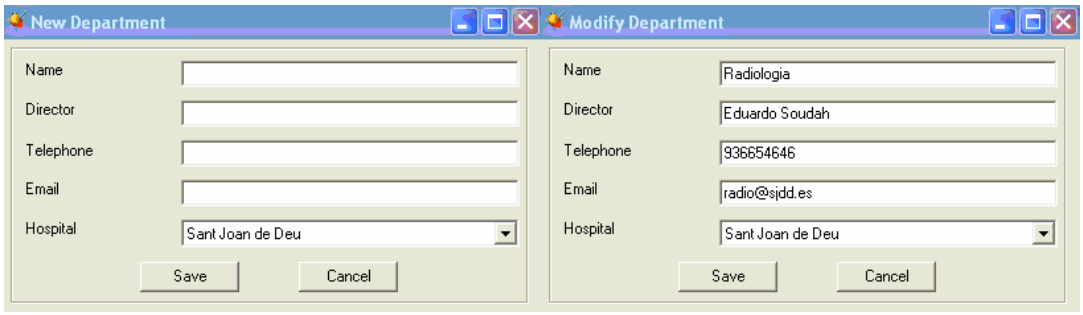

Figure 32 Modify Department

The modification of the data associated to a department is showed in the before picture (Figure 32), the fields associated with the department are:

- *Name of the department*
- *Department Director*
- *Telephone number of the department.*
- *Email address of the department*
- *Hospital which the department belongs. This field is compulsory, and it is only possible to choose a hospital inserted in the database.*

When all the data will be correct we can save it. Other action who the system can do it is Cancel of the information with the button in the bottom side of the window.

14.5 Doctor Management

Another possible area that the expert user has the control is the management of the personal staff in the hospital.

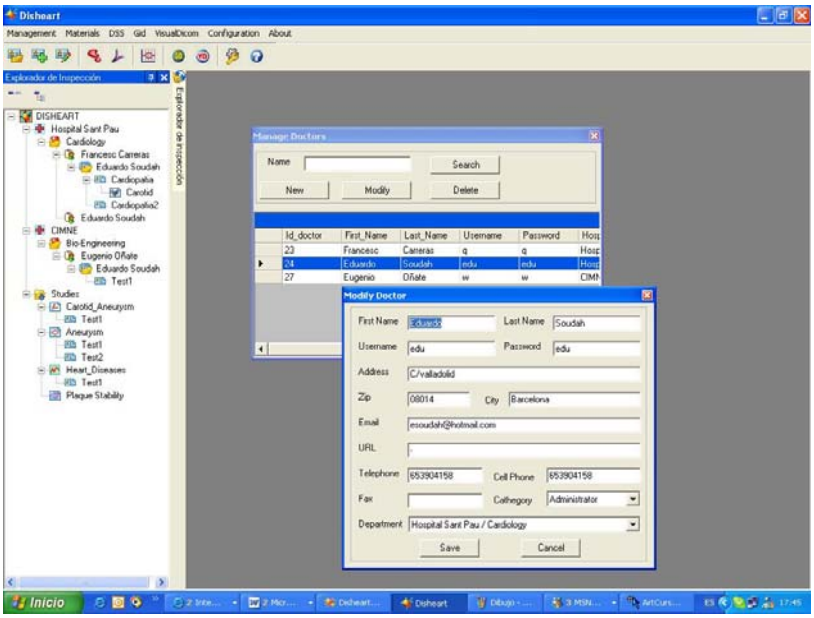

Figure 33 Insert a new Doctor

Through this window he can manage:

- *Management of the doctor added in the database.*
- *Add of New doctor.*
- *Modify the information of the doctor.*
- *Delete a doctor.*
- *Search a doctor added in the system.*

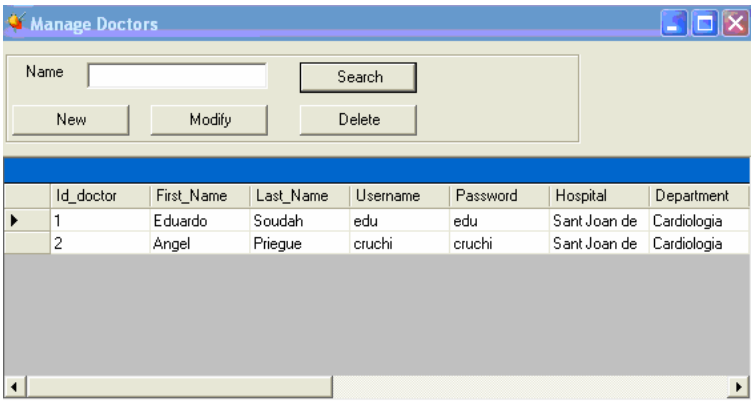

Figure 34 Search a Doctor

The next information, the first name, last name, address username, password, address, e-mail, telephone, URL, fax, Cell phone, relation Hospital/department and Category are required to define a new doctor. The category field can be System manager, Expert user or User in function of the requirements of the system. At beginning of the system only will have one System manager to management the hospital, departments and doctor and all the doctors solely can be a normal User, (to further information about the task of user see Deliverable 1st, "Specification of DisHeart System".) The button Save and Cancel are used to manage the adding or deleting the new data inserted

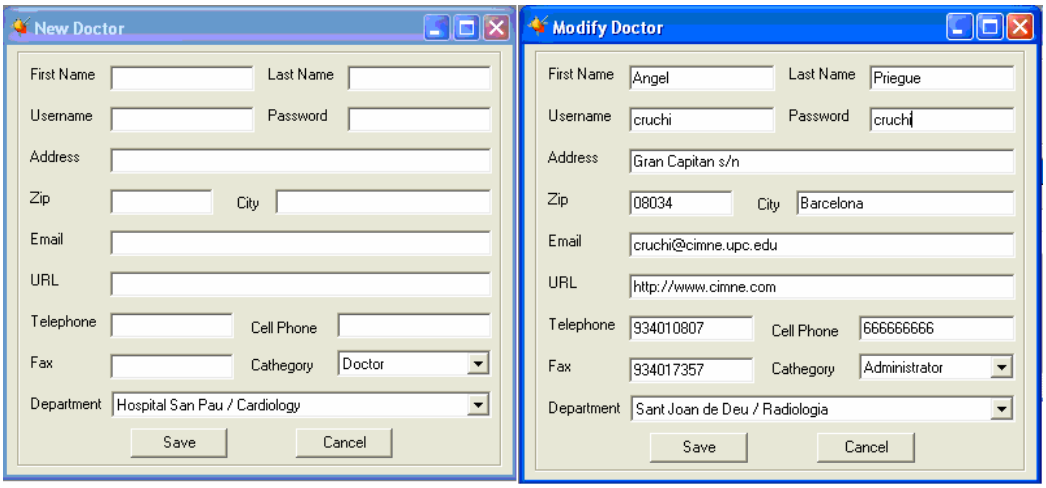

Figure 35 Insert or Modify Doctor data

The same window allows modify of the doctor. The tools used are the same of the window used to insert new data. The next picture shows how the interface permits to manage or modify the data present in the database of the hospital personal

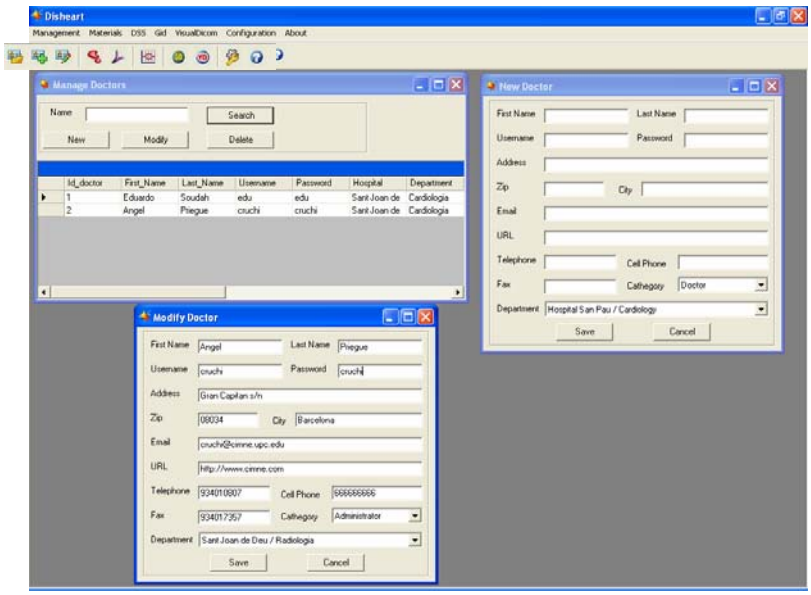

Figure 36 Modify Data Doctor

14.6 Patient Management

This section explains how a normal user can management (Add, Modify, Delete, Creation a New medical report…) the information of the patients.

To create a report, the user can go to Management → Pacient or click on the first icon that is shown on the tool bar. The system DISHEART DSS shows the next dialog windows, where all patients are listed.

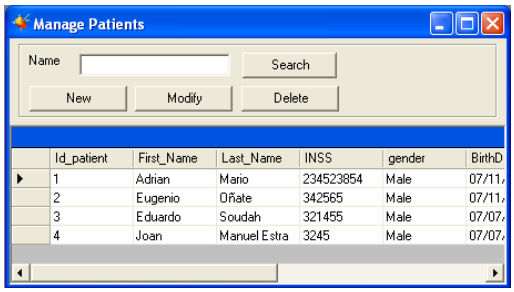

Figure 37 Manage Patients

 In the case of needing to introduce a new patient, the users simply have to press the New button and the next informative dialog will automatically appear for the doctor or user to fill it in. The parameters to fill in are:

- *INSS Num, Social Security number*
- *First name, last name, patient's first and last name*
- *Gender, birth day, address, phone and movil phone.*

Warning: It is not possible to register two patients with the same INSS number.

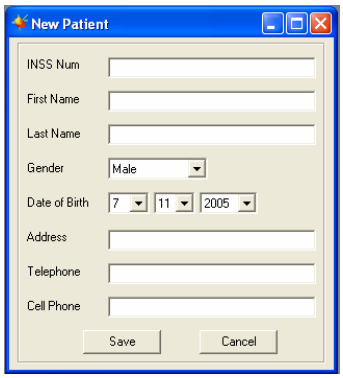

Figure 38 New Patients

Once filled all patient's data, they are stored on the database by pressing the Save button. Also these data can be modified.

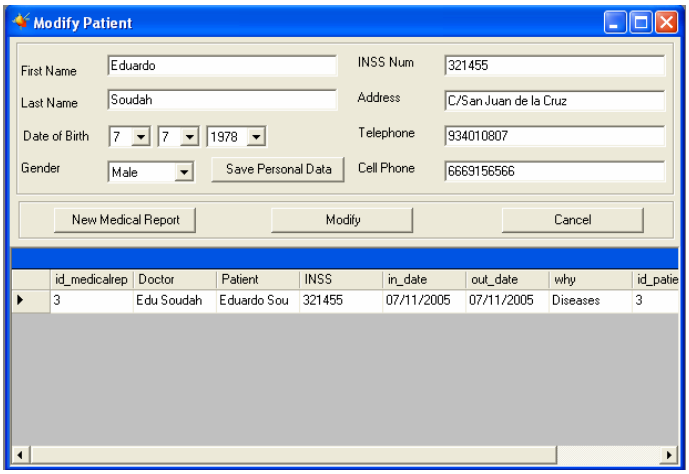

Figure 39 Modify Patient

In the case that a new medical report needs to be done, the user only need to press the New Medical Report button, and the next window will appear with the following fields.

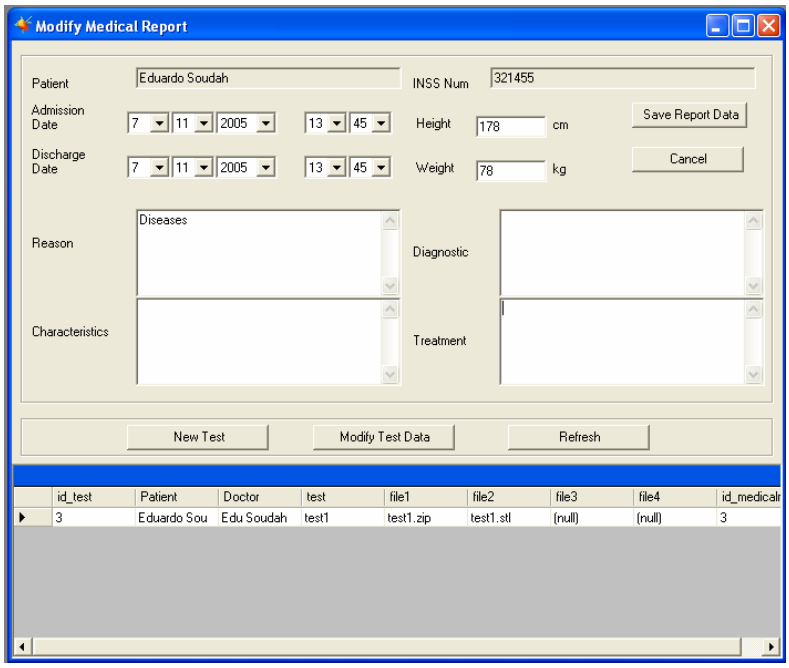

Figure 40 Modify Medical Report

Patient's personal details, Patient's admission details, Weight, Height, Reason, Diagnostic, Characteristics, Treatment. Once these fields have been filled in, the user is required to create a new test - New test –, modify a test already introduced in the database – Modify Test Data –, or refresh the database with the existing tests – Refresh.

However, when the user wants to make a test to the patient in order to complete the report, it is necessary to push the New Test button. A Wizard will then guide the user through the report completion process.

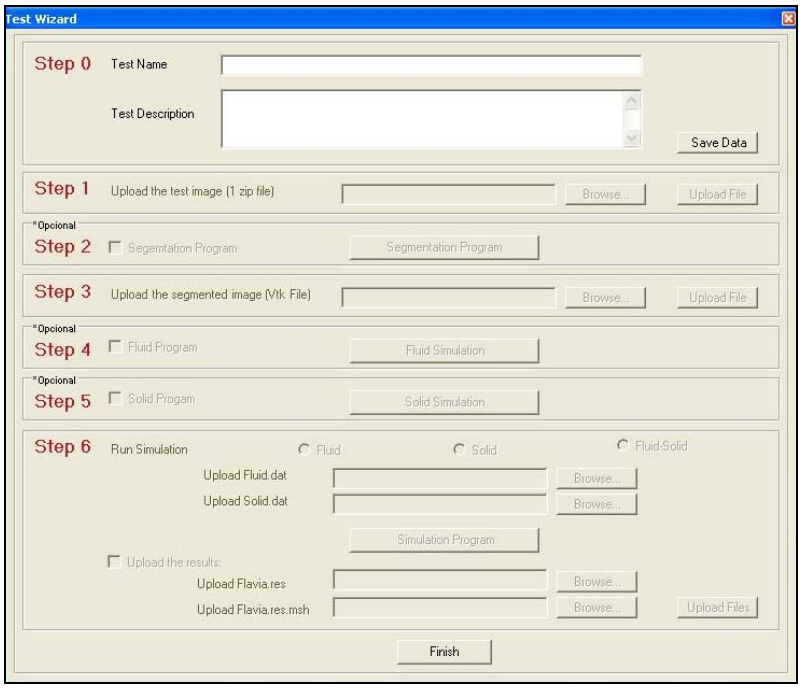

Figure 41 Help-test Interface (Wizard)

Once a stage has been successfully accomplished, it is depicted in green, and the user can follow on with the next stage. The pending steps are depicted in red.

Thanks to the Wizard, it is possible to store in the data base all kind of images in DICOM format, a divided into segments, their corresponding meshes, and the results that will later be used to train the neural network.

To know more about the management of the image segmentation, see WP2. System functionalities will be detailed in Visual Dicom User Manual.

With this brief explanation we aim at presenting the methodology to store medical images, and the materials needed for the analysis in the database through the DISHEART.DSS system.

A medical report can also be managed through Management → Test, by selecting the test patient from the patient list stored in the database. Next, a new window appears, where all the medical reports associated to that patient are listed. In case the user wants to modify an existing report, he only needs to press the Modify Test Data button.

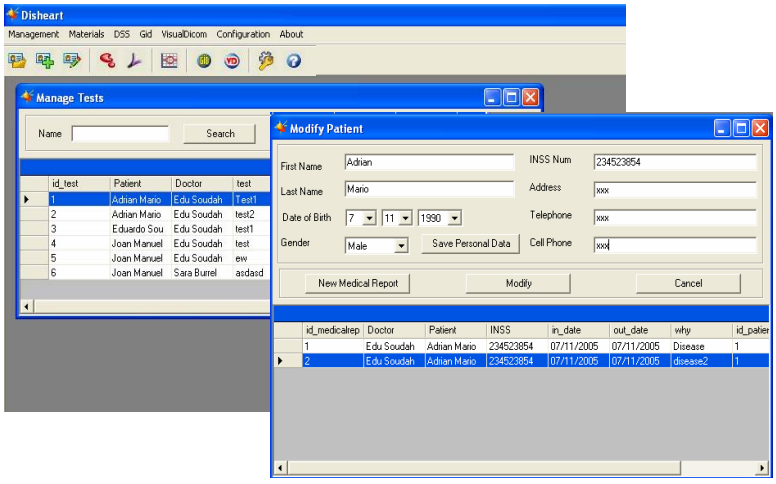

Figure 42 Management test

In case a report test has not been concluded, the user will be able of taking it up again where he left it. On that case, the user has introduced the image in the database, in DICOM format, has divided the image into segments using the software developed by the University of Zaragoza "Visual DICOM", and the image has been stored in the database until its simulation.

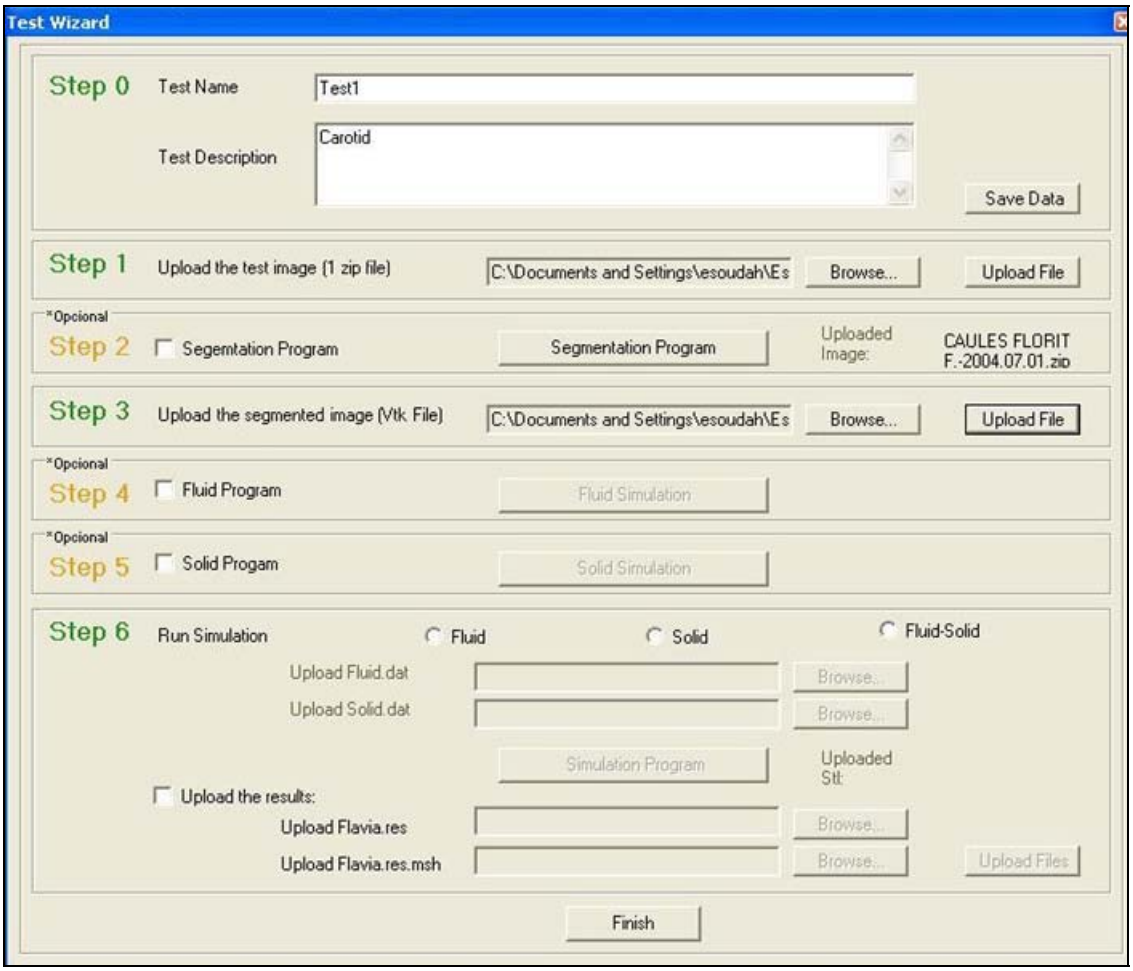

Figure 43 Help-test Interface

In order to the system can integrate other input files, the step 2, 4 and 5 are optional.

This idea gives more flexibility to the system. If for example, the user has a VTK file can be upload without the necessity to use VisualDicom, the segmentation file will save in the database.

The same fact happens with the fluid.dat and solid.dat in the Step 4 and Step 5.

In the Step 6, three different simulations(Fluid problem, Solid Problem and Fluid-Solid interaction problem) has been implemented with the idea of the create a flexibility program.

This new option gives to the user the possibility of study new problems according to the future applications in Disheart.DSS.

14.7 Material Management

There are two ways of managing the materials, by means of the tool bar Materials → Fluid or Materials → Solid, or pressing the following buttons:

Management of fluid materials

Management of solid materials

Figure 44 Disheart Interface

The management of solid materials is done by means of the following work windows:

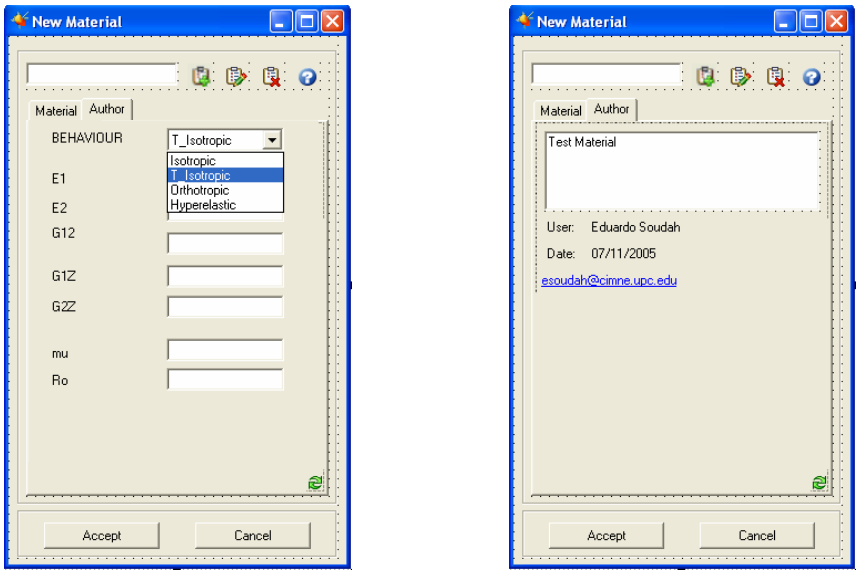

Figure 45 New Material

14.7.1 Description of the Disheart Icons.

 Adding new Material

 Delete existing Material

 Modify existing Material

 Help

 Refresh the information.

With the first window, the user selects the material behaviour and assigns to it the corresponding properties. With the second window, the user can add extra information to the material, together with the user name and the creation date of the material. Once this information has been introduced, the new material is stored in the database by pressing Accept

---

Note: To establish the types of material behaviour, we used the specifications drawn up by the University of Zaragoza. We have defined four types (Isotropic , T_isotropic, Orthotropic and hyperelastic), which are used for the artery behaviour.

Note: A material can only be modified by its creator.

15 DISHEART SYSTEM.

In Disheart.DSS two different methods have been implemented to fulfil all the specification of the features and the SME´s requirements set by the partners.

The first model is "Specific Patient Case"(SPC) and the second are the artificial neural networks for the aneurysm rupture, carotid profile and heart diseases(DSS). All the results obtained by the user will be stored in disheart-database.

15.1 Specific Patient Case.

The target of this method is to study a specific disease of the specific patient. The doctor can get images of the patient, segmentation the images, create the mesh, impose the boundary conditions, start the simulation and analyze the results with Disheart.DSS.

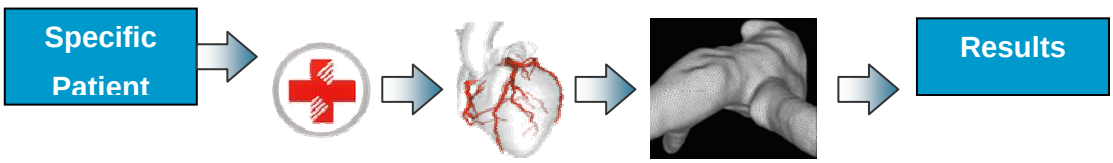

This method allows analyzing the results for implantation of the stent, graffing process, stability plaque, among others, by the user. For example, which will be the maximum wall stress in a stent implant? O which is the best angle in by-pass (graffing) operation?

15.2 How?

A Wizard guides the user through the whole process of introducing a study in the database. The different stages are thus reached in an ordered, synchronized way. The stages that have been successfully finished are depicted in green, and the pending steps are depicted in red.

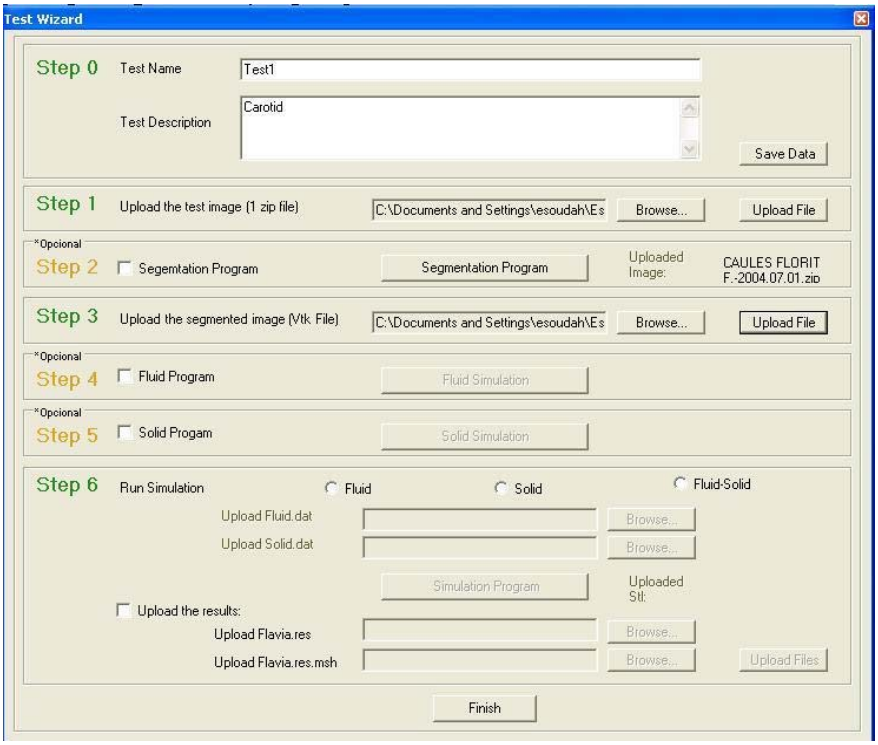

Figure 46 Test-help Interface

We show as follows the different steps in a SPC.

Step 0: Test name and description. The name of the test to be done is introduced, together with a brief description of it.

Step 1: Upload the test image. At this stage the user selects the image in DICOM format to be assigned to the patient. To assign this DICOM, a browser is automatically opened when pressing the button Browse…, as shown below.

Note: The images in DICOM format need to be zipped before uploading them to the database. This speeds the data transmission process, and enhances the storage capacity of the database. The browser allows exploring the system folders. Once selected the image, it is stored in the database by pressing the button Upload File.

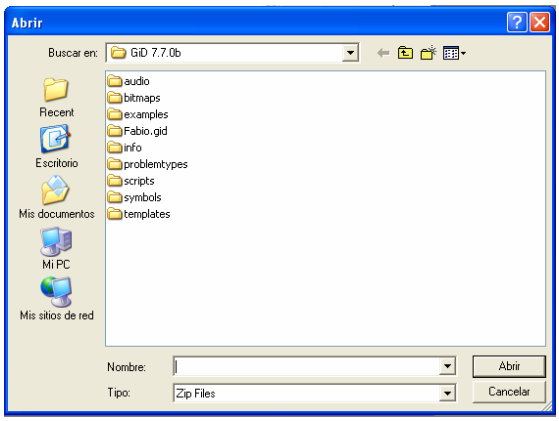

Figure 47 Browser

Step 2: (Optional) Perform the segmentation of the image. At this stage, the image is divided into segments by using the software VISUAL DICOM, developed by the University of Zaragoza (see WP2 and Section 3 for more information). By pressing the button Segmentation Program, a window is automatically opened with the loaded image, and it is cleaned and filtered (segmented) using the several available tools.
The step 2 is optional because if the user wants to create his own geometry, he could do it in a few steps. It allows a system more tolerant with the requirements needed by the user. (Section 2-Create geometry with GiD)

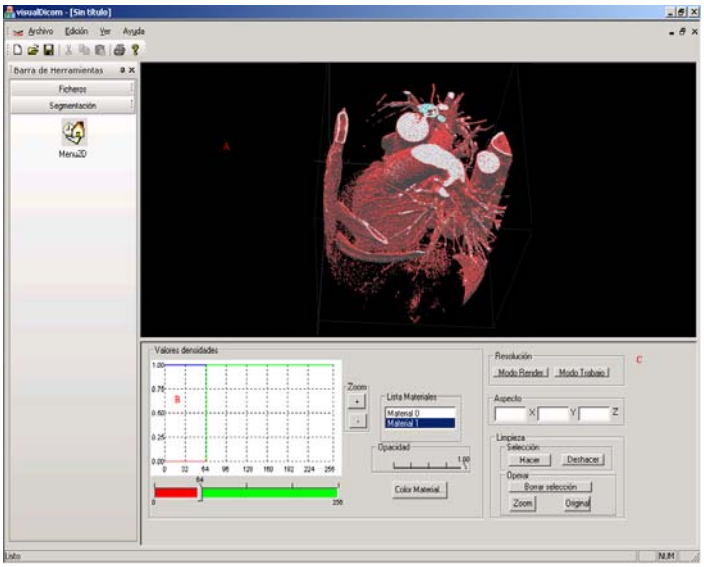

Figure 48 Visual Deco

Step 3: Upload the segmentation image. Once an image has been divided into segments, VisualDICOM offers the possibility of storing it with format STL or VTK(See Section 3)

Step 4: (Optional) Perform Simulation. The STL or VTK file – depending on the storage format chosen in the previous step – is read and a mesh of the image geometry is done to be analyzed later. For this post-process stage we use the software GiD developed by CIMNE. Further more information in Annex 1-"Medical images with GiD."

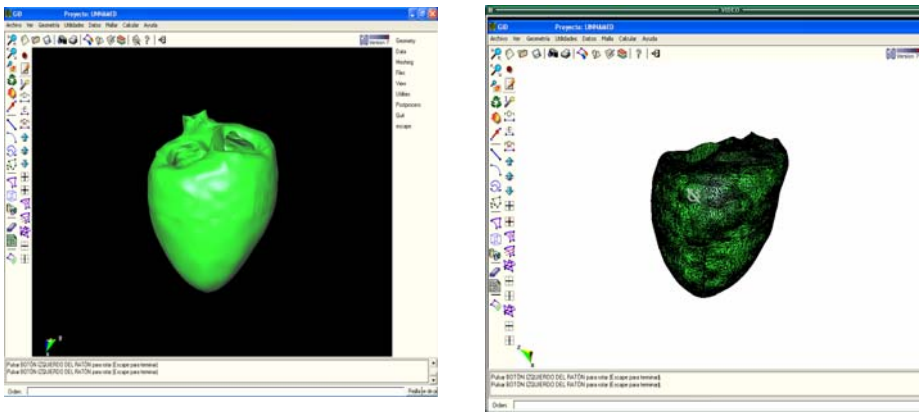

Figure 49 Mesh GiD

After the mesh has been generated (See Annex 1- "Medical Images with GiD-Section 4), the boundary conditions for the fluid and solid

Step 5 :(Optional) After the mesh has been generated (See WP3), the boundary conditions for the fluid (See Annex 1-"Impose the boundary conditions with TDYN") and the solid are established, and then the numerical simulation – based on the FEM method – starts.

Step 6: The user can select 3 different options, fluid, and solid, fluid-solid, to assign the corresponding files and run the simulation. Once finished the calculations, the results are uploaded to the database.

When the calculation process has finished, the SPC record can be consulted to verify that the new test has been successfully added.

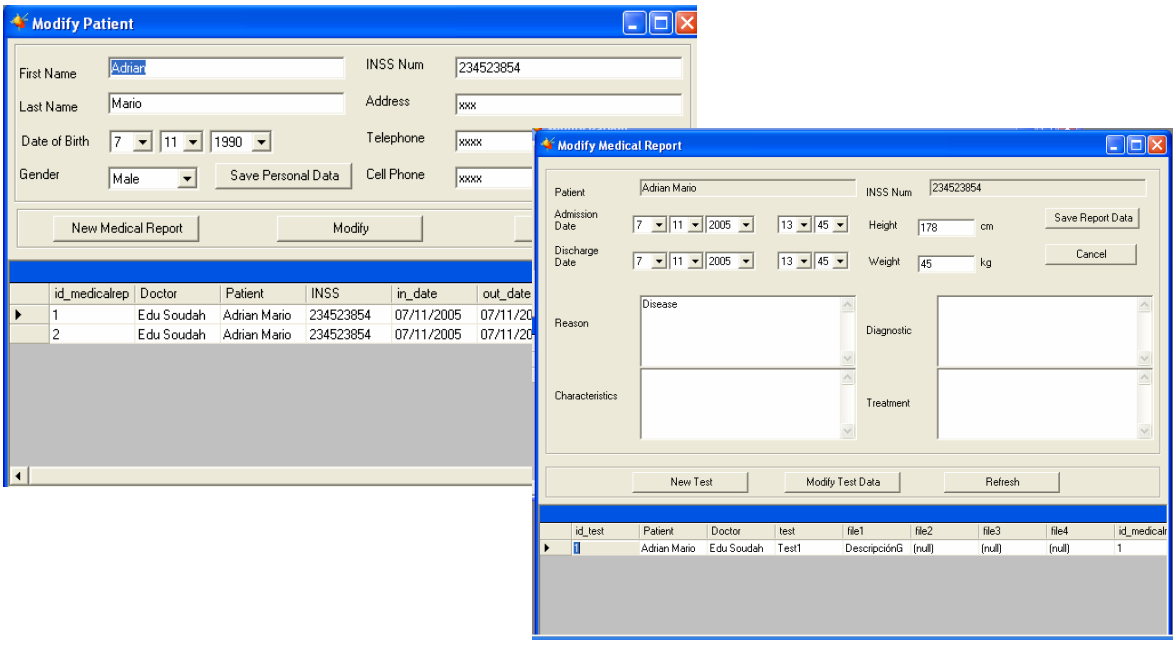

Figure 50 Modify Medical Report

This method helps the doctors to analyze results and understand which the best solution is for a specific disease. All the results will be stored in the Disheart database so other doctors could seek advice in the results of the similar disease (Decision support System)

15.3 Artificial Neuronal Networks.

The second method implemented in Disheart.DSS is the Artificial Neural Network (ANN) (See WP 6). The idea of this method is to define a disease, to characterize the geometry, to generate a lot of study cases, to save in the Disheart-Database and to train the neural networks to create a Decision Support System (DSS) for disease defined. Three different artificial neural networks (aneurysm ruptures, carotid profile and heart diseases) have been implemented according to the specification of Disheart.DSS (See WP1).

The process to create a DSS of one disease is explaining in the follow picture.

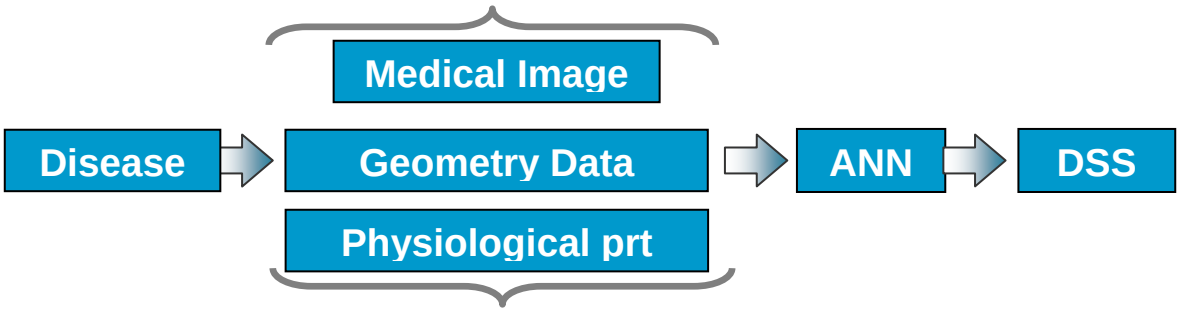

The user to define the disease will have to characterize the disease and to assign the geometry factors and physiological parameters. When the disease is defined, the user will be able to generate all the data files and save in the Disheart Database using the SPC wizard, but the only person who is able to train the neural network would be the expert user.

 The user can selected among the three different DSS through DSS in the Main Interface or a the DSS-Windows (figure 32). To see further information about the DSS, see in Deliverable 6_1

Aneurysm, DSS to calculate the stresses produced in the wall of the different geometry aneurysm.

Velocity profile in carotid, DSS to calculate the velocity inside the carotid aneurysm.

Heart Attack, DSS to calculate the probability to suffer heart diseases.

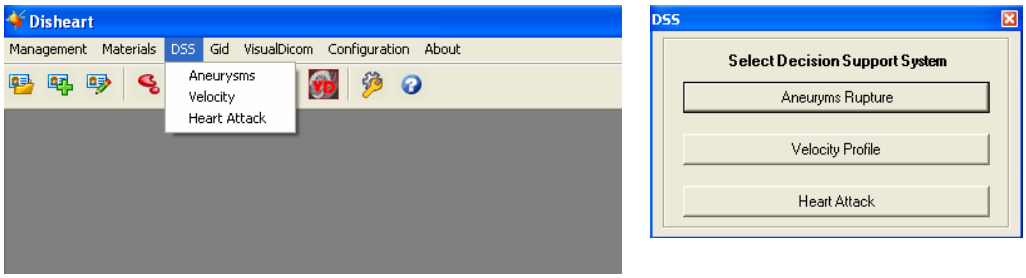

Figure 51 Manage Test

15.4 Carotid Aneurysm under different inlet conditions.

Through this window, figure 35, the doctor will be able to introduce the data-parameter of the inflow profile and he will obtain in real time the velocity profile in this area. The doctor carries out studies about different velocity profile, that's mean, different cardiac pulses.

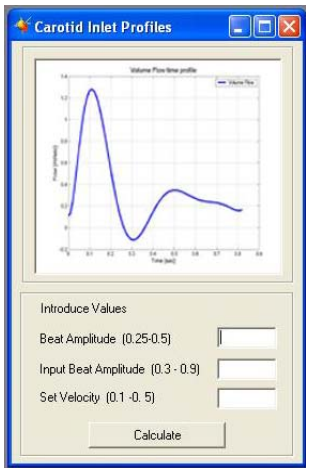

Figure 52 Carotid Aneurysm ANN

To characterize the inflow profile, three variables have been used, the beat amplitude, the input beat amplitude and the velocity set. In the following picture the meanings of the variables are shows.

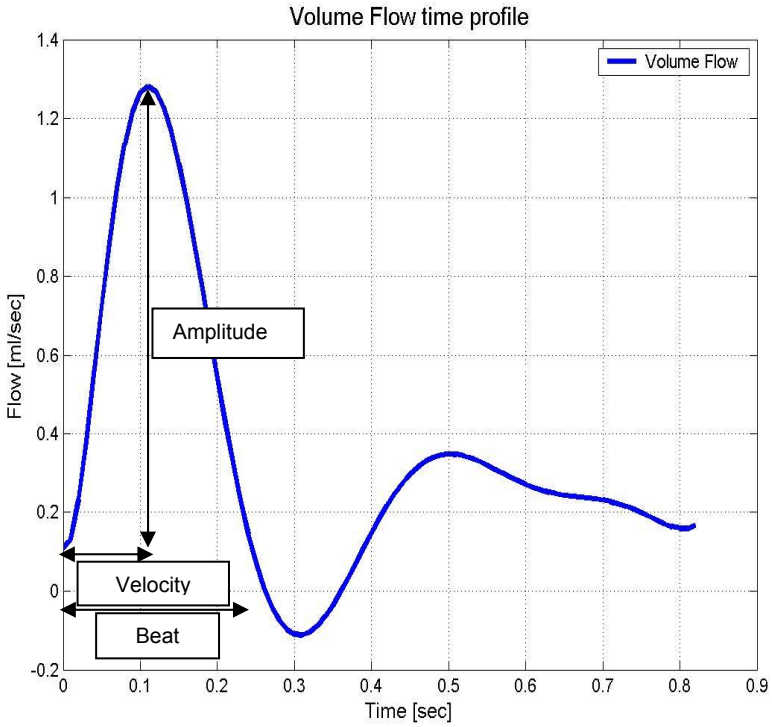

Figure 53 Carotid Aneurysm Profile

When the user creates a new case the system will save the results and will show in the tree in the folder Studies Carotid-Aneurysm.

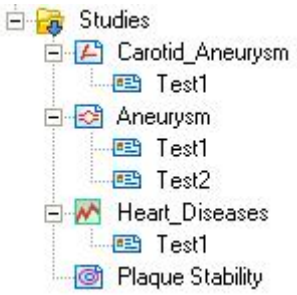

Figure 54 Tree-ANN

If the user select one study will be able to view, edit (document word See in Annex 3) and delete the study.

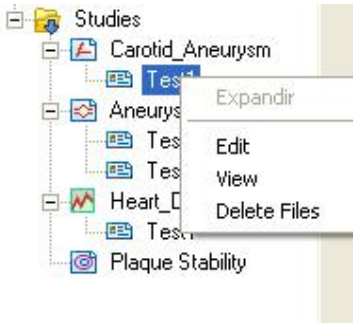

Figure 55 Menu Tree

Further information about the ANN see WP6 ("Integrated prototype Disheart.DSS"), WP7 –D7.1 ("Validation of Disheart DSS for different cardiovascular problem").

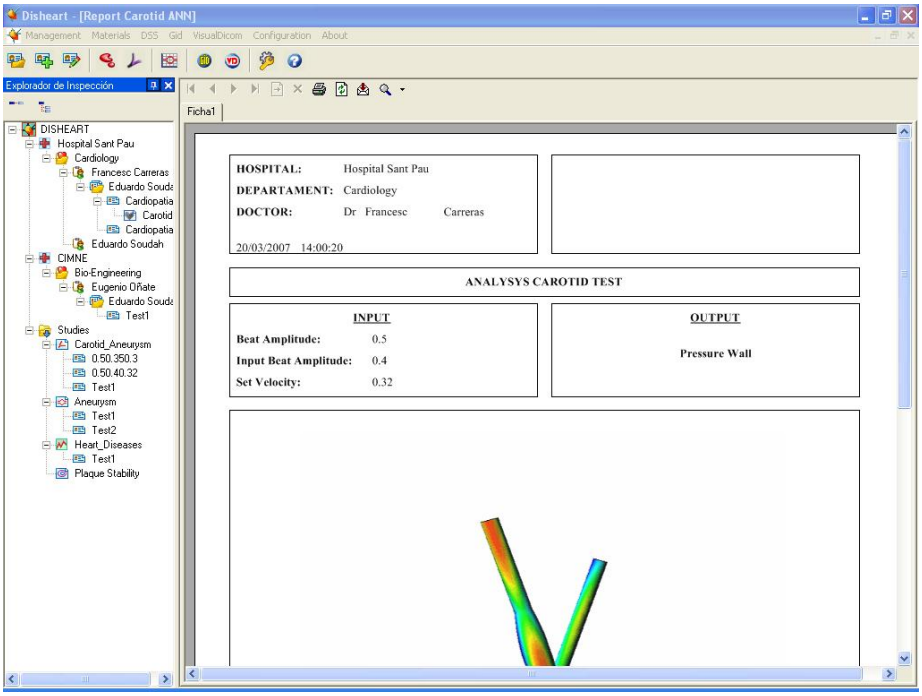

Figure 56 View Carotid ANN.

15.5 Aneurysm Rupture.

ANN, Artificial Neural Networks for Aneurysm Rupture. If the doctor wants to study a specific case of aneurysm rupture, only it is necessary select one of the four classes of the aneurysm, sphere, Cosine-Exponential… and introduces the values who determine its behavior.

Through the first windows figure 36 the doctor select the Aneurysm type.

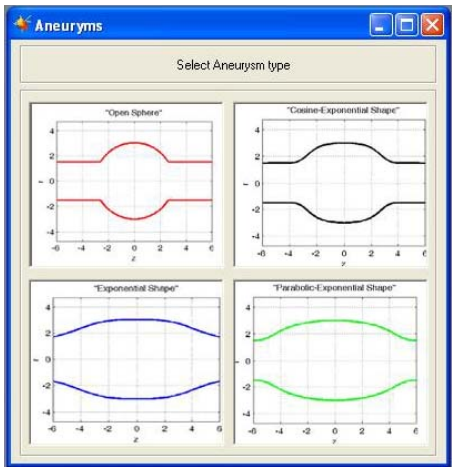

Figure 57 Aneurysms Rupture ANN

And through the following picture, figure 36, he introduces the characteristic values.
When the doctor runs the ANN, in few second, the system shows the main stresses in the wall of the aneurysm. With these results the doctor will be able to decide if it is necessary to do other test to the patient.

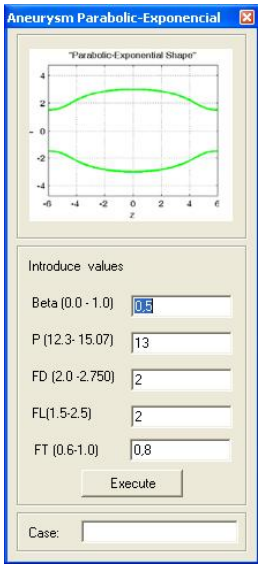

Figure 58 Sphere Aneurysm ANN

When the user creates a new case the system will save the results and will show in the tree in the folder Studies-Aneurysm. If the user select one study will be able to view, edit (document word- See in Annex 3) and delete the study.

To characterize the geometry the next equations have been used.

$$R(Z) = R_a + \left(R_{an} - R_a - c_3 \frac{Z^2}{R_a^2} \right) \exp\left(-c_1 \left| \frac{Z}{R_a} \right|^{c_2} \right),$$

Where,

$$c_2 = \frac{4.605}{(0.5 L_{an} R_a)^{c_1}},$$

$$c_3 = \frac{R_{an} - R_a}{R_a (0.8 L_{an} / R_a)^2},$$

The meanings of the variables are shown in the following picture.

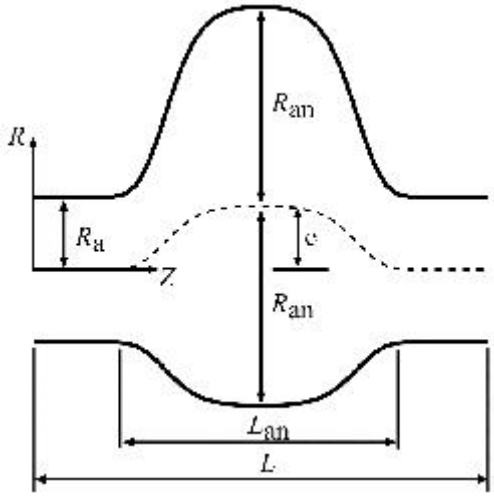

Where the dimensionless parameters are:

$$F_R = \frac{R_{an}}{R_a}, \qquad F_L = \frac{L_{an}}{R_{an}},$$

$$F_E = \frac{e}{R_a (F_R - 1)} \qquad F_T = \frac{t_{an}}{t_a}$$

And P means the pressure inside the aneurysm.

Further information about the ANN see WP6 ("Integrated prototype Disheart.DSS"), WP7 –D7.1 ("Validation of Disheart DSS for different cardiovascular problem")

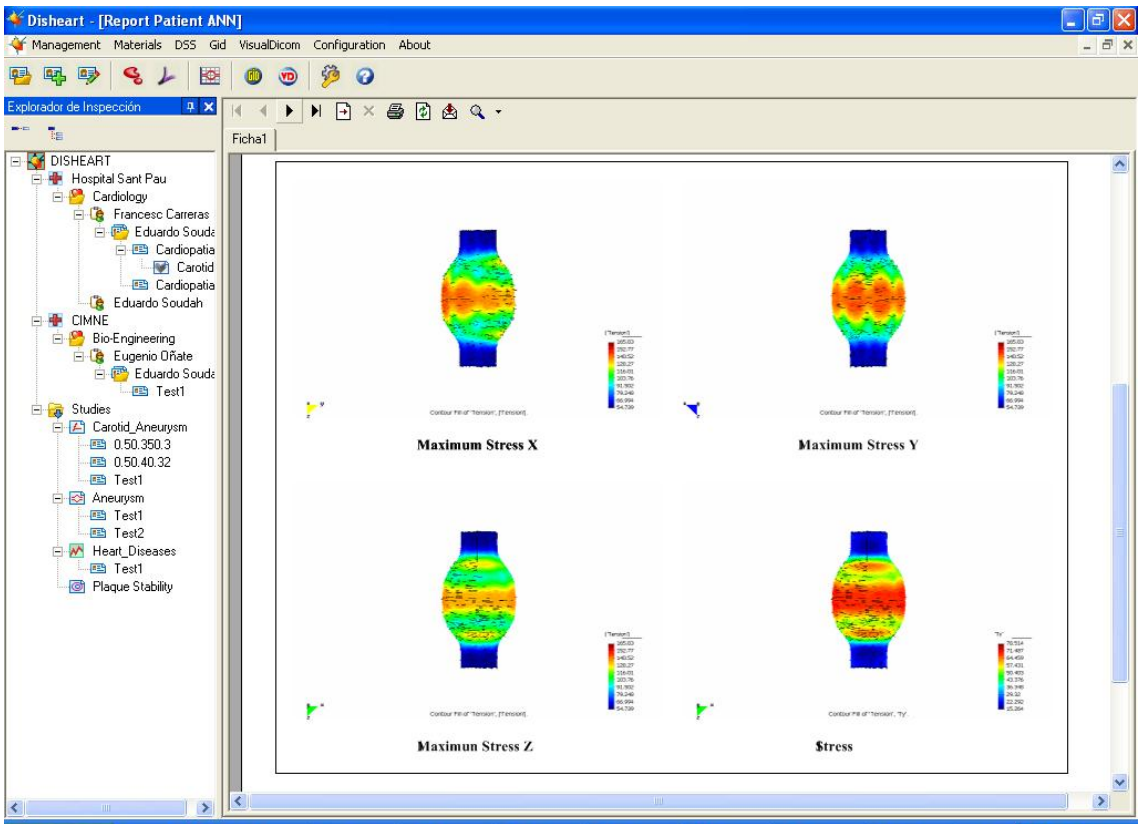

Figure 59 View aneurysm ANN.

15.6 Heart attack.

Through this window, figure 38, the doctor will be able to introduce the data-patient and he will obtain in real time the heart-disease of the patient.

The patient will only have to answer the questions showed in the test and he will be able to know if he suffers some heart-disease.

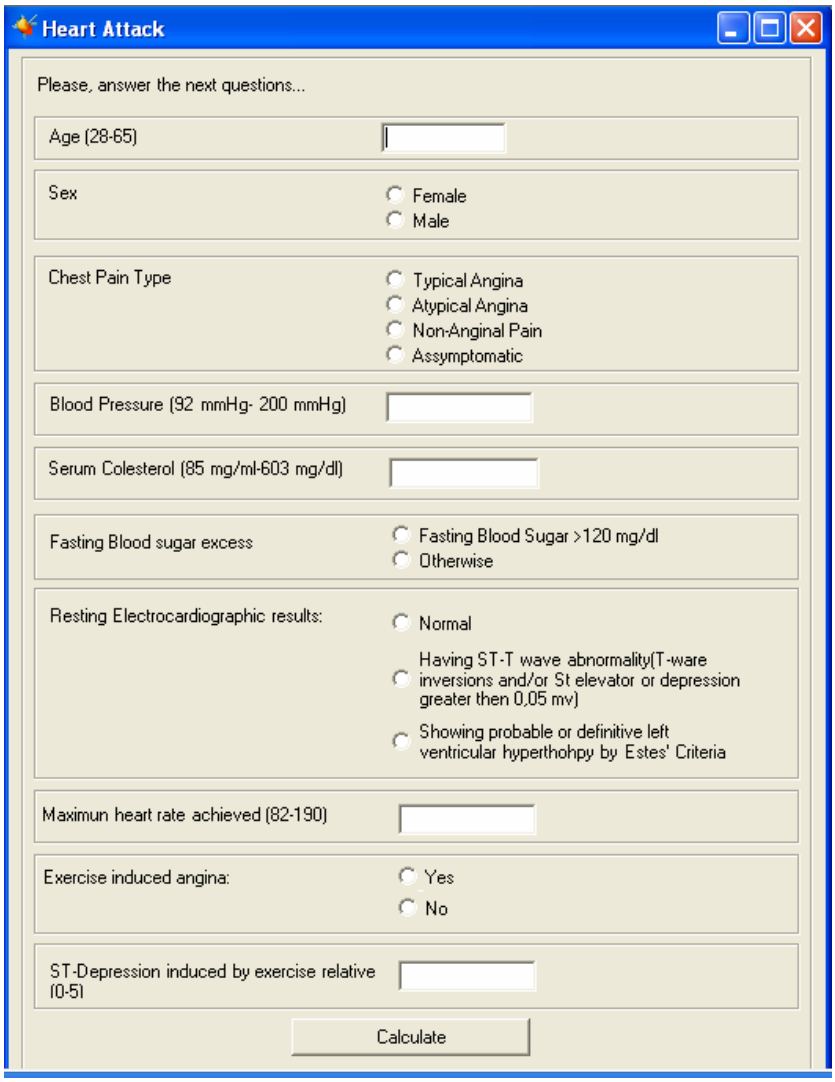

Figure 60 Heart Attack ANN

When the user creates a new case the system will save the results and will show in the tree in the folder Studies-Heart Diseases. If the user select one study will be able to view, edit (document word-See in Annex 3) and delete the study.

Further information about the ANN see WP6 ("Integrated prototype Disheart.DSS"), WP7 –D7.1 ("Validation of Disheart DSS for different cardiovascular problem").

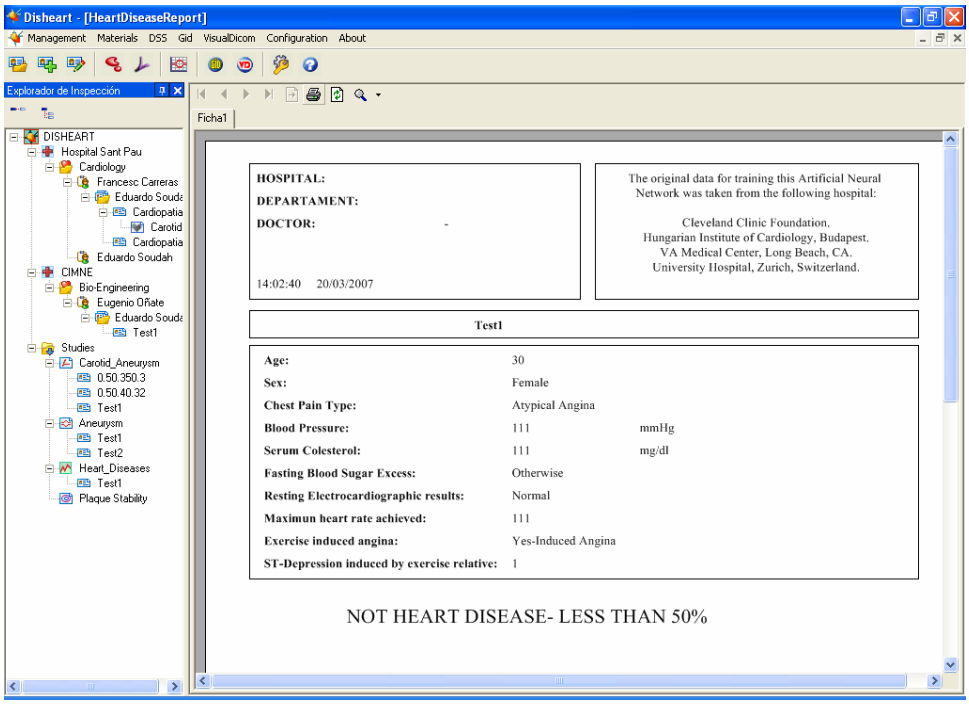

Figure 61 Heart diseases ANN.

15.7 System Preferences.

For begin to use DisHeart.DSS is necessary to configure different paths. In the first tab, the first path explain where is Pre-post Processor (GiD), the second path where is the fluid program (TDyN) and the third path where is solid program

In the second tab the user has to assign the segmentation program path. In the third tab is where the simulation of ANN are generated. And in the last tab is a temporal DisHeart.DSS folder in which it saves some information about the configuration of the system.

To define these paths are the preferences of Disheart.DSS and it is the first thing what the user has to do it when he uses Disheart.DSS.

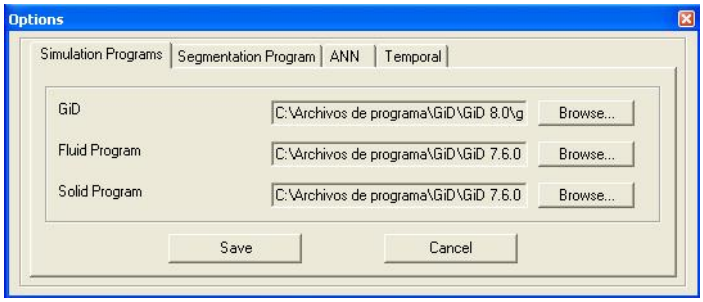

Figure 62 System Preferences

16 GiD.

Introduction.

 In the case of needing to use GiD only have to press this Icon and automatically will open it. Further more information about Gid in http://gid.cimne.upc.es or www.cimne.upc.es. To download the manual and tutorial go to http://www.gidhome.com/support/su04.subst.
Gid had been integrated in the system how another new tool. To know the new tools implemented in GiD see WP6 and this section..

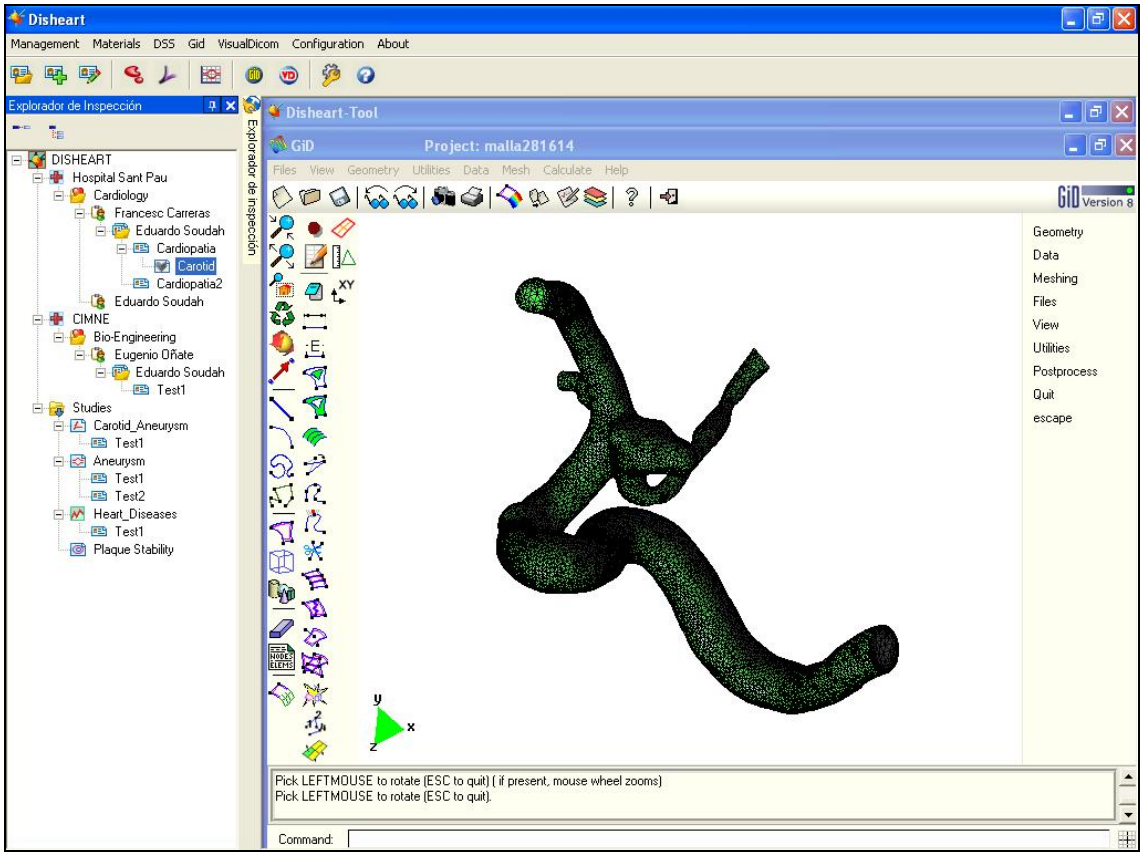

Figure 63 Disheart-GiD

16.1 Medical images with gid.

GID is the Personal Pre/Post-processor used in this project to generate finite element meshes from three-dimensional medical
images.

Digital medical images are normally distributed in DICOM format. The Digital Imaging and Communications in Medicine (DICOM) standard was created by the National Electrical Manufacturers Association (NEMA) to aid the distribution and viewing of medical images, such as CT scans, MRIs, and ultrasound [Dicom-Home, idoimaging.com].

A single DICOM file contains both a header (which stores information about the patient's name, the type of scan, image dimensions, etc), as well as all of the image data (which can contain information in three dimensions). Normally the original DICOM file contain information which is

not relevant to the process of mesh generation: original data is noisy and contain information regarding other structures.

In any case, a preprocessing stage must be applied to the original data in order to:

- Volumetric denoising: noise is present in the process of data acquisition. Accurate segmentation techniques and filters are applied in [Visual DICOM].

- Isovalue selection: mesh extraction from imaging data requires the selection of suitable boundary isosurfaces in order to the boundary volume be well defined.

This preprocessing is described in [Visual DICOM]

After the preprocessing what we have is a file with the image data and the value of the isosurface value defining the boundary of the volume of interest.

The imaging data V is given in the form of sampled function values on rectilinear grids. We assume a continuous function is constructed through the trilinear interpolation of sampled values for each cubic cell in the volume.

The format used to read the medical data is VTK structured point as it is agreed in [Visual Dicom]. The description of this format can be found in [VTK-Format]. The image in this format can also be visualized and manipulated with Insight Itk [Itk].

The overall process is depicted in figure [84]

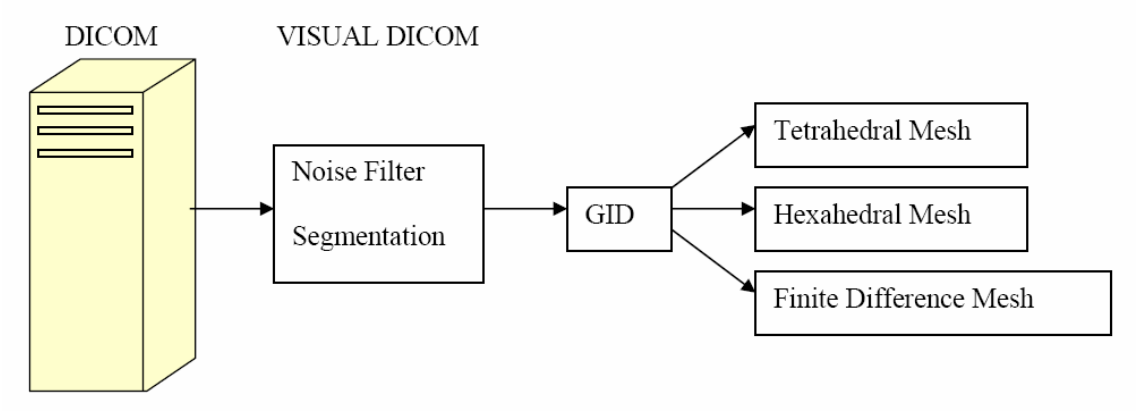

Figure 64 VTK Process

16.1.1 Reading VTK structured points inside GiD.

Having segmented the 3D image we end with a .vtk file and an isosurface value. Within GiD we can read and convert it into a discretized model suitable to be used in analysis module. A routine was implemented in this project in order to be able to read VTK structured points format either binary or ASCII.

Besides three methods has being implemented:
Marching cube: generate a triangle mesh from which a tetrahedral mesh can be generated.
Dual contour: generate an hexahedral mesh.
Finite difference: generate an orthogonal hexahedral mesh.

In the following a model corresponding to carotid artery is used to describe the three options inside GiD. As mentioned before the original model was preprocessed as it is described in [Visual DICOM]. The file used in the examples is venabifu3_fil2.vtk

The geometry of the volume is:

	X	Y	Z
DIMENSIONS	512	512	89
ORIGIN	0.0	0.0	0.0
SPACING	0.695	0.695	0.25

The model contains 23330816 data points and the isovalue used is 1.0.

16.1.2 Marching Cube.

The Marching Cubes algorithm [MC] visits each cell in a volume and performs local triangulation based on the sign configuration of the eight vertices. If one or more vertex of a cube have values less than the user-specified isovalue, and one or more have values greater than this value, we know the voxel must contribute some component of the isosurface. By determining which edges of the cube are intersected by the isosurface, we can create triangular patches which divide the cube between regions within the isosurface and regions outside. By connecting the patches from all cubes on the isosurface boundary, we get a surface representation.

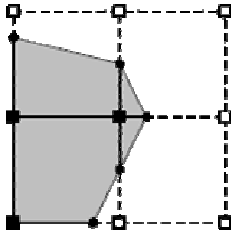

Figure 65 Marching Cube sample in 2D mc_sample.png

In GiD we can read volume in VTK structured point format and generate the boundary mesh for an isosurface using the command GiD_VTKsp2MCube:

-np- GiD_VTKsp2MCube venabifu3_fil2.vtk 1.0

The generated mesh contains 27049 nodes and 10486 triangles. See figure mc_venabifu3_fil2 .png to see a rendering of the resulting mesh inside GiD.

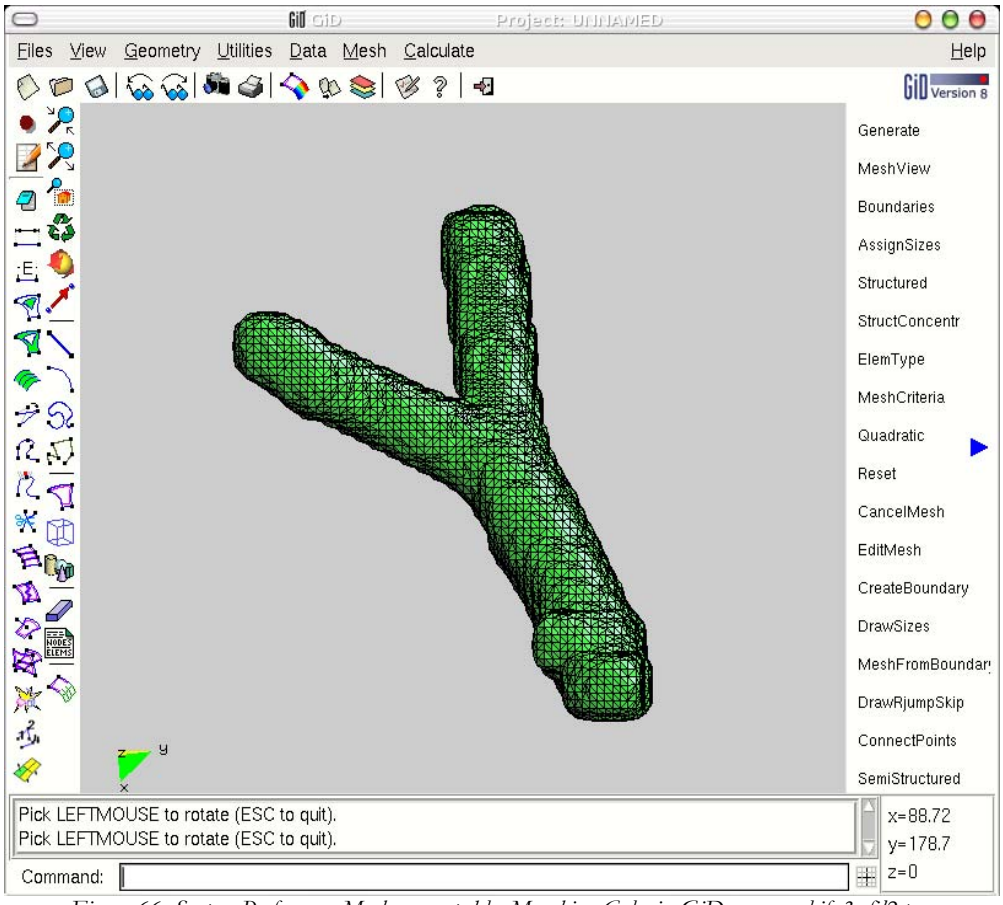

Figure 66 System Preferences Mesh generated by Marching Cube in GiD mc_venabifu3_fil2.png

After generating the triangle mesh the tetrahedral mesh can be generated by issuing the command: "Meshing MeshFromBoundary 1"

The resulting tetrahedral mesh contains 51429 tetrahedral. See figure following

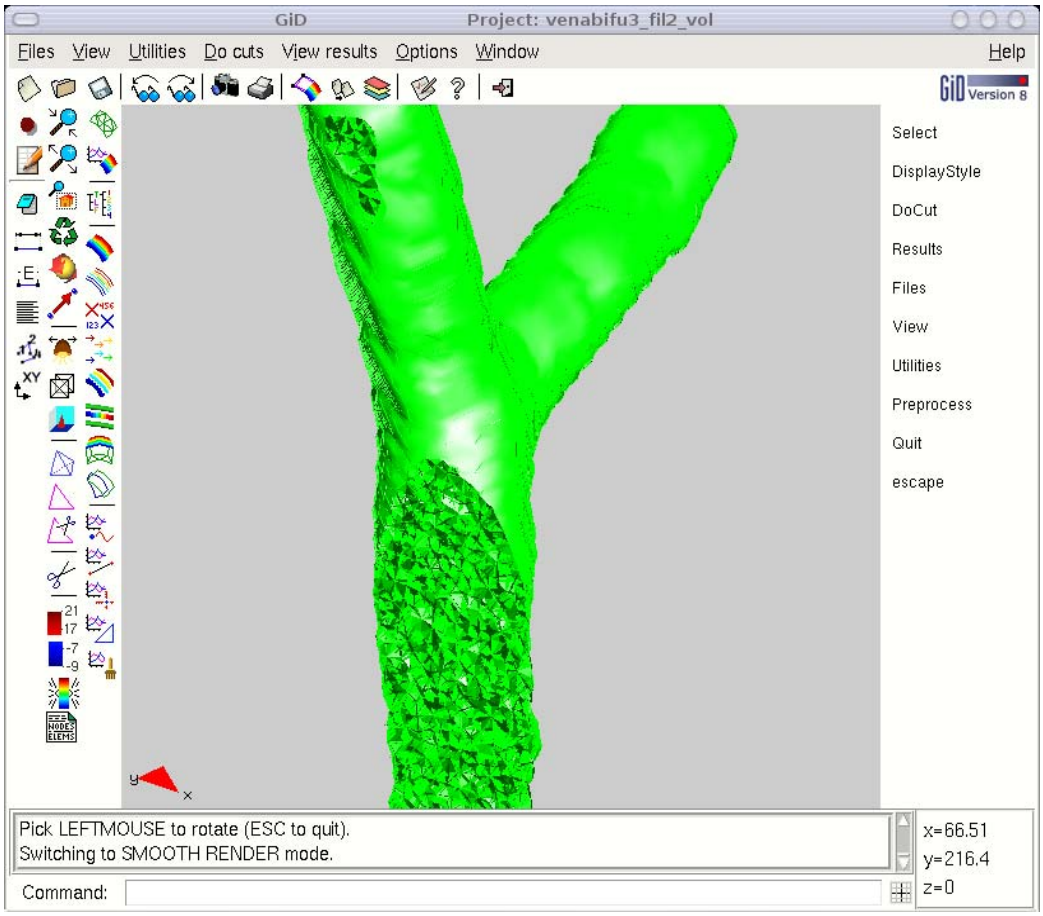

Figure 67 mc_vol_cut.png.

16.1.3 Dual contours.

Dual Contouring [DC] analyzes those edges that have endpoints lying on different sides of the isosurface, called sign change edge.

Each sign change edge is shared by four, and one minimizer is calculated for each of them by minimizing a predefined Quadratic Error Function.
The QEF is defined as follows:

$$QEF(x) = \sum n_i (x - p_i)^2$$

where n_i, p_i represent the position and unit normal vectors of the intersection point respectively.

For each sign change edge, a quad is constructed by connecting the minimizers. These quads provide an approximation of the isosurface.

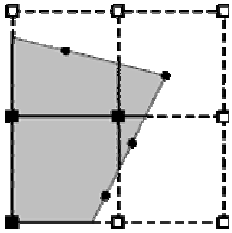

Figure 68 Dual contour sample dc_sample.png

The uniform hexahedral mesh extraction algorithm is simple. We analyze each interior vertex (a grid point inside the volume) which is shared by eight cells. One minimizer is calculated for each of them, and those eight minimizers construct a hexahedron.

In GiD we can read volume in VTK structured point format and generate the an hexahedral mesh for the volume bounded by the given isosurface using the command GiD_VTKsp2Hexa:

-np- GiD_VTKsp2Hexa venabifu3_fil2.vtk 1.0

Resulting hexahedral mesh is made of 18941 nodes and 15091 hexahedral elements. See figure dc_venabifu3_fil2.png for a rendering of the resulting mesh.

16.2 Finite difference mesh

A finite difference mesh is a mesh of orthogonal hexahedra which are axis aligned.

In GiD we can read volume in VTK structured point format and generate the finite difference mesh (orthogonal hexahedra) for the volume bounded by the given isosurface using the command GiD_VTKsp2OrthoHexa:

-np- GiD_VTKsp2OrhoHexa venabifu3_fil2.vtk 1.0

Resulting hexahedral mesh is made of 16442 nodes and 12859 orthogonal hexahedral elements. See figure df_venabifu3_fil2.png for a rendering of the resulting mesh

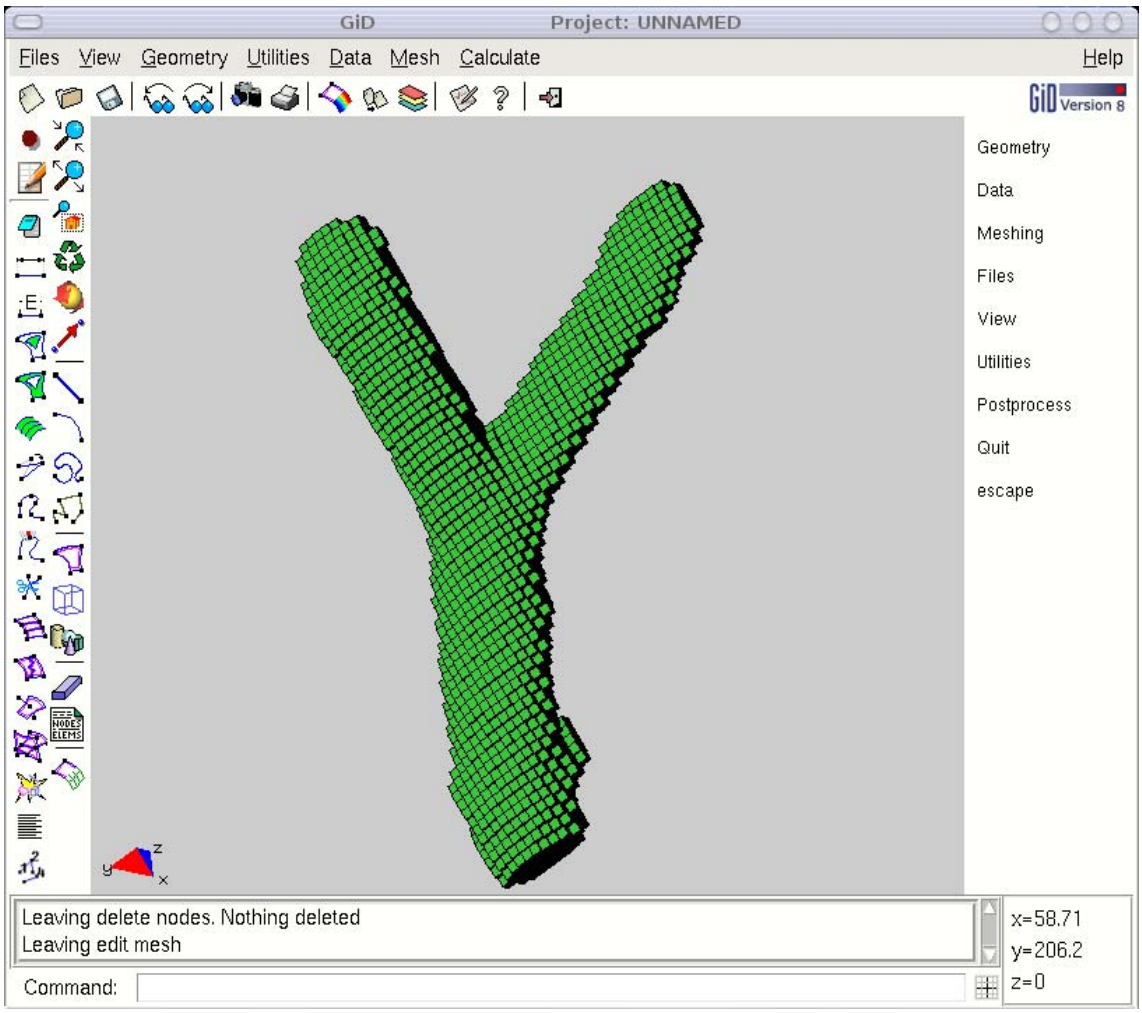

Figure 69 Finite difference mesh df_venabifu3_fil2.png

Mesh Extrude to impose the boundary conditions.

16.2.1 Artery meshing.

The target of this test is to take medical image (DICOM) of a carotid artery bifurcation that defines its internal surface; with the surface will be tried to create a mesh of volume finite elements of the vessel wall to impose the boundary conditions. The walls thickness will be 0.05 cm.

The GiD starting point was been the file VTK "venabifu3_fil2.vtk", that is a rectangular matrix with in this case binary values 0 or 1. Extracting in GiD the iso-surface of value 1 , through a Marching-cubes algorithm. With the command GiD-Tcl: GiD_VTKSP2MarchingCubes venabifu3_fil2.vtk 1.0

After the marching-cubes operation will remain some very near nodes, and for this cause there will be elements with volume close to zero. Collapsing the corner lines with a very little tolerance is possible to reach the elimination of this problem.

The typology of the mesh remains the same and will clos a volume too. It will be obtained a triangles mesh of the artery with 12585 elements but it has the problem that a lot of noise is still present in the nodes position. This noise makes also problem in the creation of prismatic elements with an extrusion process of "offset", because the "normals" fields is too much discontinuous within near elements, and some elements intercrossing will occur.

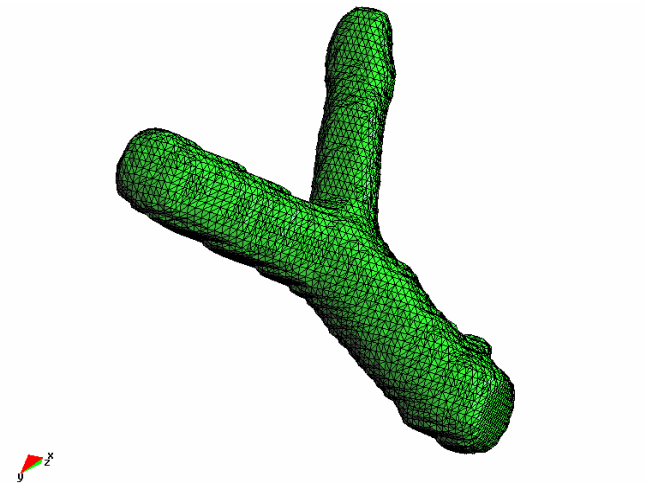

Figure 70 Mesh in its primary state

With a "Laplacian smoother" aplicated at the triangulation will treated the mesh to eliminate noise and to obtain the "middle form"

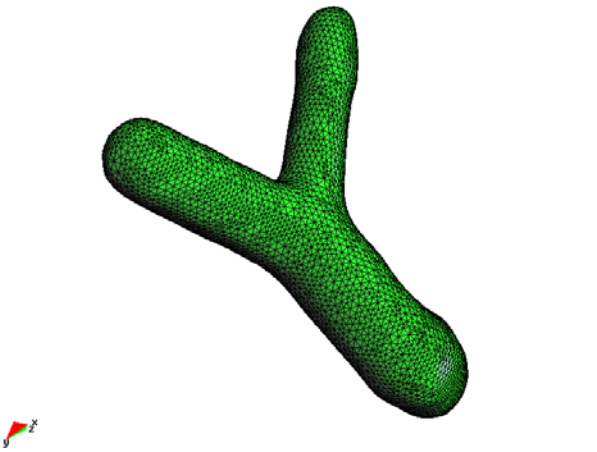

Figure 71 Mesh in its finally shape

The "laplacian smoother" standard causes that the shape shrinks, a posteriori the nodes are displaced following the final normal, measured in the nodes, trying to keep constant the closed volume, finally all the body was be scaled respect to the center of the object, to impose to the volume the exact shape.

With this step is already possible try to do the offset operation.

The model is construed in mm, wanting an offset of 0.5 mm. We create 5 elements layers of 0.1 mm of thickness, across the tool Utilities -> Copy

With these steps we obtain prisms and triangles (initial surface and 4 copies) , eliminating the triangles trough a selection made by a element type filter.

Filter:ElementType = triangle obtained 52.430 prisms and 31.470 nodes

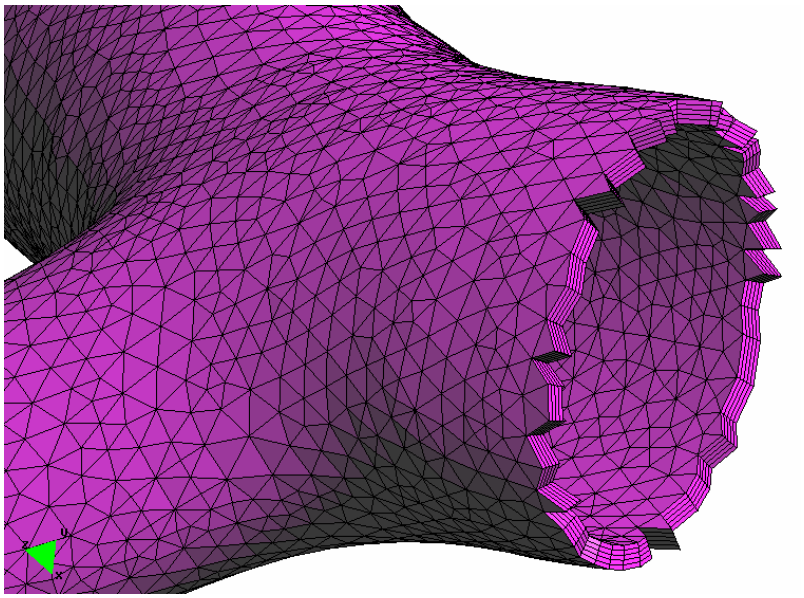

Figure 72 mesh shape eliminating external elements

No negative Jacobians were been detected in the prisms

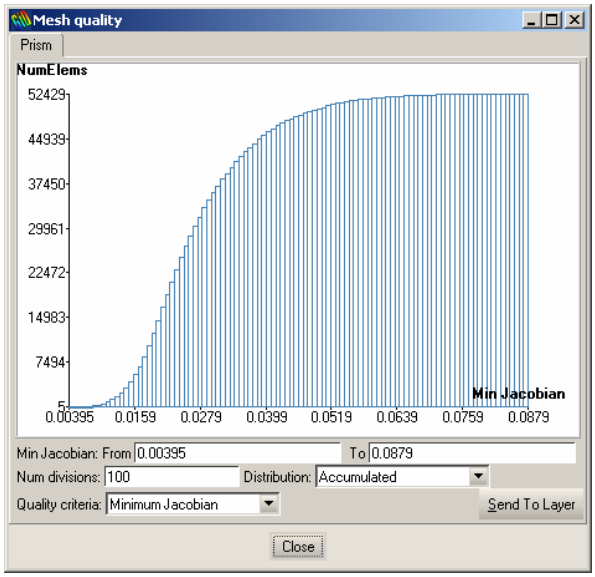

Figure 73 Any null jacobians are present

If will be desired GiD gives the possibility to subdivide the prisms in tetrahedras, in case of the program do not support the anterior element.
(menú: Mesh->Edit mesh->Split elements->Prism-Tetrahedra)
It is possible that we obtain the extrusion only with a triangulation of the contour, and try to fill up the interior side of the mesh in a no structured form, with de method of Delaunay. This method will be utile if the prisms extroduted will be unacceptable for the calculation, but even if the buondry will be acceptable can improve with a "smoothing".
In this case it's hard to control the quantity of elements in the thickness, because this dimension is quite littler than the two others and a isotropic tetrahedra can stay inside.
Example with this mesh: 32.588 tetrahedras y 10.636 nodes

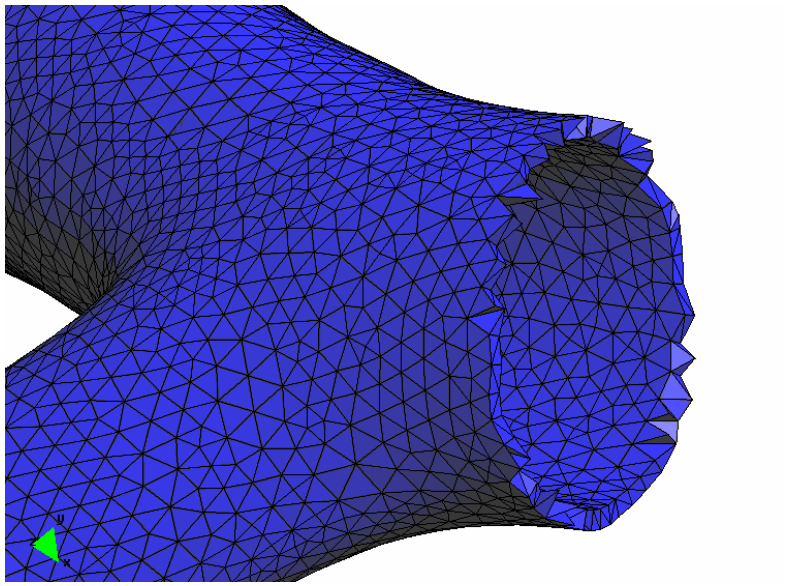

Figure 74 No structured mesh

Another way to reach this results may be a "ri-geometrization" of the triangulation:

Create "surf-meshes", an entity pseudo-geometric of GiD,; its form subjacent is the triangulation, that may be ri-meshed in some cases, generally today present a lot of problems. The reduction of the number of elements may be help the algorithms, for example trough a collapse of lines.
Trying to create "patches" NURBS that approximate the shape given with triangulation. We do not dispose of a instruments that can make this automatically. A manual work will miss to construct auxiliary curves starting to the position of some nodes, divide the domain in topologically rectangular zones, and create surfaces basing on those boundary curves…etc.

Like advantage the geometry can usually be manipulated in a simpler way that the mesh, to modify it, to put conditions and ri-meshing it.

17 CREATE GEOMETRY WITH GID.

Before explaining how boundary conditions are imposed, the geometry processing will be explained briefly. GiD has special tools to create our geometry over it the boundary conditions will be imposed.

Using Gid-geometric-tool is possible to create a new geometry with a specific shape, with this tool the user can create an infinite models based in the real models, for example in this case, the 3D geometry created was proposed by Bharadvaj et. al.. In the follow picture 75, it possible to see the shape and the measures of the carotid artery used to recreate the geometry. Any way, also it will be possible to work with a real carotid geometry (figure 87) that it was acquired from a MRA. The input image was segmented using a novel segmentation method based on Topological Derivative [Annex 1]. From this segmentation, by means of Marching Cubes algorithm, the 3D mesh of the carotid artery internal wall was reconstructed. This initial mesh was post-processed to obtain the final surface mesh and then, using a frontal method, a hexahedral mesh was constructed from the hexahedral surface. Resulting hexahedral mesh is made of 16442 nodes and 12859 orthogonal hexahedral elements. See figure 90 for a rendering of the resulting mesh. For further information see Annex 1.

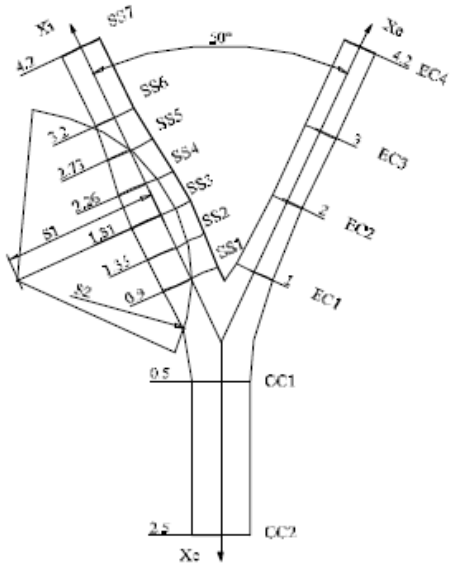

Sección	Diámetro [cm]	
CC1	0.74	
CC2	0.74	
SS1	0.77182	
SS2	0.8214	
SS3	0.8214	
SS4	0.76368	
SS5	0.6364	
SS6	0.5254	
SS7	0.5254	
EC1	0.51356	
EC2	0.42032	
EC3	0.42032	
EC4	0.42032	
Referencias (estenosis)	Medida [cm]	
	80%	95%
S1	2	1.5
S2	2.20535	1.835

Figure 75 Geometry model and graphical data.

17.1 Creating geometry with GiD.

The reasons necessaries to parametrize the geometry in many surfaces, see the figure 75, is to create a regular volume, and for create this volume is necessary to divide the full-volume in different partial-volume to create many lines that GiD will use to generate the mesh. Also it is important do not have angles with small degree, so that the tetrahedras constructed does not have a small volume.

The tools that we have to use are in the main menu. See further information in the GiD manual and tutorial go to http://www.gidhome.com/support/su04.subst

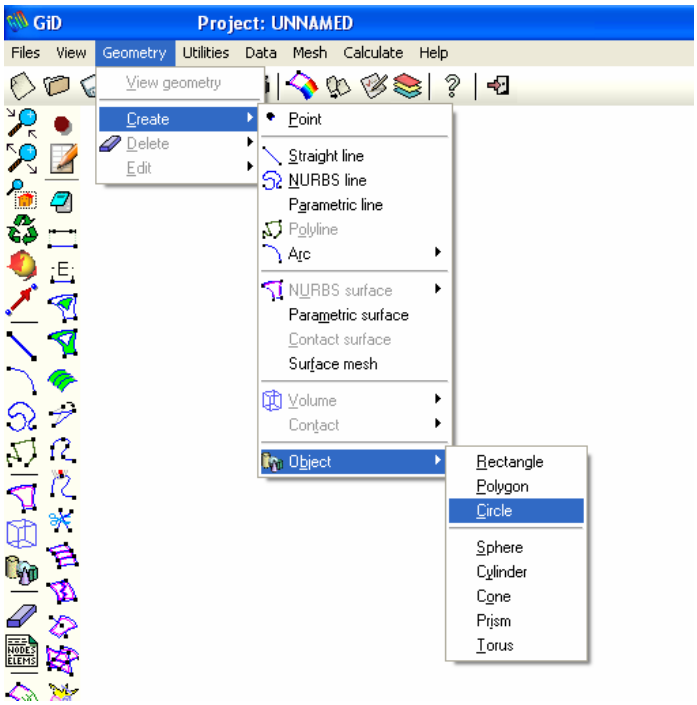

Figure 76 Creation geometry-Circle

The first step to create the geometry is to create all the contours of our carotid. To create the circular contours press geometry, create object, circle (figure 76) and GiD will ask about the radio and position of the circle, for example for the contour CC2,:

Creating a circle given center,normal and radio:
Enter a center for the circle: 0 0 0
Enter a normal for the circle: Positive Z
Enter a radius for the circle: 0,37

All the contours would be introduced in this way see figure 75

To generate the volume, first is necessary creating all the sections between the circles. Geometry-Create-Straight line. To create the cylinder only it is necessary join the points with Straight-line(Blue) between two consecutive circles and the cylinder-surfaces will be created selecting different contours, Geometry-Create-NUBS Surface-By contour. (Figure 77)

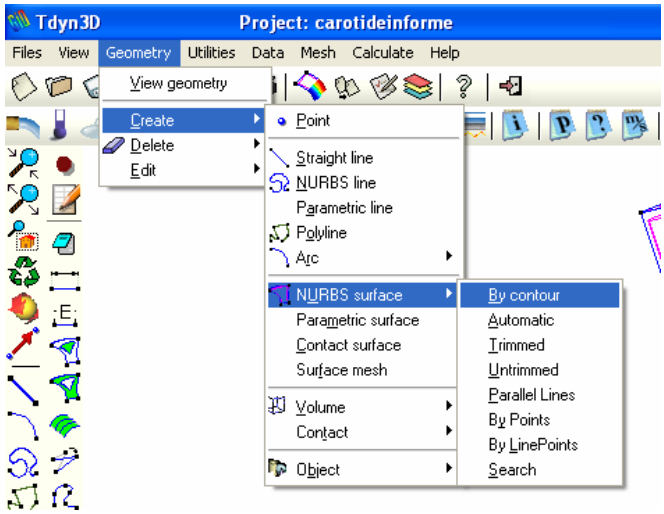

Figure 77 Creation geometry- Surface

In the carotid-bifurcation some surfaces are intersection itself, and for create a volume it is necessary the geometry will be perfect. To avoid this problem, GiD has a special tool to create intersection between surfaces. Geometry-Edit-Intersection-Surface-Surface. (Figure 78)

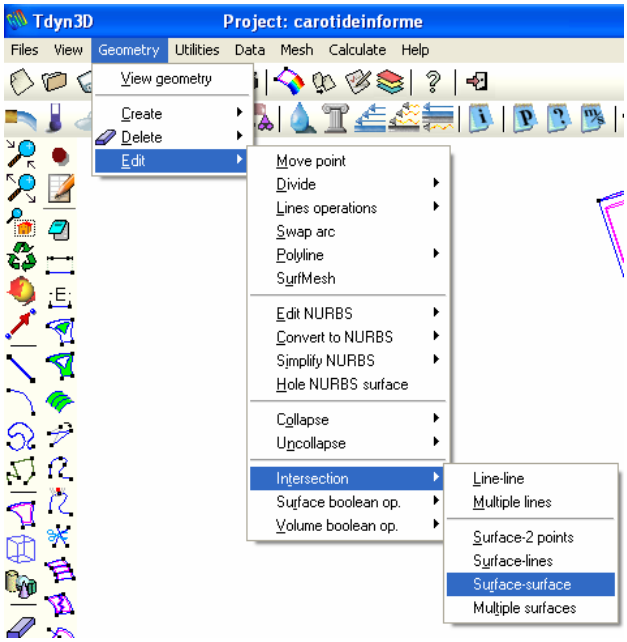

Figure 78 Creation geometry-Intersection

Created all the surfaces(pink) we can create the volume of our figure selecting the contour surface Geometry-Create-NUBS Volume-By contour.

Finished this process our geometry is done, figure 79 and the boundary conditions can be imposed.

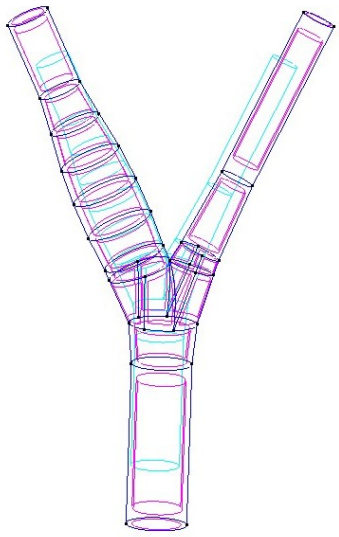

Figure 79 Geometry model realized for carotid test. Dark Blue means Line

Pink means Surface. Blue means volume In the following picture the real and artificial carotid are compared.

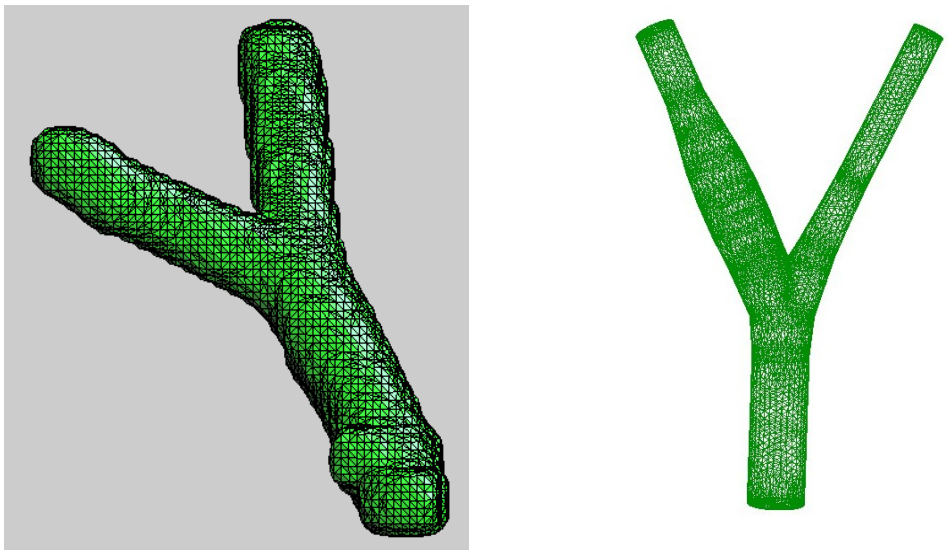

52430 Tetrahedral elements.

72452 Tetrahedral elements.

Figure 80 Real-Artificial Carotid

18 VISUAL DICOM.

The main objective of the present manual is to specify the usage of the VisualDicom software and to familiarize the user with all the options offered by the tool. The main characteristics of this application are:

- Management of DICOM files.
- Simultaneous opening of several files in DICOM format.
- Simultaneous visualization of the images in the opened DICOM files.
- Merging of multiple DICOM files in a unique *.dat extension file.

18.1 The VisualDicom Application

The main display of VisualDicom that appears once the application is initiated has this form:

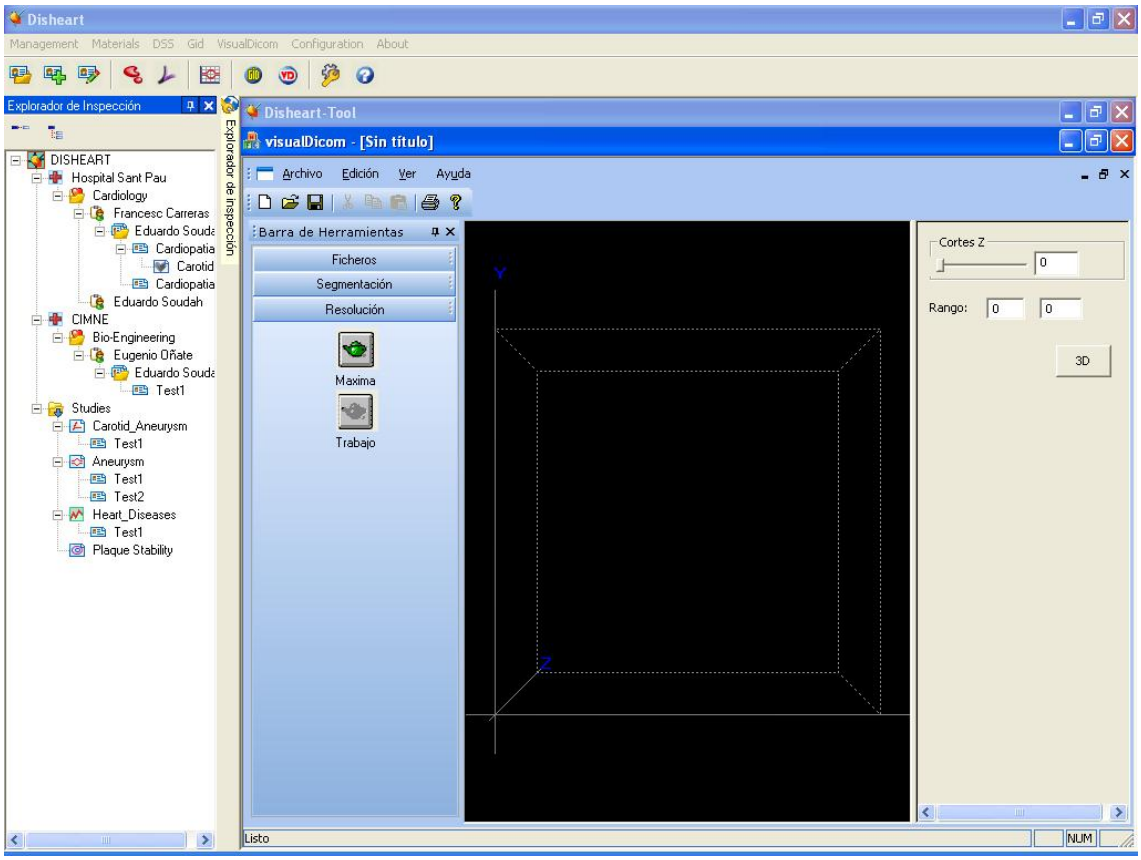

Figure 81 . Starting window for the VisulaDicom application

The main display is composed of different zones: a menu display, a tools panel and a state display, as shown in Figure 81. The contents of each menu will be described below, as well as the options of the tools panel, explaining the usage of each one.

Menu

There are four menus:

File menu

The different options of the File menu are depicted in Figure 82.

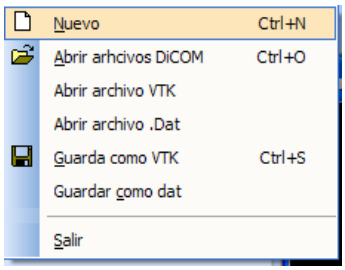

Figure 82 . The File menu.

Some of the options within the menu have an icon on the left indicating that the option can be directly accessed from the tools bar (see Figure 83).

Figure 83. The tools bar.

The different options of the File menu are described in the following. The New option allows creating a new working window in order to upload new slices for visualization. It is necessary to create a new working window before opening DICOM files for visualization.

The option "Open DICOM files" allows opening one or more DICOM files for visualization. Figure 84 shows the dialog displayed after choosing the option:

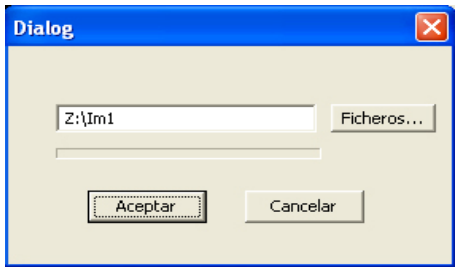

Figure 84. Open DICOM files Menu Option.

Clicking on the File button within the dialog displays the typical "Open" Windows dialog from where it is possible to select the DICOM file to visualize (see Figure 85). In this dialog, it is possible to open either one DICOM file with the data corresponding to a unique slice, or to open multiple DICOM files associated to several slices.

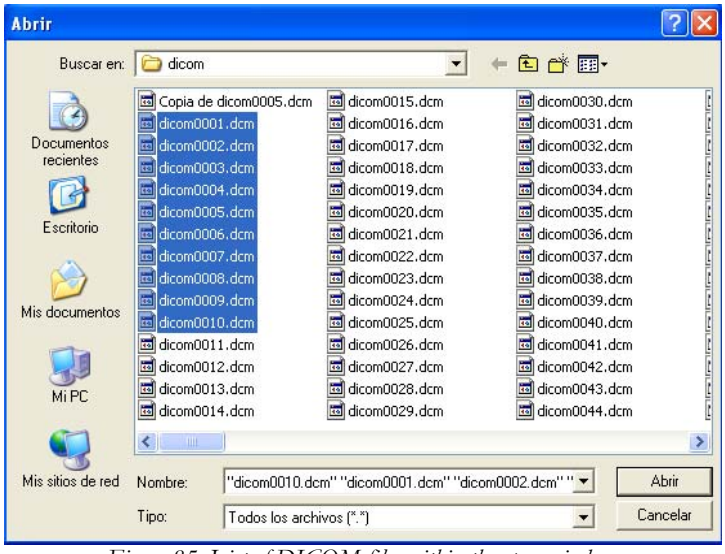

Figure 85. List of DICOM files within the open window.

Once the required files have been selected, click on the Open button. And the dialog shown in Figure 86 will appear where some information related to the set of open files is shown.

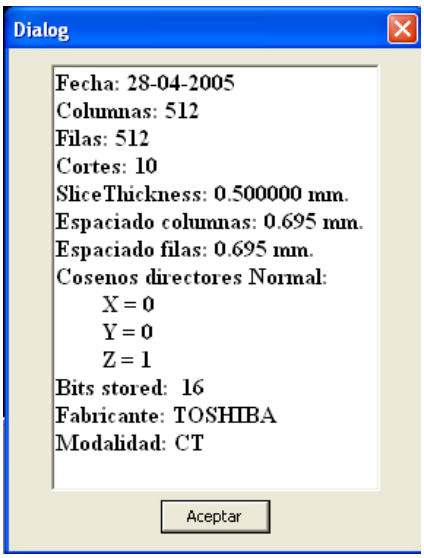

Figure 86. Information related to the opened DICOM files.

Alter reading this information, click on the "Accept" button. The window will be closed, and the working window will appear again. At this moment, a first visualization of the loaded data will appear in the display (see Figure 87). In this window, it is possible to select the desired range of slices to be shown in the 3D option.

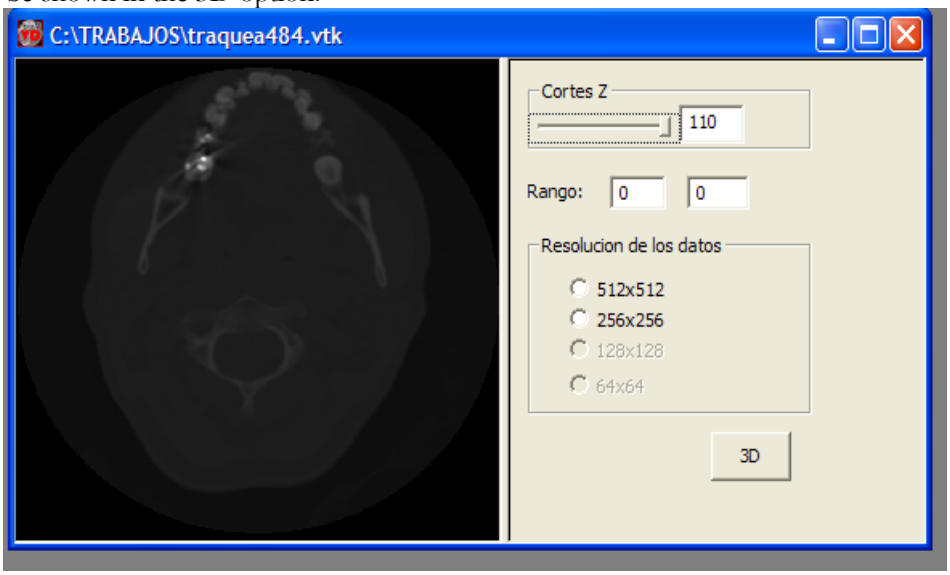

Figure 87 .Working window with the first visualization of the DICOM files. Here, the range of images to visualize can be set.

The options "Open .VTK files" and "Open .DAT files" allow to open files with different extension, (These files contain 3D data from 1 to N slices.), passing directly from the dialog "open file" to the 2D visualization. The way to proceed is as described previously for the Open DICOM File option. Once the file has been selected and the number and range of slices to be visualized has been set, the 3D button must be clicked. A new window appears with a 3D visualization of the selected data, as shown in Figure 88.

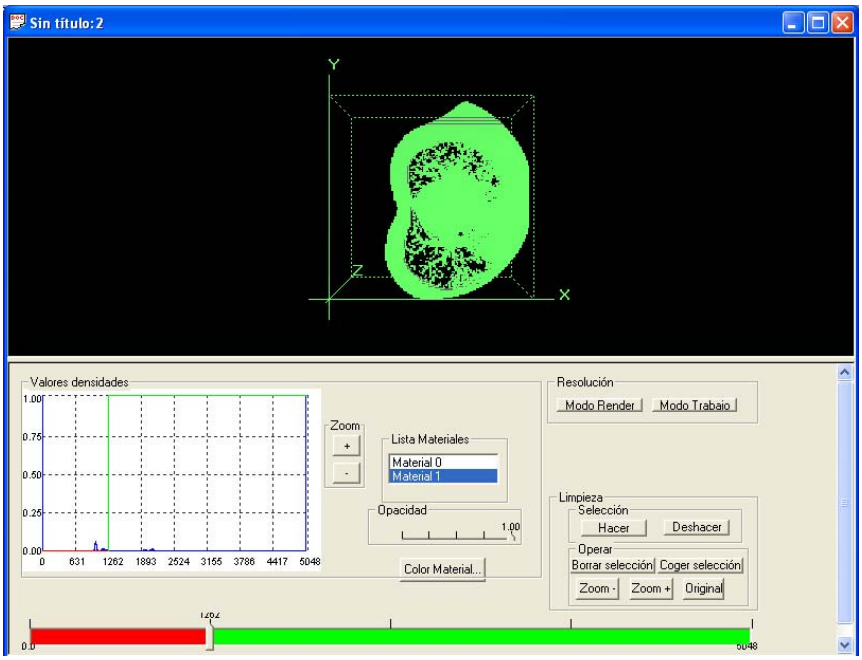

Figure 88. Segmentation Display window. The window pops-up after the 3D button has been clicked.

This display is called "segmentation display". All segmentation tools are represented in left side of the dialog. These tools will be described below. The display is divided in two areas: the display area, and the segmentation area, both of which can vary in size according to the user's necessities. For example, Figure 89 shows the visualization area which has been maximized.

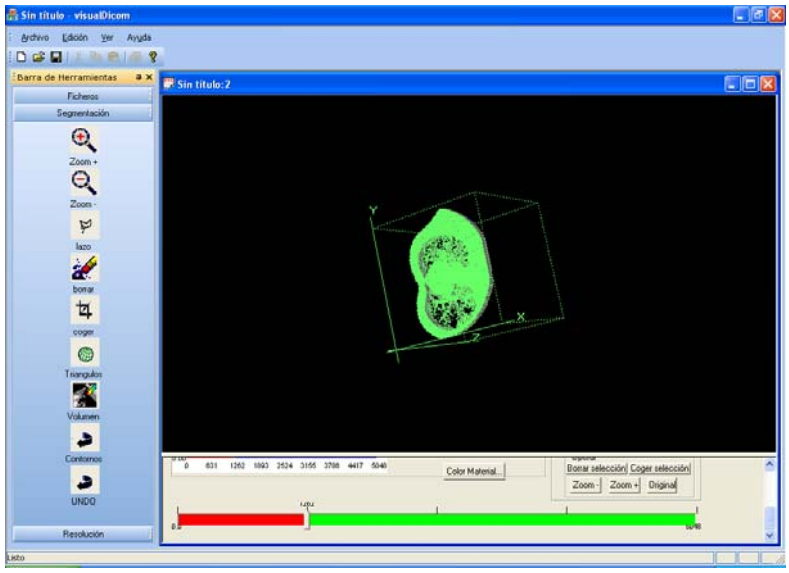

Figure 89 Segmentation Display window depicting the segmentation tool bar and the variable size characteristics of each window.

The display is shows a 3D visualization of the range of slices previously selected. The segmentation area (the lower window) shows a histogram used to establish the thresholds of the image.

The initial and final values of the x axis of the histogram represent the minimum and maximum grey values found in the DICOM file. It is possible to define, within this window, up to 8 different materials in each image and to assign a different color tag to each of them.

It is also possible to activate or deactivate this material for visualization, or to modifying the opacity of the material i.e., opacity of 0 represents an invisible material, while opacity values away form 0 means the material is visualized on the top window with different degrees of translucency (see Figure 90).

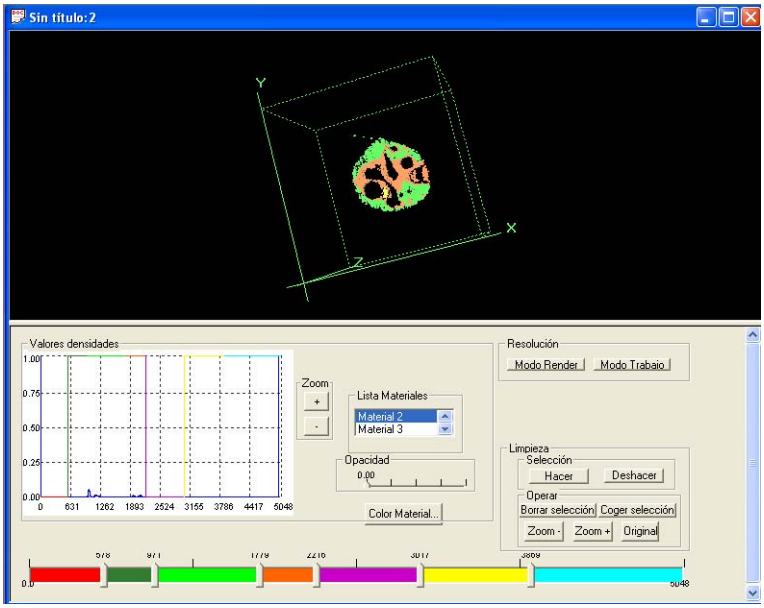

Figure 90 Visualization with different materials.

The procedure explained before represents the easier way to open and manage a DICOM file. But there is another possibility to upload a file using VisualDicom. It is possible to open a file using the option "Open as…" that allows to open files with extension .dat. These files must have an adequate format to be opened with the application. The best way is to create them within the own VisualDicom software. These files represent a much efficient way of handling merged DICOM files. The format of these .dat files is as follows.

Three numeric values are stored in the first line of the file. The first two represent the resolution (number of voxels per slice), and the third one the total number of slices in the file. In the second line, two numeric values represent the minimum and maximum values of the uh units. (unit of the DICOM files). The third line has number that takes values of 0 or 1, depending if the image is of high or low resolution. The fourth line has the number of bytes per pixel. The fifth line has three values. The first two represent the separation in the x and y axes, respectively, (the cell size) and the third one represents the separation between slices (slice thickness). The remaining lines contain the information, in bytes, contained in the DICOM files.

18.1.1 View Menu

The different options of the View menu are shown in Figure 91.

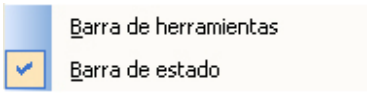

Figure 91 View menu.

They activate or deactivate the state and tool bars display.

18.1.2 Help menu

The drop-down submenu for the Help menu is shown in the next image

Figure 92. Help menu.

18.1.3 Tool Menu

There are three different subsections with different tools in each of them: Files, Segmentation and Resolution.

18.1.4 Files

A image with the tools included in the group Files is showed below. These tools are described in the next paragraphs.

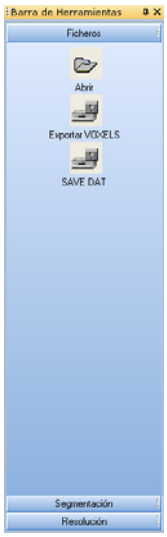

Figure 93 File option of the Tool Menu

Open: This option allows to upload one or more DICOM files to visualize them. It is important to remember that it is necessary to open a working window before uploading a DICOM file. This working window is opened with the option New of the Files menu or by its access icon. After launching the VisualDicom application and selecting the Open icon of the Files tool menu, a dialog shown in Figure 94 pos-up.

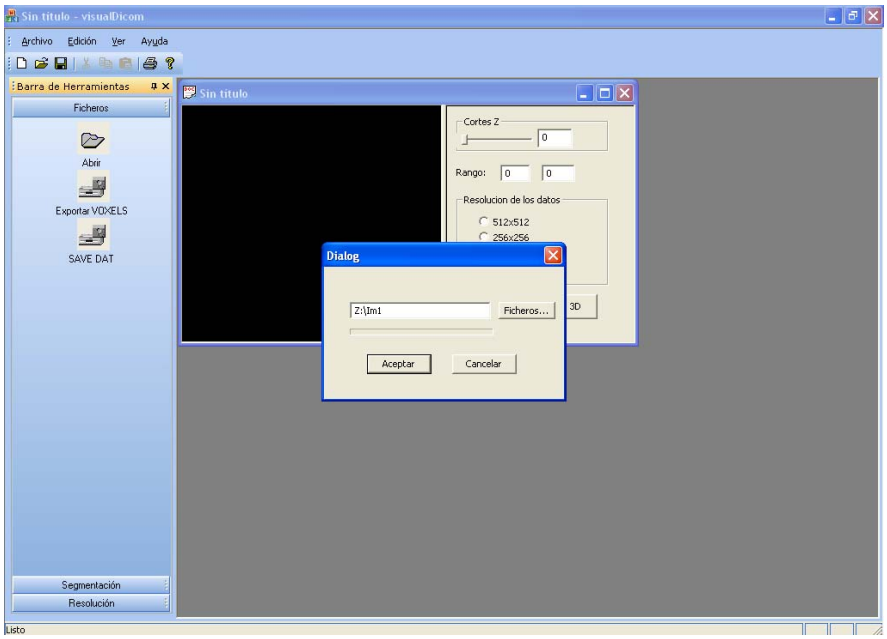

Figure 94 .Dialog displayed after slecting the Open option within the File option of the Tool Menu

Now, the way of proceeding is the same as the one described in the section of the File menu. The options Open and Open as… are available to begin the VisualDicom application.

The next option of this menu is "Export Voxels". The third and last option of this tools group is "Save dat" that allows to marge the slices uploaded in the application up to the moment and saving it in a *.dat file. So, it will be possible to visualize the selected slices only by opening this *.dat file, without the need for uploading all DICOM files again.

18.2 Segmentation

The Segmentation tool bar is shown in Figure 15.

Figure 95. Segmentation tool bar

These tool automatically activates with the segmentation display of the VisualDicom application previously described. The Zoom+ and Zoom- options allow to amplify and reduce the size of the visualized image in the visualization zone (top window) of the segmentation display as shown in Figure 96.

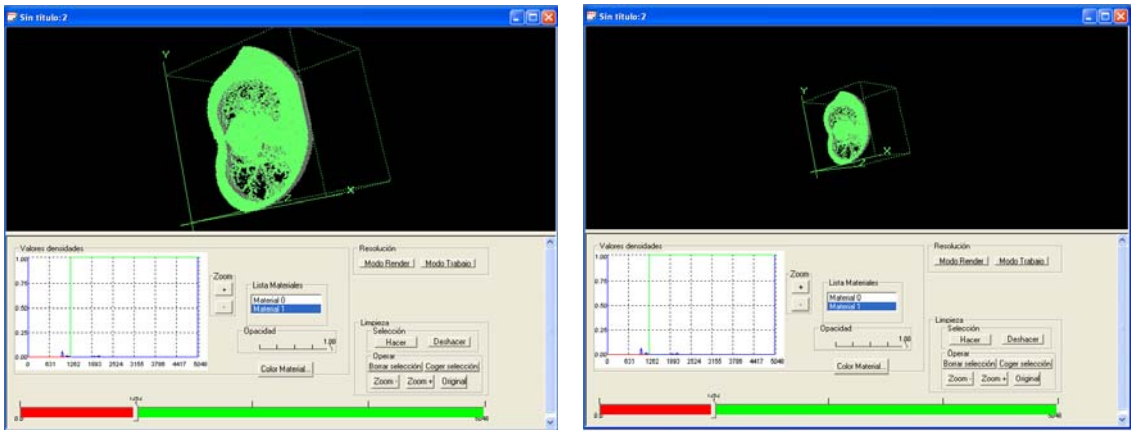

Figure 96. Example of the use of the Zoom+ and Zoom- options of the toolbar menu.

The third available tool in this group is the "Lasso" option. This tool allows to select different zones of the image. When the mouse is clicked and moved, a white line appears on the display indicating the area being selected (see Figure 97).

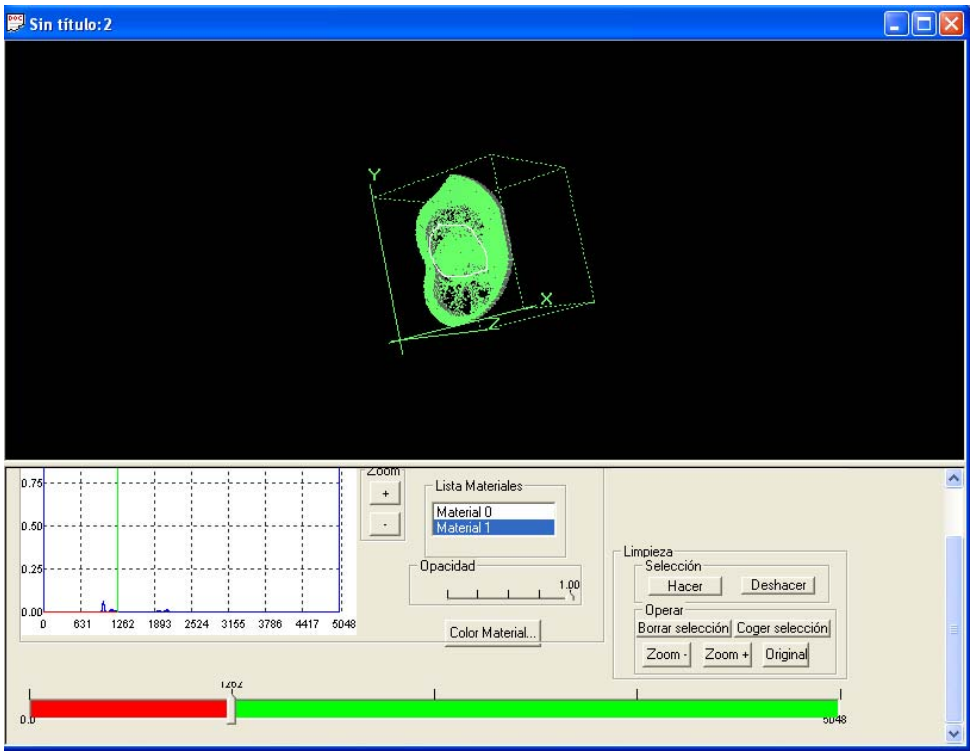

Figure 97 Example of Lasso option.

Once the desired selection is delimitated the following tools can be applied: Delete or Take. The first of them deletes the selected area maintaining the rest of the image. The second option just do the opposite, and only remain the delimitated area by the "Lasso" option, as shown in Figure 98.

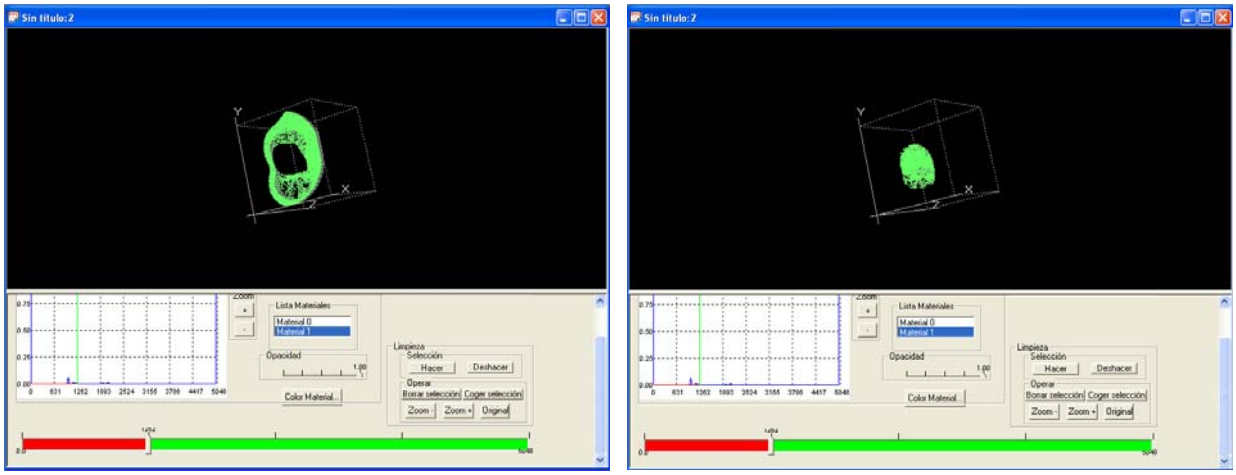

Figure 98 . Example of the delete and take options.

The "Triangles" tool allows to extract the voxel iso-surfaces by means of the marching cube algorithm. When this tool is selected, a new vtk window divided in two is opened. In the left of the window, the rendered volume is displayed as shown in Figure 99.

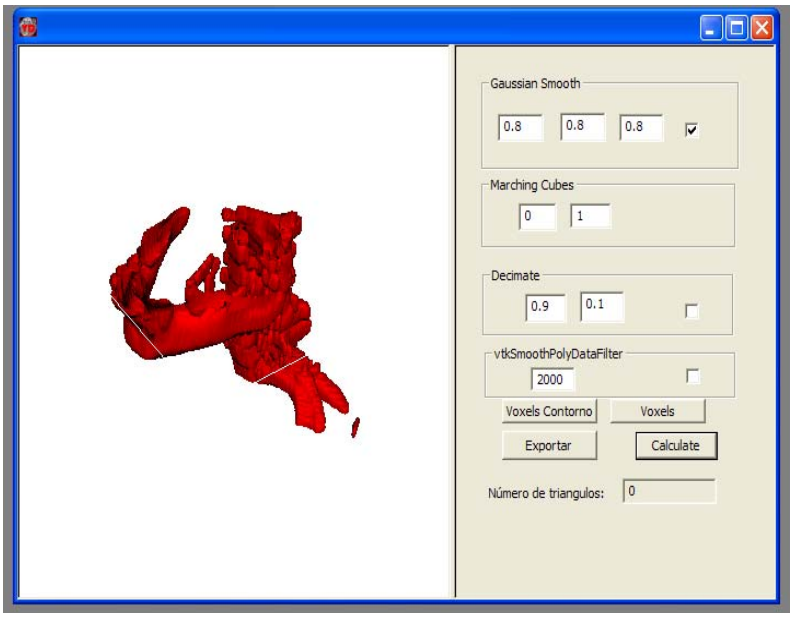

Figure 99. Isosurface visualization of the voxel data.

The mouse can be scrolled to zoom in and out the image, to move and rotate it to improve the visualization of a given area. When dealing with an picture composed of many triangles, the intense computation involved may cause a temporary loss of image visualization. In this case, an slight mouse movement is enough to recover the visualization. Figure 100 shows a zoom of the image depicted in Figure 99.

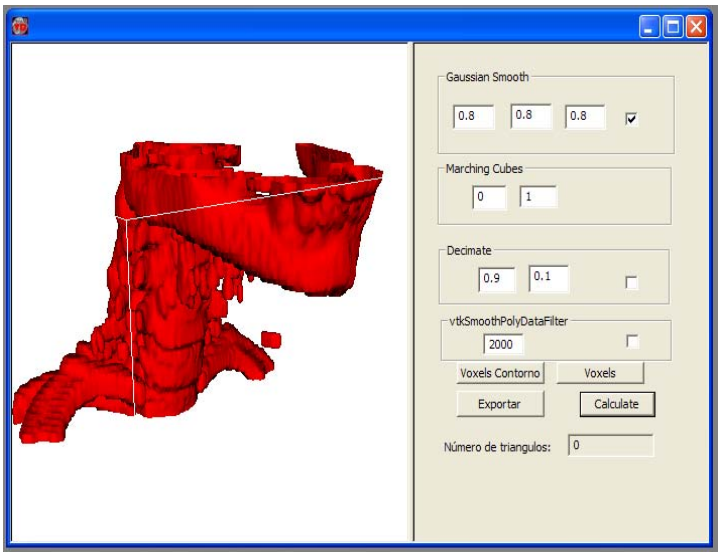

Figure 100. Zoomed image of the Isosurface.

The right of the window has options related with the isosurface rendering. Gaussian Smooth, allows to specify parameters for the Gaussian filter in the three axis for boundary smoothing. The second box, Marching Cubes, defines parameters applied in the marching cube algorithm. The box Decimate allows to increase the size of the triangularization (to replace small triangles with bigger ones when possible) for improve rendering speed.

The fourth box specifies a parameter related to smoothing the image at the triangle mesh level. When turning on/off any of the previous options, it will be necessary to click on the button "Calculate" to refresh the representation in the screen left area. The "Voxels Contour" button allows to save the boundary voxel in vtk format. The "Voxels" button allows to save the voxels supplied to the triangularization algorithm in vtk format. The "Export" button allows to export to

stl format. When pressing this button, a prompt window appears giving the user to opportunity to chose the saving directory.

The next available tool from the segmentation window is "Volume". This tool opens a new window in which it is shown the result of transforming the image from the segmentation window to a volume by means of the volumeRayCasting technique (see Figure 101).

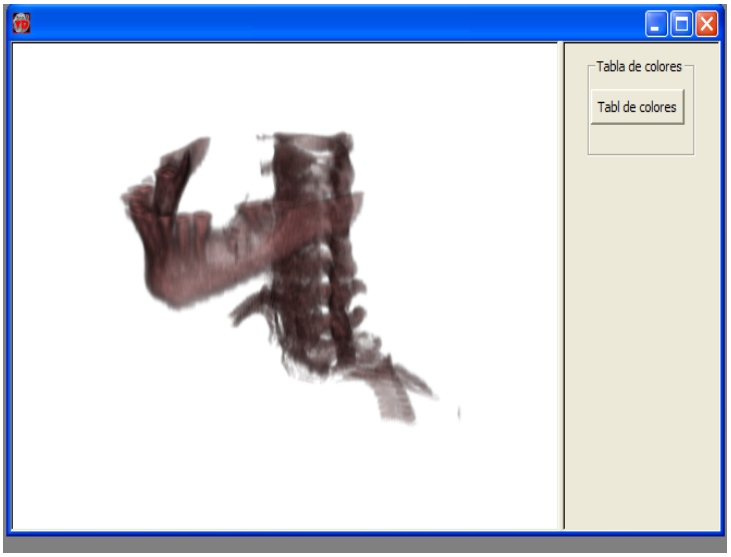

Figure 101. Example of the volumeRayCasting.

The window is divide into two vertical areas, in the left is used to display the volume rendering. By pressing the "Colour Table" button in the right, allows to change the rendering colour as shown in Figure 102.

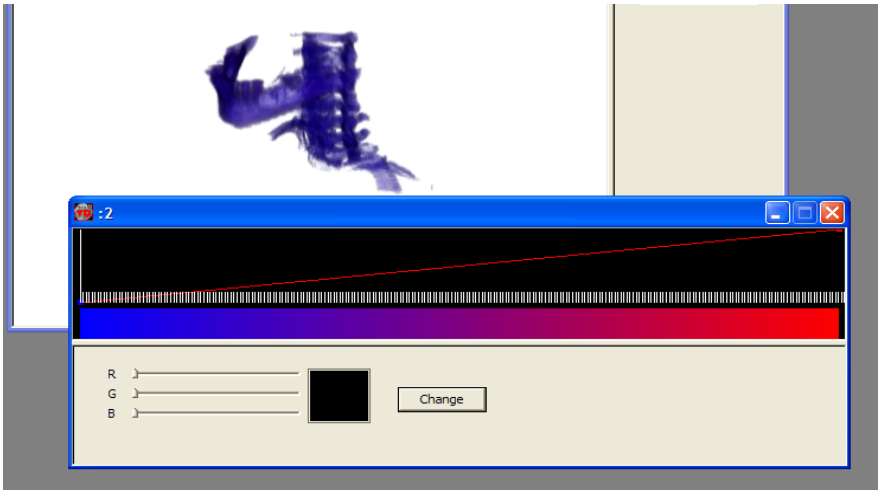

Figure 102. Example of the volumeRayCasting colour table.

The following tool is applied to the contour segmentation. When the "contour" button is pressed, the window in Figure 103 pops-up. This tool allows to navigate along the different slices, as well as to perform cuts along the x, y, and z axis.

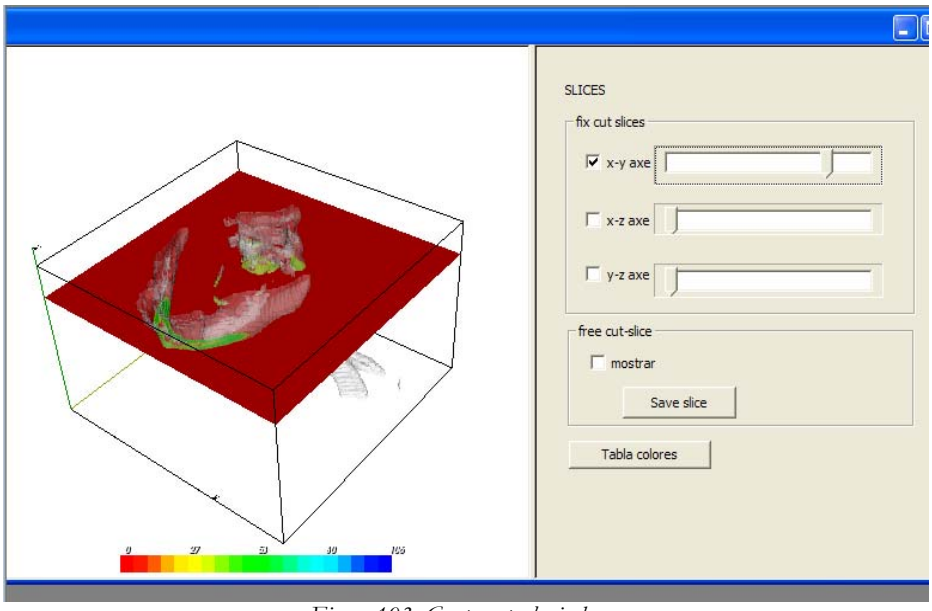

Figure 103. Contour tool windows.

The "Undo" button within the segmentation toolbox allows to undo the last change occurred in the segmentation screen.

Resolution

The resolution tab within the toolbar allows setting the working resolution during the working session. A lower resolution will allow rapid changes to be performed, leaving the high resolution for the final visualization, making therefore the work more effective.

19 –DISSEMINATION OF THE DISHEART.DSS

The following actions have been carried out in order to disseminate the Disheart project:

- Create an image and a logo of the project
- Design and develop the Web page of the Disheart project
- Dissemination of the project activities through conferences and workshops
- Dissemination via publications in relevant scientific and technical journals

The Disheart project will be presented to hospitals, medical centres and private organizations of the sector.

19.1 Image / Logo

An image for the project has been established in order to provide all partners with a corporative image; it would be useful mainly for dissemination purposes.

The project image will be used in all the project documents and dissemination actions:

- Deliverables
- Milestones
- Brochure
- Web page
- Presentations

Figure 104: Logo 1

Figure 105: Logo2

19.2 Web page of the Disheart project

The Disheart project web site has the following address: http://www.cimne.upc.es/disheart/

19.2.1 Description of the web page

The web page is structured in three different principal sections:

- About Disheart
- Diffusion
- Members' Area

The About Disheart section is divided in the following parts: Introduction, Objectives, Work Plan and Consortium.

- Introduction: a technical summary and the framework where the project is co-funded are presented.
- Objectives: in this section the expected results by DISHEART.DSS are presented
- Work plan: description of the work packages
- Consortium: the partners of the Disheart project, RTD performers and SME's are listed

In the Diffusion section would be presented the public documents and the dissemination activities.

The members' area is accessible only for the project partners. Each partner can access to it by means of a login and a password.

In the members area the following options exists:

- Information
- Documentation
- Users
- Forum
- Video-Conference
- Chat
- Calendar

A detailed description of the project and a list of the personal information of the collaborators can be found in the Information and Personal Information section respectively.

In the Documentation section every member can attach files by pressing the button add new folder.

Software for mailing is integrated in the web page, useful within the project. The user can select the addressees of the DISHEART participants from a list and send them an email, with the possibility to attach files.

Users can directly modify their project personal information (through the contact details option).

19.2.2 Description of the member's area icons

 Information about the Disheart project

 Documentation: automatic system to upload files of all kind, with the possibility to alert users when a new file has been uploaded. All the files that have been uploaded to the system (and its author) can be seen within a certain period of time

 Users: All the users of the Disheart web page are showed

 Forum: it is possible to add topics and contribute to a forum space among the registered members of the internal platform

 Videoconference: a Net Meeting based videoconference. This tool may become useful to avoid some meetings along the life of the project

 Chat: a chat with connected registered members of the Disheart project platform can be established

 Calendar: allows scheduling activities and deadlines. It may be important for the correct project development

19.2.3 Image of the Disheart web page

Figure 106: Web Page 1

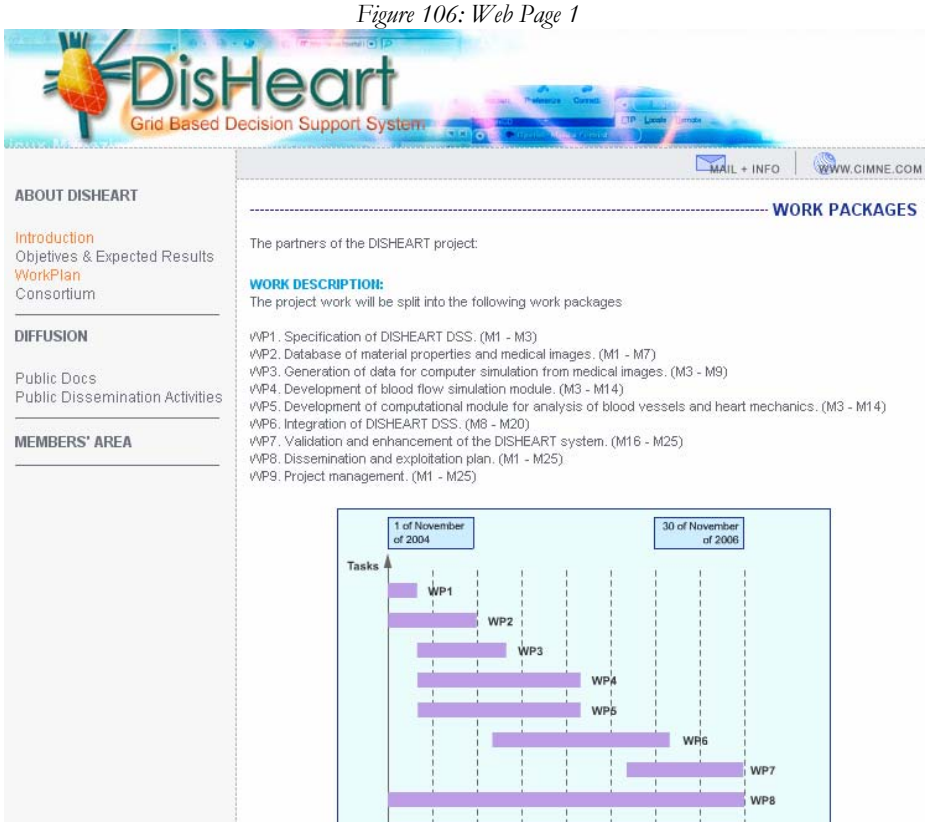

Figure 107: Web Page 2

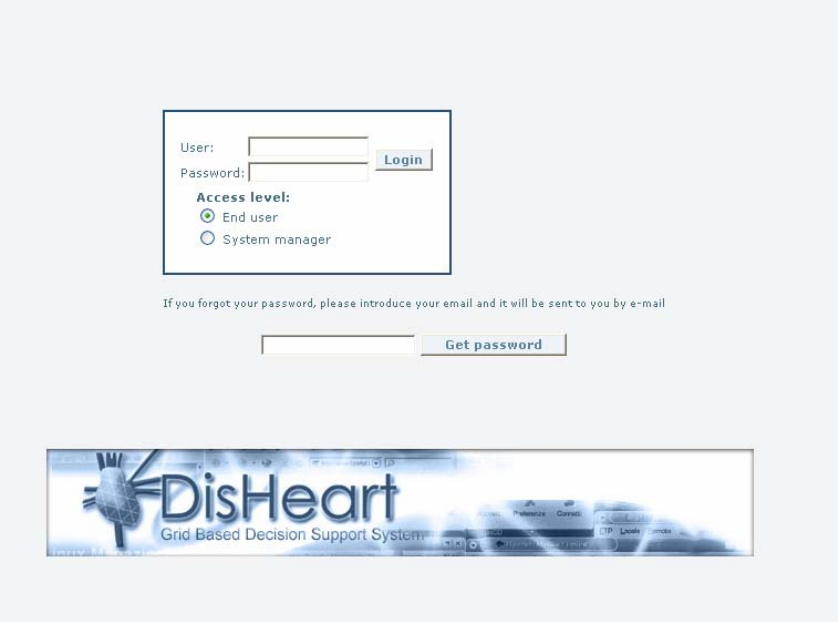

Figure 108: Restricted Area 1

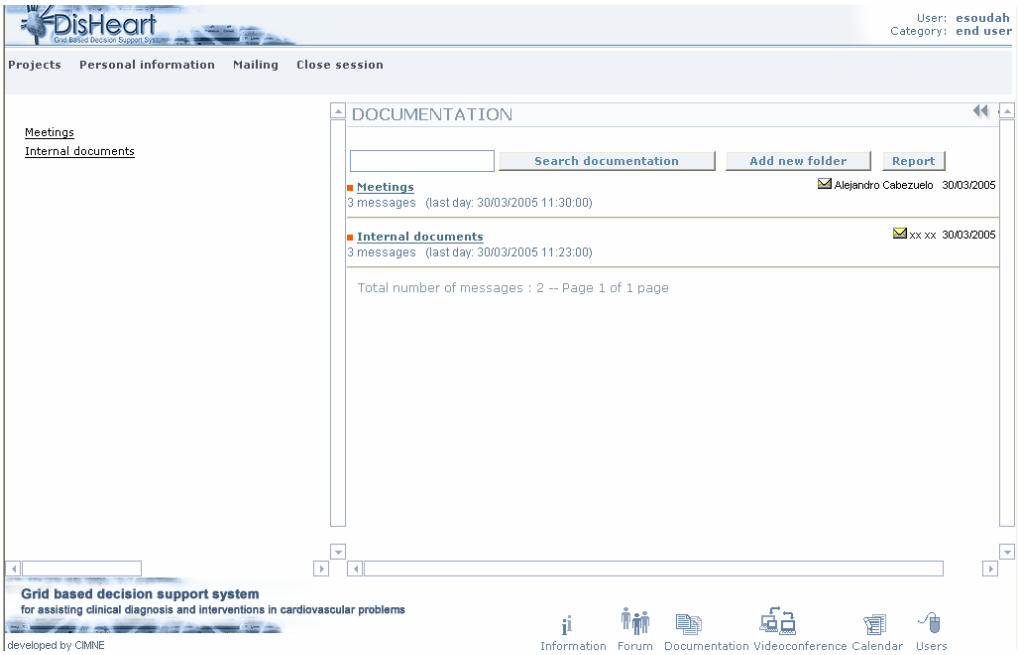

Figure 109: Restricted Area 2

20 ACNOWLEDGEMENT.

The support for the development of the DISHEART.DSS of the European Commission (EC) through the 6th Framework PROGRAMME HORIZONTAL RESEARCH ACTIVITIES INVOLVING SME'S CO-OPERATIVE RESEARCH is gratefully acknowledged.

In this work have cooperated the follow groups:

- International Center for Numerical Methods in Engineering (CIMNE). (Spain)
- The Aragon Institute of Engineering Research - University of Zaragoza (I3A). (Spain)
- Technical University Graz (Austria).
- Laboratoire Techniques de l'Imagerie, de la Modélisation et de la Cognition (TIMC) France
- Vascular Fluid Dynamics (USA).
- Sant Pau Hospital (Spain).

21 REFERENCES.

21.1 Project Deliverables

Deliverables	Authors	Reference	Date
Specification of DISHEART DSS and SME's requirements	CIMNE	D1.1.Rev 0	February 2005
Assessment and evaluation requirements	CIMNE	D1.12.Rev 0	February 2005
Material Database.	TIMC-CIMNE	D2.1.Rev 0	June 2005
Medical Images Database.	TIMC-CIMNE	D2.2.Rev 0	June 2005
Generation of data for computer simulation from medical images.	CIMNE	D3.1.Rev 0	June 2005
Consitutive model for blood flow	COMPASSIS	D4.1.Rev 0	June 2005
Blood Flow analysis module.	CIMNE	D4.2.Rev 0	February 2006
Performance and Assessment	CIMNE	D4.3.Rev 0	February 2006
Material models for blood vessel	TUG-I3A	D5.1.Rev 0	June 2005
Material model for heart mechanics	I3A-TIMC	D5.2.Rev 0	February 2006
Stochastic analysis module	I3A	D5.3.Rev 0	February 2006
Performance assessment	I3A	D5.4.Rev 0	February 2006
Integration of DISHEART DSS.	CIMNE	D6.1.Rev 0	September 2006
Validation of the DISHEART.DSS for Different cardiovascular problem.	I3A-CIMNE	D7.1.Rev 0	September 2006
Final Version of the DISHEART.	CIMNE	D7.2.Rev 0	February 2007
Guidelines for future use of the DISHEART DSS	CIMNE	D7.3.Rev 0	February 2007
Initial dissemination and exploitation plans.	CIMNE	D8.1.Rev 0	February 2007
Dissemination actions	CIMNE	D8.2.Rev 0	February 2007
Exploitation actions.	CIMNE	D8.3.Rev 0	February 2007
Project management	CIMNE	D9.Rev 0	February 2007

21.2 Manuals

[GiD], GiD - The personal pre and postprocessor, www.gidhome.com.

[DICOM-Home] DICOM Homepage, http://medical.nema.org/

[DICOM-Intro] DICOM introduction and software, www.sph.sc.edu/comd/rorden/dicom.html

21.3 Publications

"El valor de cálculo en los sistemas de ayuda a la toma de decisiones en ingeniería"
E.Oñate, Publication CIMNE Nª264, Barcelona, October 2004

"The value of computattion in engineering decision support systems"
E.Oñate, Revista de Obras Públicas N3449, Madrid, November 2004

Structural Damage Models for Fibrous Biological Soft Tissues. V. Alastrue, J. Rodriguez, B. Calvo, M Doblare, INT J SOLIDS STRUCT. In press, 2007.

An anisotropic visco-hyperelastic model for ligaments at finite strains: Formulation and computational aspects. E. Peña, B. Calvo, M. A. Martinez, M. Doblaré, INT J SOLIDS STRUCT, 44, 760-778, 2007.

An uncoupled directional damage model for fibered biological soft tissues. formulation and computational aspects. B. Calvo, E. Peña, M. A. Martinez, M. Doblaré, INT J NUMER METH ENG, 69, 2036-2057, 2007.

A procedure to simulate coronary artery bypass graft surgery. F. Cacho, M. Doblare, GA Holzapfel, 2007. MEDICAL AND BIOLOGICAL ENGINEERING AND COMPUTING (MBEC), Aceptado, 2007.

Order Compact Schemes with Adaptive Time Step for Monodomain Reaction Diffusion Equations. E. A. Heidenreich, J.F. Rodriguez, F.J. Gaspar, M. Doblaré. JOURNAL OF COMPUTATIONAL AND APPLIED MATHEMATICS. Aceptado, 2007.

A constitutive model for fibrous tissues considering collagen fiber crimp. F. Cacho, P.J. Elbischger, J.F. Rodríguez, M. Doblaré, G.A. Holzapfel INTERNATIONAL JOURNAL OF NON-LINEAR MECHANICS, In press, 2007.

A stochastic-structurally-based thgree dimensional finite-strain damage model for fibrous soft tissue. J.F. Rodriguez, F. Cacho, J. A. Bea, M. Doblaré, J MECH PHYS SOLIDS, 54, 864-886, 2006.

On the numerical treatment of initial strains in biological soft tissues. E. Peña, M. A. Martinez, B. Calvo, M. Doblaré, INT J NUMER METH ENG, 68, 836-860, 2006.

On solving large strain hyperelastic problems with the natural element method. B. Calvo, M. A. Martinez, M. Doblaré, INT J NUMER METH ENG, 62 (2), 159-185, 2005.

On the employ of meshless methods in biomechanics. M. Doblaré, E. Cueto, B. Calvo, M. A. Martinez, J.M. Garcia-Aznar, J. Cegoñino, COMPUT METHOD APPL M, 194(6-8), 801-821, 2005.

21.4 Conferences

"Neural Networks For Simulation Of Computational Processes In Bioengineering". E.Soudah, J.F.Rodriguez, R.López, M.Doblaré and E.Oñate - World Congress on Bioengineering (WACBE 2007) Thailand.

"Fluid-Structure interaction applied to blood flow simulations. Thematic conference of vision and medical processing".J. S. Pérez, E. Oñate, E. Soudah, J.García, E.Escolano, A.Mena, E. Heidenreich, J.F.Rodríguez, M.Doblaré. VIPIMAGEOctober2007

"Validation Of The One-Dimensional Numerical Model In The Ascending-Descending Aorta With Real Flow Profile". E.Soudah,F.Mussi and E.Oñate - III International Congress on Computational Bioengineering (ICCB 2007) Venezuela.

"Neural Networks for Simulation the Mechanical Stress in Abdominal Aneurysm". J.F.Rodriguez, E.Soudah, R.López, M.Doblaré and E.Oñate - III International Congress on Computational Bioengineering (ICCB 2007) Venezuela.

"Mechanical Stress in Abdominal Aneurysm: Influence Of Geometry And Material Anisotropy". José F.Rodríguez, M.Doblaré. A computational analysis, 5th World Congress of Biomechanics, Munich, Germany, 29th July - 4th August, 2006

"Transmural stress during bypass surgery: a patient-specific computational analysis". F.Cacho A computational analysis, 5th World Congress of Biomechanics, Munich, Germany, 29th July - 4th August, 2006.

"An Anisotropic Constitutive Growth Model for Soft Tissues: An Application To Aneurysm". José F.Rodríguez. 5th World Congress of Biomechanics, Munich, Germany, 29th July - 4th August, 2006.

"Modelling and Characterizing Collagen Fibers Bundles".Fernando Cacho, Poster Presentation. 2006 IEEE International Symposium on Biomedical Imaging: from Nano to Macro. April 6-9 Virgina. USA.

Annex A- Impose Boundary Conditions with TDyn

A.1 Introduction

Briefly how the boundary condition will be explained in this section. Further information in deliverables D4.2 Blood flow analysis module, D4.3 Performance Assessment and www.compassis.com/compass-site/productos/tdyn/index.html.

To impose the boundary conditions the following procedure is required, menu DATA, submenu Condition/Ransol and Boundary/Fluid and to impose the material behaviour, Material/Fluid. The boundary conditions imposed will be:

Fix velocity field in the inner section
Null value of field pressure in the section where the blood go out.
The no slip boundary condition for the vessel walls.

A.2 Velocity.

The no slip boundary condition for the vessel walls was imposed by a VfixWall in the "fluid body ransol boundary condition", so doing we can put a fix null value of velocity in all the points of the surfaces that substituting the artery walls; equally we use the VfixWall condition to fix a no slip boundary condition in the vessel lateral walls. See figure 110

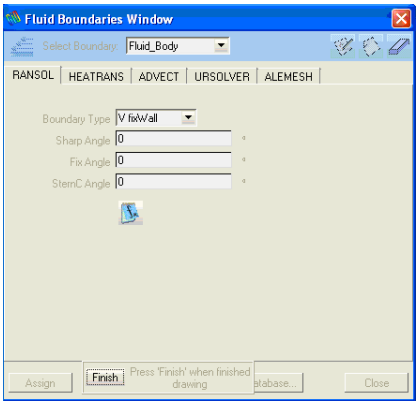

Figure 110 Fluid boundary conditions

Impose the fix wall condition, it is necessary to set the condition of the flow and impose that the lower surfaces is the one trough that the flow enters. We use an expression of a polynomial that can best emulate the flow of a real humane cardiac cycle (Figure 111). With an expression of the velocity and the pressure not much complex is possible to use a limited number of steps. The polynomial expression can give us a good profile of blood flow in velocity and pressure (Figure 112) The polynomial in the other out going sections only describes the variation of the pressure, this condition permits to the pressure to move along the route of the blood; this is a fundamental data that we have to impose when the target of the study is the effect of the pressure on the lateral vessels.

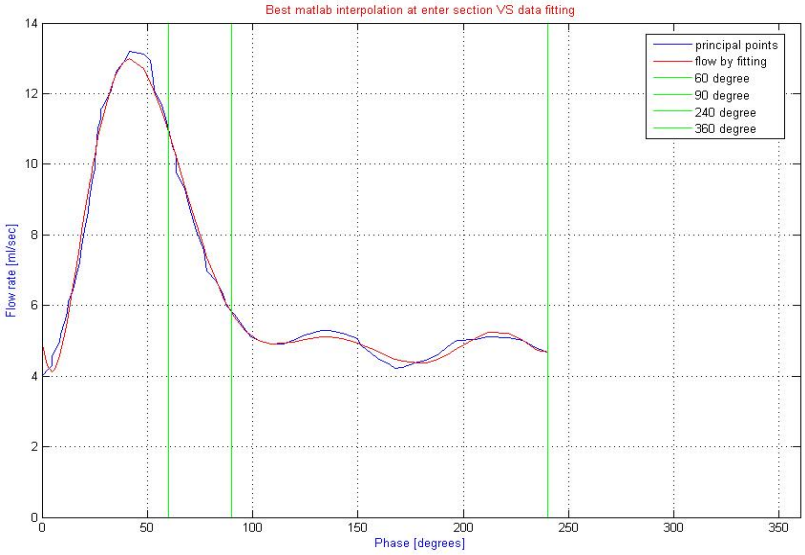

Figure 111 Cardiac cycle.

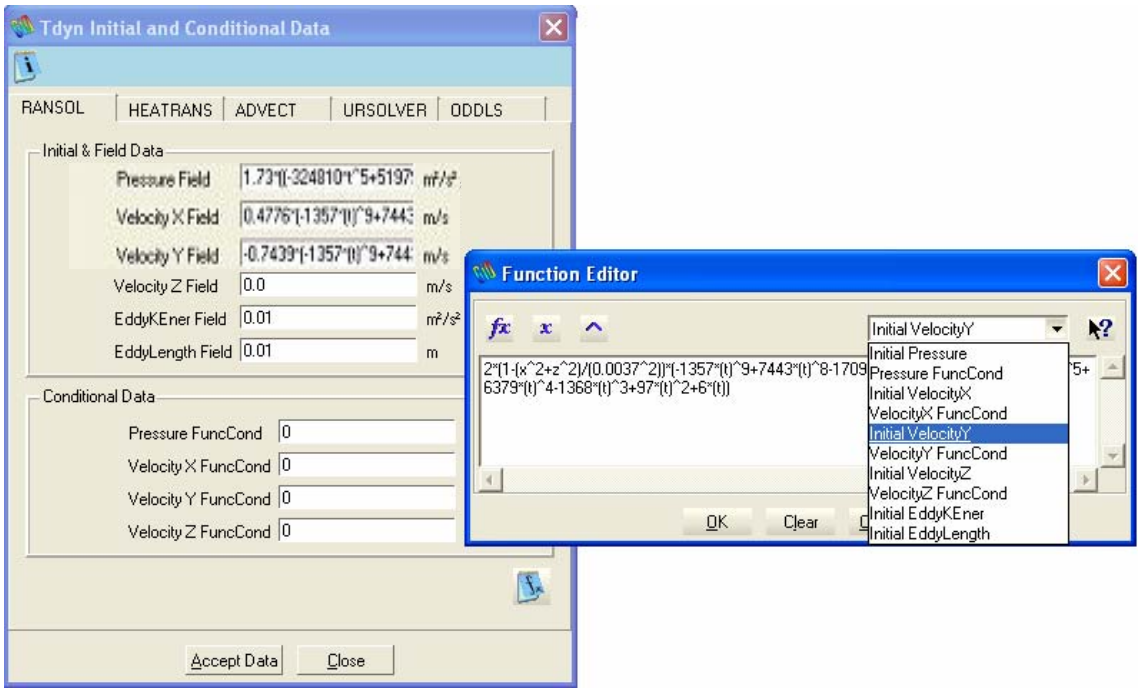

Figure 112 Initial and Conditional Data.

In figure 113, it is possible see where the boundary conditions have been imposed.

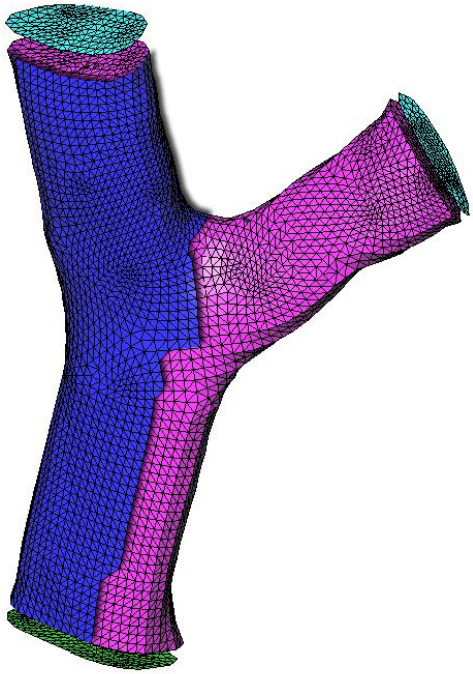

Figure 113 Boundary Conditions

Pink area, volume fluid, is the part of material that the properties of the blood have been assigned.
Dark blue, surface fluid is the surface of the material. The fix velocity and coupling (Alesmesh) boundary conditions have been imposed.
Blue, output layer. In this layer is need to imposed the pressure profile (figure 113)
Green, input layer. It is necessary to imposed the velocity profile (figure 114)

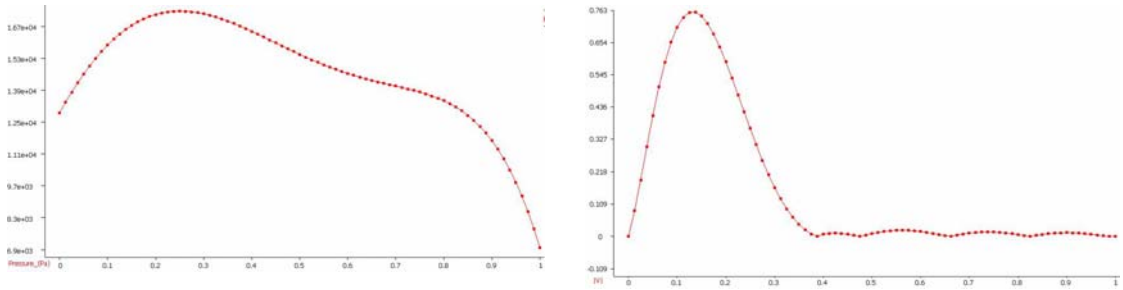

Figure 114 Pressure and Velocity Profile

A.3 Material.

To impose the material behaviour it is necessary go to DATA-Materials, and in follow windows fill in the parameters of the fluid (See figure 115)

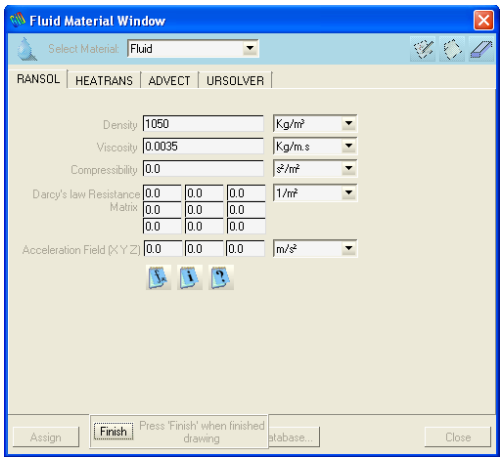

Figure 115 Fluid material

In this case, the parameters were:

Density	1050	Kg / m3
Viscosity	0.0035	Kg / m ·s
Compressibility	0.0	s2 / m2

A.4 Problem Data.

To impose the number of the steps, the time step, and the propriety of the computation the following procedure is required DATA- Problem Data. Figure 116

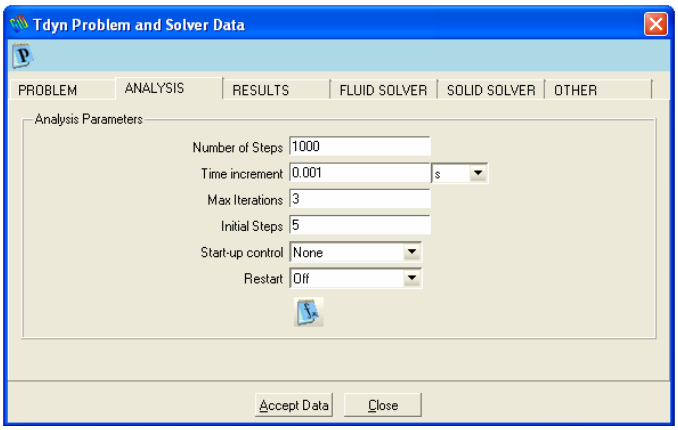

Figure 116 Problem Data Windows

In this case, the parameters were, figure 117. But to impose good parameters depend of the user-experience.

Step number	Time increment	Max iteration	Output step
6000	0.00006	5	100

Figure 117 Problem Data Parameters

A.5 Mesh

After the boundary conditions and fluid conditions were imposed, the mesh can be generated. To find the correct size of the element becomes hard due to the complex geometry and the stability of the problem.

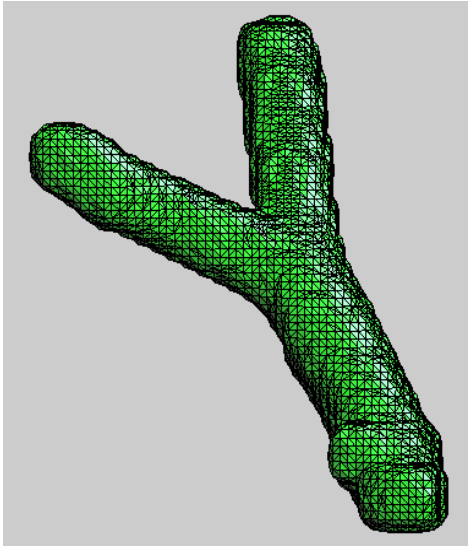

Figure 118 3D mesh representation of carotid model

This table shows an example of a mesh that we can use for the problem studied

Element size (m)	Triangles number	Tetrahedral number
0.0008	31470	52430

Create the geometry; impose the boundary conditions, material behaviour and problem data, the simulation can be running.

A.6 Icon.

 For running the problem.

 To check the state of the calculation and the converged.

 To see the graphic of the moments of forces inside the body studied.

Annex B- Disheart DSS Results

In this annex the results of the Disheart Dss will be showed.

1- Heart Disease DSS.
2- Carotid Aneurysm DSS.
3- Aneurysm DSS.

HOSPITAL:

DEPARTAMENT:

DOCTOR: -

14:02:40 20/03/200

The original data for training this Artificial Neural Network was taken from the following hospital:

Cleveland Clinic Foundation.
Hungarian Institute of Cardiology, Budapest.
VA Medical Center, Long Beach, CA.
University Hospital, Zurich, Switzerland.

Test1

Age:	30	
Sex:	Female	
Chest Pain Type:	Atypical Angina	
Blood Pressure:	111	mmHg
Serum Colesterol:	111	mg/dl
Fasting Blood Sugar Excess:	Otherwise	
Resting Electrocardiographic results:	Normal	
Maximun heart rate achieved:	111	
Exercise induced angina:	Yes-Induced Angina	
ST-Depression induced by exercise	1	

NOT HEART DISEASE- LESS THAN 50%

HOSPITAL:	Hospital Sant Pau
DEPARTAMENT:	Cardiology
DOCTOR:	Dr Francesc Carreras

20/03/200 14:00:20

ANALYSYS CAROTID TEST

INPUT	
Beat Amplitude:	0.5
Input Beat Amplitude:	0.4
Set Velocity:	0.32

OUTPUT

Pressure Wall

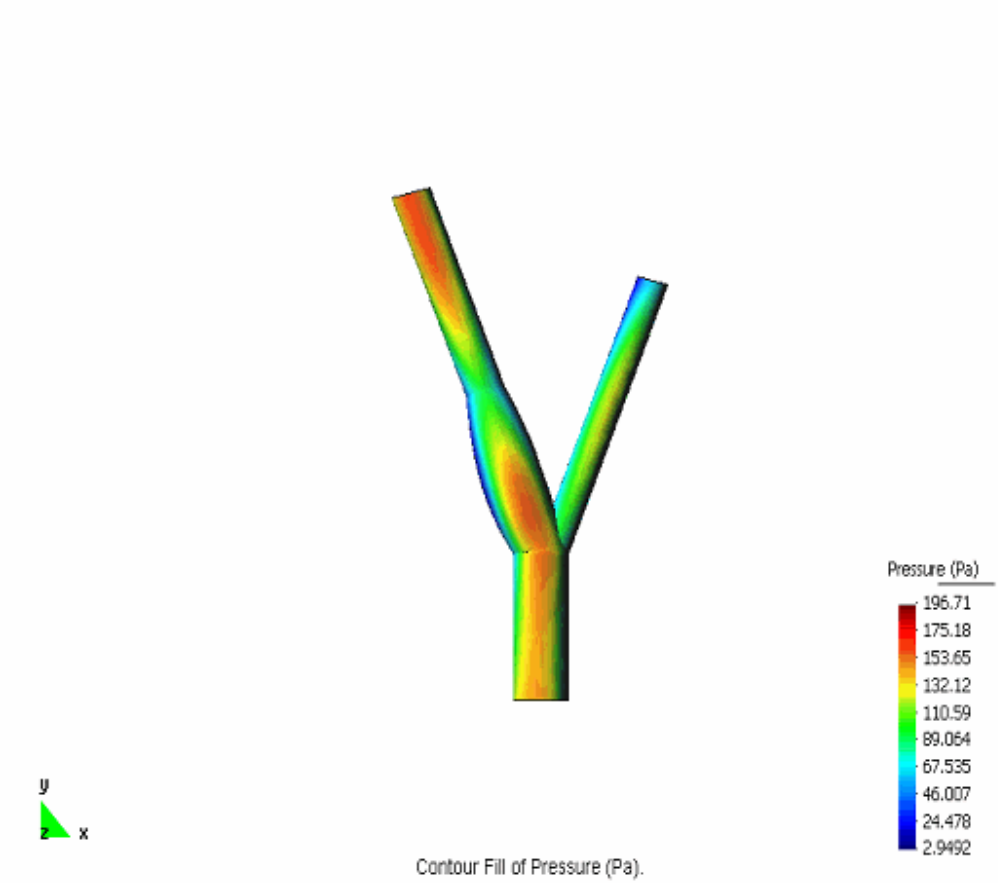

HOSPITAL:	Hospital Sant Pau
DEPARTAMENT:	Cardiology
DOCTOR:	Dr Francesc Carreras

20/03/200 13:25:36

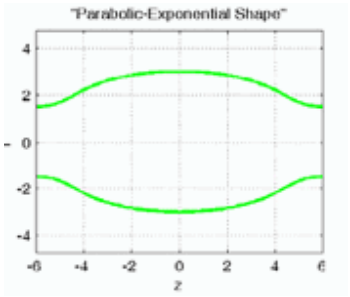

ANALYSYS OF ANEURYSM RUPTURE

INPUT	
Asymmetry	1
Thickness Factor:	2
Diameter Factor:	13
Length Factor:	2
Arterial Pressure:	1

OUTPUT

Main Tension X

Main Tension Y

Main Tension Z

| Tension |

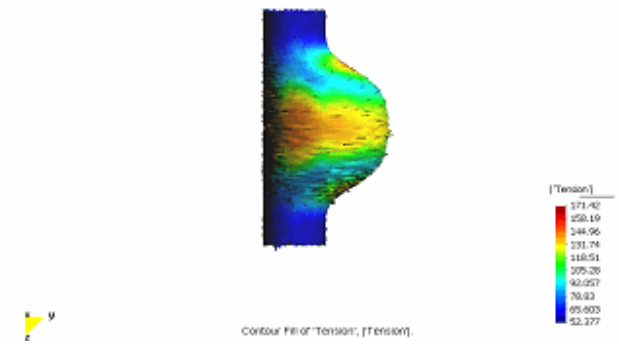

Maximum Stress X

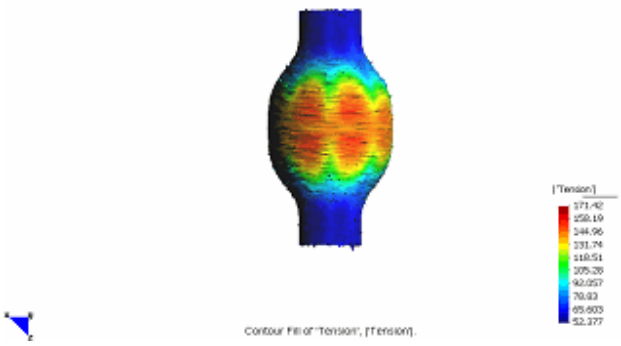

Maximum Stress Y

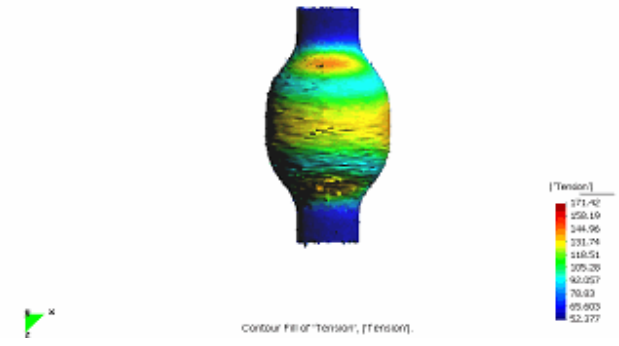

Maximun Stress Z

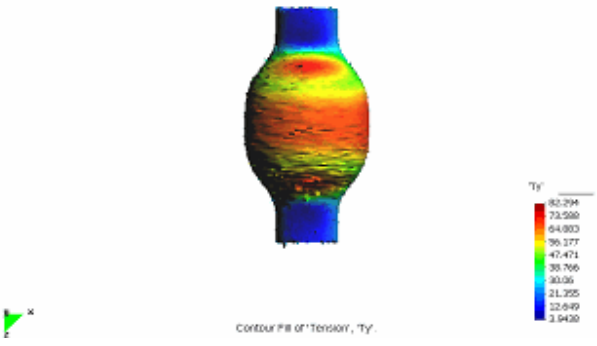

Stress

ANALYSYS OF ANEURYSM RUPTURE

INPUT	
Asymmetry	1
Thickness Factor:	2
Diameter Factor:	13
Length Factor:	2
Arterial Pressure:	1

OUTPUT

Main Tension X

Main Tension Y

Main Tension Z

| Tension |

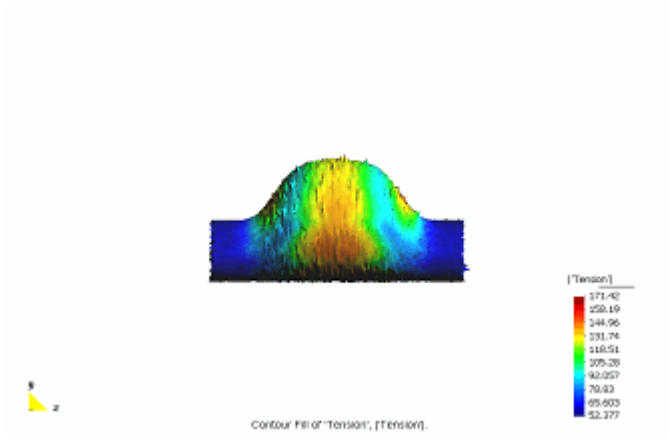

Maximum Stress X

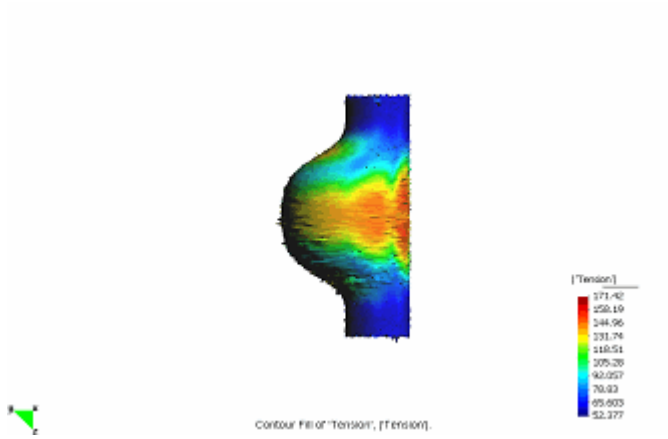

Maximum Stress Y

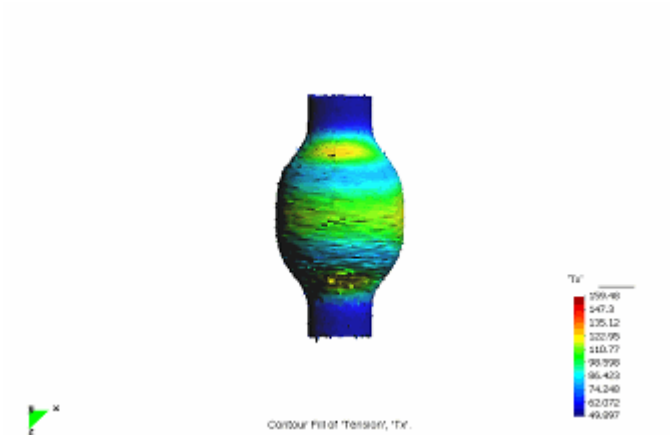

Maximun Stress Z

Stress